

TR 88-47

THE SULPHIDIZATION OF MINERAL SURFACES AS
APPLIED TO THE FROTH FLOTATION PROCESS.

Thesis

Submitted in Partial Fulfilment of the
Requirements for the Degree of

MASTER OF SCIENCE

in the Department of Chemistry at Rhodes University.

by

MUDZIMBA HUBERT RAMAGWEDE

July 1987

	Page
Acknowledgements	vi
List of Tables	vii
List of Figures	viii
List of Micrographs	xix
Abstract	xxiv

CHAPTER 1 INTRODUCTION

1.1	General	1
1.2	Sulphidizing reactions and the formation of a sulphide film	1
1.3	Sulphide Mineral flotation	17
1.4	The use of sodium sulphide as an activator of oxide and heavily oxidized sulphide minerals.	19

CHAPTER 2	EXPERIMENTAL	28
2.1	Preliminary work	28
2.1.1	General	28
2.1.2	Metal ion - soluble sulphide reactions	29
2.1.3	Sulphide analysis	30
2.2	Detailed work	31
2.2.1	Substrate choice	31
2.2.2	Reagent choice and optimum conditions suitable for study.	33
2.2.3	Experimental materials and methods	34
2.2.3.1	Materials and Reagents	34
2.2.3.1.1	Materials	34
2.2.3.1.2	Reagents.	36

2.2.3.2	Solubility of copper (II) oxide and cerussite	37
2.2.3.3	Sulphide - mineral reactions	38
2.2.3.4	Sulphide analysis	40
2.2.3.5	Starch analysis	41
2.2.3.6	Determination of CO_3^{2-} (51)	42
2.2.3.7	Xanthate-sulphidized mineral interaction	43
2.2.3.8	Scanning electron microscope and microprobe studies.	45
CHAPTER 3 RESULTS AND DISCUSSION		46
3.1.1.	Results	46
3.1.2.	Discussion	51
3.2	CuO Interactions	55
3.2.1	Solubility of CuO	55
3.2.2	Kinetics of sulphide uptake on CuO	58
3.2.3	Kinetics of sulphide uptake on CuO in the presence of Ca^{2+} and Mg^{2+}	62
3.2.4	Kinetics of sulphide uptake in the presence of starch, gum arabic and Triton X-100	72

3.2.5	Reaction of xanthate with CuO sulphidized at pH 11	80
3.2.6	Discussion	84
3.3	Cerussite interactions	92
3.3.1	Solubility of cerussite	92
3.3.2	Kinetics of sulphide uptake on cerussite	96
3.3.3	Kinetics of sulphide uptake on cerussite in the presence of Mg^{2+} Ca^{2+}	101
3.3.4	Kinetics of sulphide uptake on cerussite in the presence of 50ppm starch, gum arabic and Triton X-100	113
3.3.5	Reaction of Xanthate with sulphidized cerussite at pH 9 and 11	118
3.3.6	Discussion	120
CHAPTER 4 : CONCLUSION		126
REFERENCES		136

ACKNOWLEDGEMENTS

I would like to express my gratitude to my supervisors, Dr P.J. Harris of MINTEK and Professor D.J. Eve of Rhodes University for their enthusiastic guidance, co-operation and encouragement throughout this study.

I would also like to thank:

The Council for Mineral Technology (MINTEK) who provided the financial assistance without which this thesis would not have been possible.

Mr.R. Cross and colleagues of the Rhodes University Electron microscope unit for the production of the excellent quality micrographs.

Mr.R.Skae, Geology Department, Rhodes University for his assistance when using the electron microprobe.

Mr.N.Skeef and Mr A. Rugunanan for their help in the preparation of the final draft.

Ms T.P.Nengovhela for the excellent typing of this thesis.

The staff of Mineral Process Chemistry MINTEK and the staff of the Chemistry Department, Rhodes University.

My parents for their continual interest and support.

LIST OF TABLES

Table

I	Conditions under which xanthate experiments were conducted at pH 11 of sulphidization and pH 9 of xanthate reaction.	83
II	Concentration of various species of Pb^{2+} as a function of pH for an addition of 1×10^{-4} mol/l Pb^{2+} to water from ref (69).	95
III	Concentration of Mg^{2+} and Ca^{2+} adsorbed as a function of pH during the dissolution of cerussite.	107
IV	Conditions under which xanthate experiments were conducted at (a) pH 9* and (b) pH 11*	115

LIST OF FIGURES

Figures		Page
Fig. 1.	Zeta potential of anglesite, cerussite, galena and lead hydroxide as a function of pH in 0.005M KNO_3 . (from ref 24)	8
Fig. 2.	Zeta potential of anglesite, cerussite and galena as a function of sodium sulphide addition in 0.005M KNO_3 at pH 9.5. From ref 24)	10
Fig. 3.	Effects of time on uptake of sulphide on CuO . Curve 1 : Concentrations measured by the Colorimetric method. Curve 2 : concentration measured by the iodometric method. Curve 3 : concentrations measured by the iodometric method with mild continuous stirring. Initial concentration of Na_2S in all cases was $8.0 \times 10^{-3}\text{N}$ (from ref 29)	13
Fig. 4.	Effects of pH on the interaction of 35x48 mesh brochantite with $5 \times 10^{-3}\text{M}$ $(\text{NH}_4)_2\text{S}_2$ solution. (from ref 31)	16

Figures

Page

- Fig. 5. Kinetics of sulphide ion disappearance from solution as a function of pH for the chrysocolla/ammonium sulphide system. (from ref 31) 16
- Fig. 6. Effects of sulphidization of the surface of malachite on its wettability (ref 37). 20
- Fig. 7. Effects of Na_2S on adsorption of amyl dixanthogen and on flotation with AmDX, CCl_4 , n-hexane and cyclohexane emulsions and amyl xanthate solutions. Conditioning at pH 8 for 5 min. Curve 1 : flotation with AmDX emulsions : Curve 2 : flotation with 20 mg/l solutions of AmX : Curve 3 : AmDX adsorption : Curves 4,5 and 6 : flotation with CCl_4 , n-hexane and cyclohexane emulsions respectively (from ref 38). 23
- Fig. 8. Proportion of total sulphide present as S^{2-} , HS^- and H_2S in aqueous solution as function of pH. (from ref 45) 35
- Fig. 9 a. Apparatus used for sulphidization. 39

- Fig. 9b. Cross section of the apparatus used for sulphidization. 39
- Fig. 10a. Apparatus used for xanthate-sulphidized mineral interaction. 44
- Fig. 10b. Cross section of the apparatus used for xanthate-sulphidized mineral interaction. 44
- Fig. 11. Relationship between the mmoles of sulphide reacted and the mmoles of copper added at pH 9 and 11. $[Cu^{2+}] = 1 \times 10^{-2} \text{ mol/l}$, $[S^{2-}] = 1 \times 10^{-3} \text{ mol/l}$. Sulphide was determined by the MB and ISE. 47
- Fig. 12. Relationship between mmoles of sulphide reacted and the mmoles of copper added. $[Cu^{2+}] = 1 \times 10^{-2} \text{ mol/l}$, $[S^{2-}] = 1 \times 10^{-3} \text{ mol/l}$. Sulphide was determined by the MB after its modification. 50
- Fig. 13. Relationship between the mmoles of sulphide reacted and the mmoles of lead added $[Pb^{2+}] = 1 \times 10^{-2} \text{ mol/l}$, $[S^{2-}] = 1 \times 10^{-3} \text{ mol/l}$. MB was carried out on a filtered solution. 50
- Fig. 14. The solubility of 1g CuO after 1 hour conditioning in a borax buffer solution. 55

- Figure.15. Distribution of hydrolysis products (x,y) at $l = 1M$ and $25^{\circ}C$ in solutions saturated with CuO . The heavy curve is the total concentration of copper (II) the minimum is dashed because of the uncertainty with which the $Cu(OH)_2$ and $Cu(OH)_3^-$ species are known (ref 59). 56
- Figure.16. Kinetics of sulphide uptake on CuO at various pH values, $1 \times 10^{-4} mol/l$ sulphide was used. 59
- Figure.17. First order plot for sulphide interaction with CuO . Initials $[S^{2-}] = 1 \times 10^{-4} mol/l$. 59
- Figure.18. Kinetics of sulphide uptake on CuO at various pH values. $1 \times 10^{-3} mol/l$ sulphide was used. 61
- Figure.19. Variation with pH of the reaction velocities. 61
- 1) after conditioning CuO with $1 \times 10^{-4} mol/l$ sulphide.
 - 2) after conditioning CuO with $1 \times 10^{-3} mol/l$ sulphide.

- Figure.20. The variation with pH of the bulk precipitate after sulphidization using 1×10^{-3} mol/l sulphide. The bulk precipitate is also represented as % of initial concentration. 65
- Figure.21. Kinetics of sulphide uptake on CuO in the presence 1.25×10^{-3} mol/l Ca^{2+} at various pH values. 1.10^{-4} mol/l sulphide was used. 65
- Figure.22. Kinetics uptake on CuO in the presence of 2.06×10^{-3} mol/l Mg^{2+} at various pH. 1×10^{-4} mol/l sulphide was used. 56
- Figure.23. Kinetics of sulphide uptake on CuO in the presence of 1.25×10^{-3} mol/l Ca^{2+} at various pH values. 1×10^{-3} mol/l sulphide was used. 66
- Figure.24. Kinetics of sulphide uptake on CuO in the presence of 2.06×10^{-3} mol/l Mg^{2+} at various pH values. 1×10^{-3} mol/l sulphide was used. 58
- Figure.25. Variation with pH of the reaction velocities after sulphidization in the presence of 1.25×10^{-3} mol/l Ca^{2+} and 2.06×10^{-3} mol/l. 68

- Figure.26. Variation with pH of the bulk precipitate after sulphidization in the presence of Ca^{2+} and Mg^{2+} using 1×10^{-3} mol/l sulphide. The bulk precipitate is also represented as % of the initial sulphide concentration. 69
- Figure.27. Variation with pH of Ca^{2+} and Mg^{2+} uptake on CuO after 1 hour conditioning with 1.25×10^{-3} mol/l Ca^{2+} and 2.06×10^{-3} mol/l Mg^{2+} . 69
- Figure.28. Kinetics of sulphide uptake on CuO in the presence of 50ppm starch. Initial $[\text{S}^{2-}] = 1 \times 10^{-4}$ mol/l. 73
- Figure.29. Kinetics of sulphide uptake on CuO in the presence of 50ppm gum arabic. Initial $[\text{S}^{2-}] = 1 \times 10^{-4}$ mol/l. 73
- Figure.30. Kinetics of sulphide uptake on CuO in the presence of 50ppm Triton X-100. Initial $[\text{S}^{2-}] = 1 \times 10^{-4}$ mol/l. 74
- Figure.31. Kinetics of sulphide uptake on CuO in the presence of 50ppm starch. 1×10^{-3} mol/l sulphide was used. 74

- Figure.32. Kinetics of sulphide uptake on CuO 75
in the presence of 50ppm gum arabic.
 1×10^{-3} mol/l sulphide was used.
- Figure.33. Kinetics of sulphide uptake on CuO in 75
the presence of 50ppm Triton X-100.
 1×10^{-3} mol/l sulphide was used.
- Figure.34. Variation with pH of the reaction 78
velocities after sulphidization in the
presence of 50ppm starch, gum arabic
and Triton X-100.
- Figure.35. Variation with pH of the bulk precipitate 78
after sulphidization in the presence of
50ppm starch, gum arabic and Triton X-100
using 1×10^{-3} mol/l sulphide. The bulk
precipitate is also represented as % of
the initial sulphide concentration.
- Figure.36. Variation in xanthate uptake on CuO with 82
sulphidization level.
- Figure.37. Logarithmic concentration diagram for 87
 1×10^{-3} M Ca^{2+} Equilibrium data from ref (20).
- Figure.38. Logarithmic concentration diagram for 87
 1×10^{-4} M Mg^{2+} Equilibrium data from ref (20).

Figures		Pages
Figure.39.	Solubility of cerussite after 30 minutes of conditioning.	93
Figure.40.	Comparison of bulk precipitate (bp) and the surface precipitate (sp) measured after complete reaction of sulphide with cerussite surface, concentration of sulphide used = 1×10^{-4} mol/l.	93
Figure.41.	Kinetics of sulphide uptake on cerussite concentration of sulphide used = 1×10^{-4} mol/l.	93
Figure.42.	First order rate plot for sulphide interaction with cerussite.	98
Figure.43.	Cerussite particles produced after sulphidization under various conditions.	99
Figure.44.	Kinetics of sulphide uptake in the presence of 2.06×10^{-3} mol/l Mg^{2+} . Concentration = 1×10^{-4} mol/l sulphide was used.	103
Figure.45.	Kinetics of sulphide uptake on cerussite in the presence of 1.25×10^{-3} mol/l Ca^{2+} .	103

- Figure.46. First order plot for sulphide interaction with cerussite in the presence of 1.25×10^{-3} mol/l Ca^{2+} and 2.06×10^{-3} mol/l Mg^{2+} at pH 9. 105
- Figure.47. Variation with Ca^{2+} concentration of the rate of sulphide uptake on cerussite at pH 11, 0.5g of cerussite was used, concentration = 1×10^{-4} mol/l sulphide was used. 105
- Figure.48. Variation with pH of the bulk precipitate (1) in the presence and (2) absence of calcium. 106
- Figure.49. Solubility of cerussite in the presence of 50ppm Triton X-100, Ca^{2+} , gum arabic and starch b1 = solubility in the absence of other species. 106
- Figure.50. Variation of equilibrium carbonate concentration with Ca^{2+} concentration during sulphidization at pH 11. Concentration = 1×10^{-4} mol/l sulphide was used. 111

- Figure.51. Kinetics of sulphide uptake on cerussite in the presence of 50ppm starch at various pH values 1×10^{-4} mol/l was used. 111
- Figure.52. Kinetics of sulphide uptake on cerussite in the presence of 50ppm gum arabic at various pH values 1×10^{-4} mol/l sulphide was used. 112
- Figure.53. Kinetics of sulphide uptake on cerussite in the presence of 50ppm Triton X-100, 1×10^{-4} mol/l sulphide was used. 112
- Figure.54. Variation with starch concentration of the rate of sulphide uptake on cerussite at pH 11, 0.5g of cerussite was used. 1×10^{-4} mol/l sulphide was used. 115
- Figure.55. Variation with gum arabic concentration of the rate of sulphide uptake on cerussite at pH 11, 0.5g of cerussite was used. 1×10^{-4} mol/l sulphide was used. 115

Figures

Pages

- Figure.56. The variation with pH of the bulk precipitate after sulphidization in the presence of (1) starch and (2) gum arabic and (3) Triton X-100. 116
- Figure.57. Variation in xanthate uptake on cerussite with sulphidization level. 116
- Figure.58. Kinetics of cerussite dissolution at pH 12. 124

LIST OF MICROGRAPHS

Micrographs		Page
Micrograph.1.	CuO conditioned with 1×10^{-4} mol/l sulphide at pH 9.	63
Micrograph.2.	CuO conditioned with 1×10^{-3} mol/l sulphide at pH 9.	63
Micrograph.3.	CuO conditioned with 1×10^{-3} mol/l sulphide at pH 10.	63
Micrograph.4.	CuO conditioned with 1×10^{-4} mol/l sulphide at pH 9 in the presence of 1.25×10^{-3} mol/l Ca^{2+} .	63
Micrograph.5.	CuO conditioned with 1×10^{-4} mol/l sulphide at pH 9 in the presence of 2.06×10^{-3} mol/l Mg^{2+} .	54
Micrograph.6.	CuO conditioned with 1×10^{-3} mol/l sulphide at pH 9 in the presence of 1.25×10^{-3} mol/l Ca^{2+} .	64
Micrograph.7.	CuO conditioned with 1×10^{-3} mol/l sulphide at pH 9 in the presence of 2.06×10^{-3} mol/l Mg^{2+} .	64

Micrograph.8.	CuO conditioned with 1×10^{-3} mol/l sulphide at pH 10 in the presence of $1.25 \text{ mol/l Ca}^{2+}$.	64
Micrograph.9.	CuO conditioned with 1×10^{-3} mol/l sulphide at pH 10 in the presence of 2.06×10^{-3} mol/l Mg^{2+} .	71
Micrograph.10.	CuO conditioned with 1×10^{-4} mol/l sulphide at pH 9 in the presence of 50ppm starch.	71
Micrograph.11.	CuO conditioned with 1×10^{-4} mol/l sulphide at pH 9 in the presence of 50ppm gum arabic.	71
Micrograph.12.	CuO conditioned with 1×10^{-4} mol/l sulphide at pH 9 in the presence of 50ppm Triton X-100.	71
Micrograph.13.	CuO conditioned with 1×10^{-3} mol/l sulphide at pH 9 in the presence of 50ppm gum arabic.	79

Micrograph.14.	CuO conditioned with 1×10^{-3} mol/l sulphide at pH 9 in the presence of 50ppm gum arabic.	79
Micrograph.15.	CuO conditioned with 1×10^{-3} mol/l sulphide at pH 10 in the presence of 50ppm starch.	79
Micrograph.16.	CuO conditioned with 1×10^{-3} mol/l sulphide at pH 10 in the presence of 50ppm gum arabic.	79
Micrograph.17.	CuO conditioned with 1×10^{-3} mol/l sulphide at pH 9 in the presence of 50ppm Triton X-100.	81
Micrograph.18.	CuO conditioned with 1×10^{-3} mol/l sulphide at pH 10 in the presence of 50ppm Triton X-100.	81
Micrograph.19.	CuO sulphidized with 1×10^{-3} mol/l sulphide at pH 12.	81
Micrograph.20.	X-Ray image for sulphur for micrograph 19.	81

Micrograph.21.	Cerussite conditioned with 1×10^{-4} mol/l sulphide at pH 9.	100
Micrograph.22.	Untreated cerussite particles.	100
Micrograph.23.	Cerussite conditioned with 1×10^{-4} mol/l sulphide at pH 10 (4000 x magnification).	100
Micrograph.24.	X-Ray image for sulphur for micrograph 23 (4000 x magnification).	100
Micrograph.25.	Cerussite conditioned with 1×10^{-4} mol/l sulphide at pH 11.	102
Micrograph.26.	Cerussite conditioned with 1×10^{-4} mol/l sulphide at pH 12.	102
Micrograph.27.	Cerussite conditioned with 1×10^{-4} mol/l sulphide at pH 11 (4000 x magnification).	102
Micrograph.28.	X-Ray image for sulphur, for micrograph 27 (4000 x magnification).	102
Micrograph.29.	Cerussite conditioned with 1×10^{-4} mol/l sulphide at pH 9 in the presence of 1.25×10^{-3} mol/l Ca^{2+} .	110

Micrographs		Page
Micrograph.30.	Cerussite conditioned with 1×10^{-4} mol/l sulphide at pH 11 in the presence of 1.25×10^{-3} mol/l Ca^{2+} .	110
Micrograph.31.	Cerussite conditioned with 1×10^{-4} mol/l sulphide at pH 12 in the presence of 1.25×10^{-3} mol/l Ca^{2+} .	110
Micrograph.32.	Cerussite particles conditioned with 1×10^{-4} mol/l sulphide of 50ppm starch at pH 11.	110
Micrograph.33.	Cerussite conditioned with 1×10^{-4} mol/l sulphide in the process of 50ppm gum arabic at pH 11.	117
Micrograph.34.	Cerussite conditioned with 1×10^{-4} mol/l sulphide in the presence of 50ppm Triton X-100 at pH 11.	117
Micrograph.35.	Cerussite conditioned with 1×10^{-4} mol/l sulphide in the presence of 50ppm Triton X-100 at pH 11.	117

Abstract

This work constitutes a fundamental study of the interaction between soluble sulphide, copper (II) oxide and cerussite particles in the presence of Ca^{2+} , Mg^{2+} starch, gum arabic and Triton X-100. A detailed investigation of the effect of pH of the system on the rate of sulphide uptake was made. In addition, the structural form of the surface precipitates were determined with the aid of scanning electron microscopy. On the basis of these results, it was concluded that adsorption of sulphide on cerussite in the presence or absence of Ca^{2+} , Mg^{2+} , starch, gum arabic and Triton X-100 could either lead to the formation of a non-uniform or a uniform sulphide layer depending on the experimental conditions. However, the interaction of copper (II) oxide with soluble sulphide in the presence or absence of the above mentioned species always led to the formation of a non-uniform sulphide layer. Preliminary experiments of the interaction between xanthate and sulphidized surface showed that oxide surface covered with metal sulphide layer reacts with less xanthate than the free oxide surface.

CHAPTER I

INTRODUCTION

1.1. General

Separation of minerals by the flotation process was first used on a commercial basis in Australia at Broken Hill in the early part of the 20th century (1). The importance of this process in modern mineral technology especially in the separation of sulphides from high grade ores, needs no emphasis. However, since there is a steady decline in the grade of ores, and the fact that many of the ores remaining are finely disseminated mixtures of minerals with the majority of them being highly oxidized, mineral processing chemists are now faced with a problem of improving and modifying conventional flotation techniques to separate these refractory types of ores efficiently.

Froth flotation processes are used throughout the world for the concentration of a large number of different minerals such as gold bearing pyrites and copper, zinc and lead sulphides (2,3)

The process starts with the grinding of the ore to a chosen average grain size to secure maximum release of the discrete mineral particles. Only a relatively narrow size range of particles from approximately $10\mu\text{m}$ to $250\mu\text{m}$ can be floated successfully (4). The finely divided solids are conditioned in water with a combination of reagents e.g. collectors,

depressants, frothers, etc. These reagents make the surface of the selected mineral hydrophobic, so that upon the introduction of air into the system only particles of the selected mineral become attached to the air bubbles and are carried to the top of the flotation cell, where they are retained in the froth which is automatically scraped off. The concentrates are then dried and treated further.

The flotation separation of sulphide minerals from non-valuable gangue minerals with thio-type collectors (usually alkyl xanthates) has been extensively applied (5). This separation is possible because thio-type collectors either do not adsorb at the non-sulphide mineral-water interface, or if they do, they do not contain a sufficiently large non-polar group to render the minerals hydrophobic (3).

Most oxides and highly oxidized sulphide minerals containing copper, lead and zinc, interact well with thio-type collectors. But their response to flotation after treatment with collectors is rather poor. This is believed to be caused by the detachment of unevenly distributed thick patches of metal xanthates from the surfaces. The floatability of these minerals can be improved by increasing collector addition to such an extent, that, the multilayer patches of collector reaction products are no longer isolated, but form a continuous layer which envelopes each particle. The adhesion of the substrate

is now strengthened by lateral bonds existing within the continuous layer surrounding the particle (2). The use of xanthate collectors in the flotation of these minerals is uneconomic because it will lead to high consumption of the collector.

Some investigators have looked at the possibility of using chelating reagents as substitutes for xanthate collectors (6-11). Fundamental laboratory tests have shown that these reagents have potential, but they have not yet been adopted commercially.

Mineral processing chemists have long been using the sulphidization process prior to flotation in the treatment of oxide and heavily oxidized sulphide minerals (2,3,12,13). This is an efficient process and recoveries ranging between 80 and 100% have been reported (14-18). The mineral is conditioned first with soluble sulphide. After the reaction between soluble sulphide and metal ions from the soluble oxide mineral is complete, collector is added and flotation is carried out. The amount of the collector needed for flotation after sulphidization is low. However, this procedure can be complicated by an inadequate control of the sulphide concentration. Sulphide concentration should be controlled in such a way that during xanthate addition there are no free sulphide ions present in

solution since sulphide ions can act as depressants during flotation (19-22). Sulphidization can be accomplished by using a low sulphide concentration such that during addition of xanthate, there is a minimum of free sulphide ions present, or by conditioning the mineral with a solution of high sulphide concentration, followed by the decantation of the solution containing the excess free sulphide ions prior to xanthate addition (13,23). It should be mentioned that some workers have found that over-sulphidization can lead to the depression of flotation (23,24).

Several investigators have shown that sulphidization leads to changes in surface properties of the mineral (12,24,25). It was postulated that this change was caused by the reaction of all soluble metal ions with sulphide, followed by the deposition of the metal sulphide on the mineral surface. The resultant mineral surface is less soluble and more hydrophobic than its precursor. The hydrophobic surface will give a better response to flotation after a relatively low amount of xanthate has been added. However, results of these investigators have not provided evidence of the nature of the sulphide layer that is formed, i.e. whether it is a uniform layer or a non-uniform one, and under what conditions it is formed. Since the sulphidization step is the most crucial one in this process,

it is of interest to establish the manner in which sulphide ions are adsorbed by the oxide minerals and the conditions required to reduce continuous reaction of sulphide with the metal ions and, if possible, to form an impervious surface coating.

The purpose of this investigation was to study some of these aspects, and to establish the parameters that influence the manner in which the sulphide layer is formed on certain oxide mineral surfaces. This was accomplished by studying the adsorption of sulphide on cerussite (PbCO_3) and CuO at controlled pH values since the available literature (26,27) shows that similar studies have only been done at pH values determined by the hydrolysis of Na_2S in solution. Further studies on the adsorption of sulphide were conducted in the presence of Mg^{2+} , and Ca^{2+} because these metal ions are known to have an effect on the flotation of oxides when the sulphidization process is used (14).

It has been suggested that sulphidization involves the deposition of the metal sulphide on the mineral surface, consequently the influence of reagents on the sulphidization process which cause significant flocculation or dispersion such as starch, gum arabic and Triton X-100 was also investigated.

The scanning electron microscope was used to distinguish the presence of the precipitate on the surface and also to ascertain the distribution and structural nature of this precipitate. In addition the electron microprobe facility was used to confirm that the adsorbed species was a metal sulphide. Reactions between xanthate and the sulphidized surface were studied but flotation was not undertaken.

1.2 Sulphidizing reactions and the formation of a sulphide film.

Even at very small concentrations sulphide ions are able to react with metal cations to form insoluble compounds. Sulphide ions and cations of heavy metals interact predominantly at the surface of the corresponding minerals where the concentration of metal cation is high. The compounds thus formed are deposited on the surfaces of these minerals as thick sulphide films. With a sufficiently high addition of sodium sulphide on cerussite, this film can be seen clearly by naked eye (13,24,25).

Fleming (13) studied the effect of soluble sulphide on the flotation of lead minerals. He proposed that the reaction between soluble sulphide anions and cerussite should virtually go to completion. Fleming considered two factors that could complicate the matter.

1) Slow diffusion of Pb ions from the solid-liquid interface and 2) an impervious coating of the cerussite by lead sulphide. Finally it was concluded that sulphidization could only take place through direct chemical combination of Pb^{2+} and S^{2-} ions. The PbS formed nucleated on the surface forming a relatively stable film.

Marabini et al (26) studied the reaction of soluble sulphide with cerussite and smithsonite. The reaction of cerussite with S^{2-} was found to reach completion within a few minutes, with the formation of PbS on the surface. The overall uptake of S^{2-} on cerussite was thought to be a chemical-type adsorption with simultaneous solvent action on the mineral and penetration of the sulphide ion into the crystalline mass with formation of a non-uniform lead sulphide coating with a thickness equivalent to a few dozen monolayers. The modification of the surface by sulphide ions was interpreted using infra-red (IR) and X-Ray photo-electron spectroscopy (XPS) (26,28). IR results showed peaks at 466 and 374 cm^{-1} that were characteristic of galena and a peak at 986 cm^{-1} attributable to sulphoxide forms (PbS_2O_3). The XPS results showed an increase of sulphur on the surface as Na_2S concentration was increased.

Fuerstenau et al (24) investigated the sulphidization of lead minerals using electrokinetic measurements. They investigated the following minerals: anglesite (PbSO_4), cerussite (PbCO_3) and galena (PbS), and observed that unsulphidized cerussite had minima in the zeta potential at pH 6 and 10 (Fig.1). The zeta potential of anglesite was found to be higher than that of cerussite probably because anglesite has a greater solubility than cerussite.

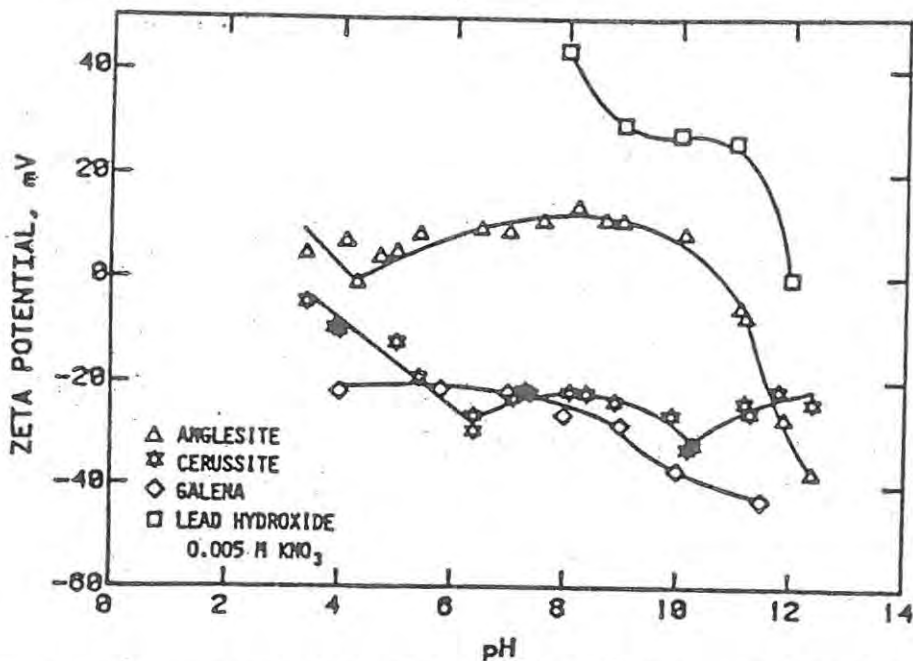
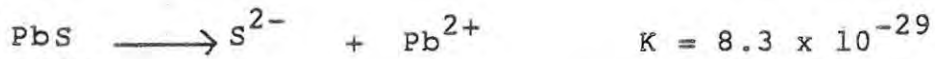
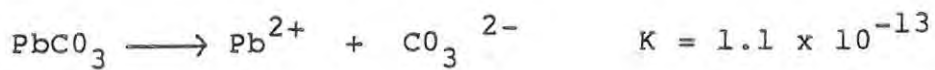
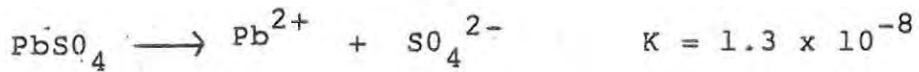


Fig. 1. Zeta potential of anglesite, cerussite, galena and lead hydroxide as a function of pH in 0.005M KNO_3 . (from ref 24)

At low pH both cerussite and anglesite are probably positively charged. In the case of anglesite, the amount of lead in solution was sufficient to cause the zeta potential to reverse its sign at about pH 5 due to the formation and readsorption of $\text{Pb}(\text{OH})^+$. With cerussite, there was a minimum in the zeta potential at about pH 6, and a further increase in pH also caused the zeta potential to become slightly less negative due to the readsorption of $\text{Pb}(\text{OH})^+$. The effect was low due to the low concentration of lead ions in solution. The zeta potential of cerussite after sulphidization at pH 9.5 was found to decrease with increasing S^{2-} concentration (Fig.2). The zeta potential of sulphidized cerussite was similar to that of galena. This further emphasizes that sulphidization can transform the surface of cerussite so that it is more like that of galena.

Massaci et al (27) observed that the interaction of cerussite with S^{2-} is an exothermic type of reaction. Their kinetic studies conducted by measuring the heat evolved during sulphidization as a function of time suggested that sulphidization of cerussite involves a more complex interaction of the solid-liquid interface than previously considered.

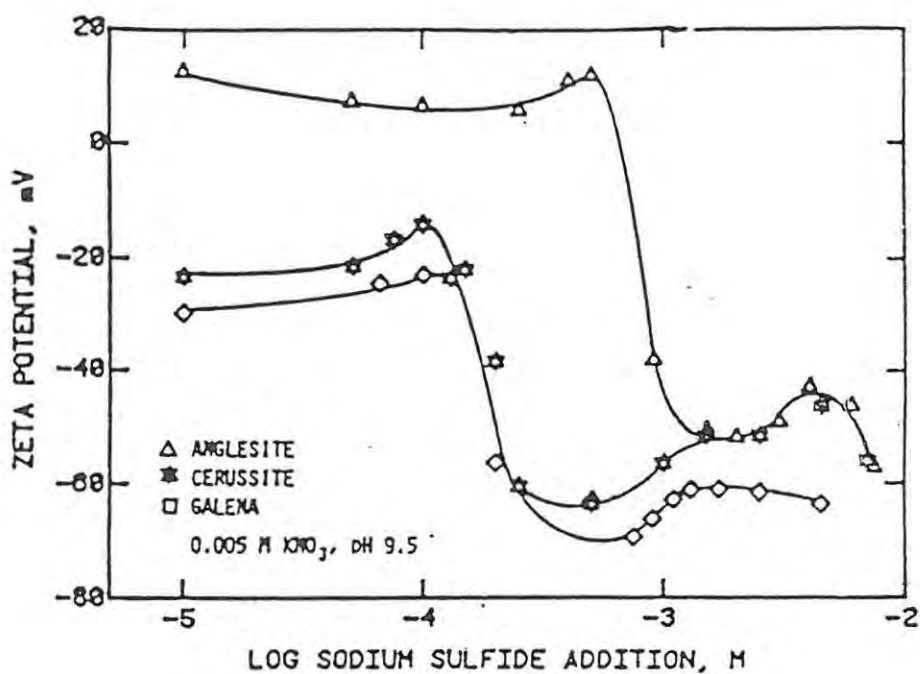
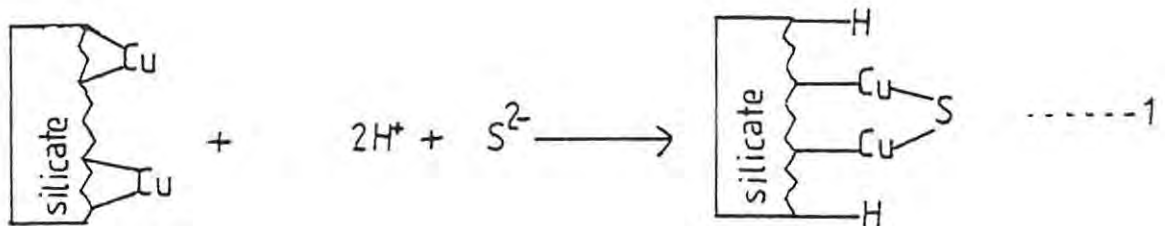


Fig. 2. Zeta potential of anglesite, cerussite and galena as a function of sodium sulphide addition in 0.005M KNO₃ at pH 9.5. (From ref 24)

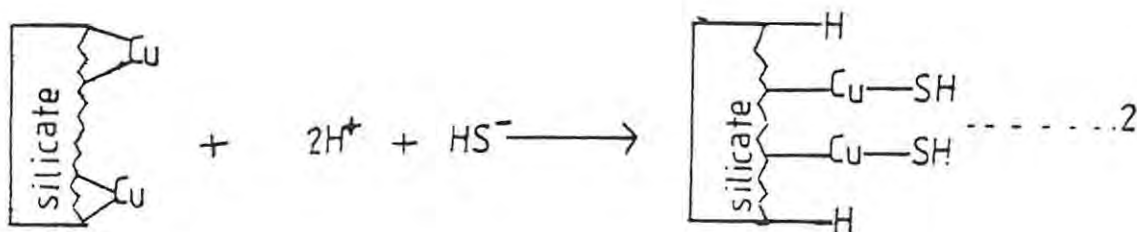
Attempts to elucidate the mechanisms of the sulphidization of copper oxide minerals have been conducted by several investigators (29,30,31).

Bowdish et al (30) studied the chemical mechanisms in the sulphidization of chrysocolla ($\text{Cu}_2\text{H}_2 (\text{Si}_2\text{O}_5) (\text{OH})_4$). They sulphidized chrysocolla at pH values ranging from 4 to 6.

Thereafter, they conditioned the sulphidized mineral in a xanthate solution followed by flotation. The authors found that as the sulphide concentration was increased from 350 to 600 mg/l of 60% Na_2S the percentage recovery decreased, but the sulphide film was thought to be always present on the surface. In postulating their mechanism of sulphidization, the authors assumed that each copper atom has two bonds to the silicate structure. The formation of the "collectable" site may be expressed as follows:



Sites that may be "non-collectable" may be formed by a similar reaction between chrysocolla and the H^+ , HS^- ion pair as in reaction 2 .



In the product formed in reaction 2 the copper ions are covered by HS^- ions and hence there is no place for xanthate ion attachment. These mechanisms were only formulated from the results of solution chemistry study, no spectroscopic work was attempted so the above mechanisms are not substantiated.

Castro et al (29) also studied the chemical factors in the sulphidization of copper (II) oxide. Synthetic tenorite was used because it can be obtained in a chemically pure state with a well defined formula and crystalline structure. They determined the amount adsorbed indirectly by measuring the residual concentration using either colorimetric technique or an iodometric method. The results obtained using the colorimetric technique indicated that sulphide uptake was complete in the first few minutes. When the iodometric technique was employed the initial uptake was found to be high but not complete and in addition, it decreased with time (Fig. 3).

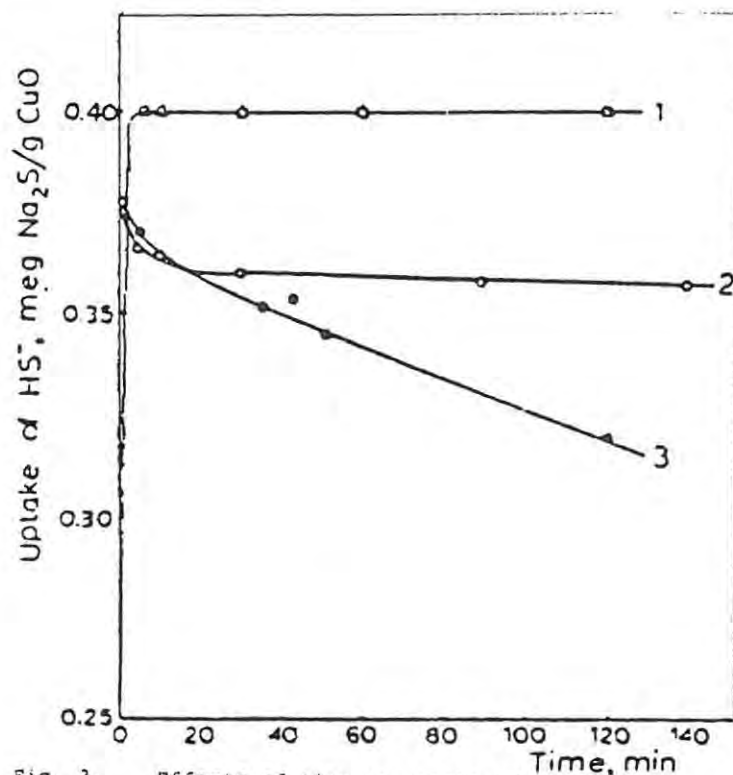


Fig. 3. Effects of time on uptake of sulphide on CuO.

Curve 1 : Concentrations measured by the Colorimetric method. Curve 2 : concentration measured by the iodometric method. Curve 3 : concentrations measured by the iodometric method with mild continuous stirring.

Initial concentration of Na_2S in all cases was $8.0 \times 10^{-3} \text{N}$ (from ref 29)

The discrepancies between the results obtained by the two techniques were accounted for by the type of ionic species detected by both methods. The colorimetric technique used was specific for sulphide ions, whereas the iodometric technique in addition can also detect a number of other species, like $\text{S}_2\text{O}_3^{2-}$, SO_3^{2-} , thionates, etc. The formation of the sulphoxide species served as an indication that there is oxidation of S^{2-} in solution.

The evidence provided by these authors suggests that the rate of sulphide adsorption on copper (II)

Oxide is high, and if the O_2 content is not controlled properly, some of the sulphide ions will form sulphoxide species. The authors did not mention the effect of pH on the sulphide uptake. Their X-Ray results showed the presence of CuS on the surface. In general the results showed that sulphide adsorption leads to changes in the surface features. However, their results do not give sufficient information to make it possible to deduce the type of surface layer formed, despite the fact that their calculations, based on monolayers, indicated multilayer formation.

Raghavan et al (31) studied the interaction of chrysocolla and brochantite ($Cu_4(OH)_6SO_4$) with S^{2-} in greater detail. They considered the following variables : (1) stirring speed, (2) particle size, (3) surface area and (4) pH, and they also conducted an electrokinetic study before and after sulphidization.

Analytical determination of sulphide adsorbed was done by measuring the residual concentration using a sulphide ion selective electrode. They eliminated oxygen from the system by bubbling nitrogen gas through the solution. Their results showed that stirring speed or mass transfer of sulphide ions through a boundary layer around the particles plays an insignificant role in the kinetics of the interaction process.

Sulphide uptake on brochantite was found to be a fast process and it was independent of particle size whereas for chrysocolla, sulphide abstraction depended on particle size. As a result the rate of sulphide uptake increased with decreasing particle size.

Investigation by Raghavan et al (31) of the dependence of the interaction of sulphide ions with brochantite and chrysocolla on the pH value of the aqueous solution showed that, below a pH of 7, the consumption of sulphide was complete within five minutes. They therefore suggested that $H_2S(aq)$ species which predominated at pH values below 7 is a much better sulphidizing agent for brochantite and chrysocolla than HS^- or S^{2-} (Fig.4 and 5 respectively). However, the apparent rapid uptake of sulphide ion at pH values below 7 could as well be due to the loss of H_2S gas during sulphidization. In addition the bubbling of N_2 gas through the solution during sulphidization is likely to cause the loss of H_2S gas. Consequently, their data cannot give a clear picture of the kinetics of sulphide adsorption at a pH value below 7.

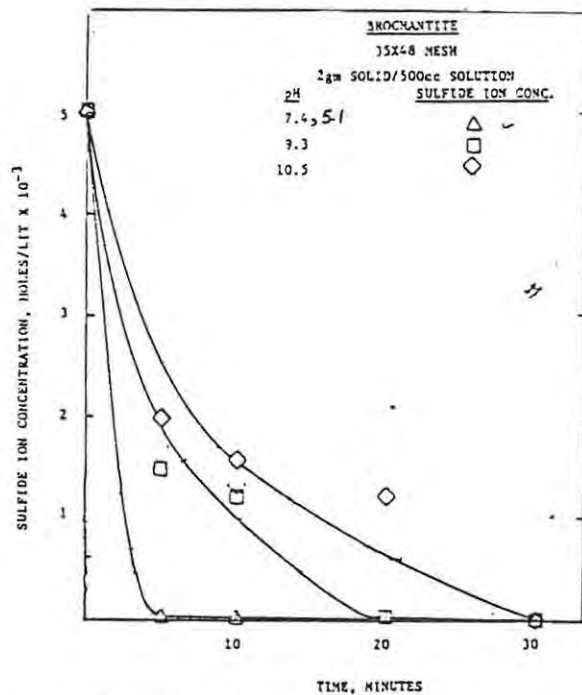


Fig. 4. Effects of pH on the interaction of 35x48 mesh brochantite with $5 \times 10^{-3} \text{ M } (\text{NH}_4)_2 \text{S}_2$ solution.

(from ref 31)

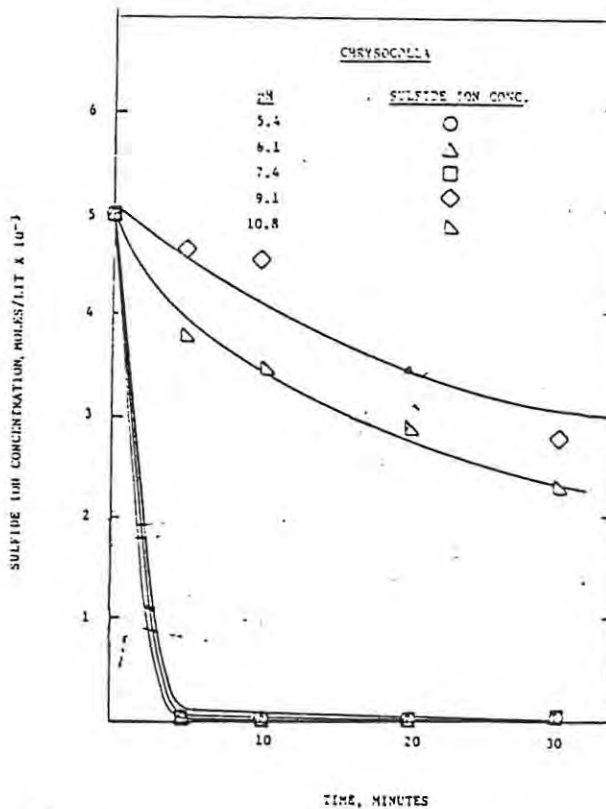


Fig. 5. Kinetics of sulphide ion disappearance from solution as a function of pH for the chrysocolla/ammonium sulphide system.

(from ref 31)

The authors also observed that sulphidization decreased the surface areas of chrysocolla and brochantite used. The reduction in surface area of brochantite was quite remarkable since its surface area was reduced from 1.884 to $0.87\text{m}^2/\text{g}$ whereas that of chrysocolla was reduced from 114.3 to $100.2\text{m}^2/\text{g}$ (i.e. after sulphidization at pH 9.3 using $1 \times 10^{-2}\text{mol/l}$ sulphide)

Raghavan et al noticed that sulphidization did not alter the electrokinetic behaviour of chrysocolla. On the other hand the electrokinetic behaviour of brochantite was changed by sulphidization using $1 \times 10^{-2}\text{mol/l}$ Na_2S and the zeta potential was found to be negative between pH 3 and 11 as opposed to the untreated brochantite which has its point of zero charge (p.z.c) at pH 9.

1.3. Sulphide mineral flotation.

Sulphide minerals which include galena (PbS), sphalerite ZnS , chalcopyrite (CuFeS_2) and pyrite (FeS_2) have been well studied in flotation research because they are the major source of non-ferrous metals. Most metal sulphides are floated effectively in the presence of oxygen with short-chain sulphhydryl collectors. This is due to a number of phenomena. First, because of its large size;

the sulphide ion, unlike oxygen, exhibits little tendency to form hydrogen bonds. Secondly, insoluble compounds form as a result of reaction between heavy metal ions and short-chain sulphhydryl collectors at relatively low concentrations.

Sulphide minerals are naturally more hydrophobic than the corresponding oxides and silicates (32,33, 34) some of them e.g. chalcopyrite, pyrite, galena, etc. do respond to collectorless flotation after the removal of hydrophilic species from their surfaces. In spite of their low solubility, sulphide minerals are thermodynamically unstable in the presence of oxygen. Although bulk oxidation does not occur, surface oxidation to SO_3^{2-} , SO_4^{2-} , $\text{S}_2\text{O}_3^{2-}$, etc (35) can take place. The oxidation products are more soluble in aqueous media than their precursors. During flotation with sulphhydryl collectors, the metal ion thus released interacts strongly with a collector to form a metal-chelate on the surface of the mineral. Therefore, in the case of the galena-xanthate interaction, the first layer on the mineral is believed to be PbX (strongly bound to the surface) over which layers of PbX_2 build up by 'sheer physical attachment' (36). This causes the mineral to be more hydrophobic and as a result, it will respond to flotation.

High selectivity is, however, only achieved by the addition of modifying agents such as depressants, activators, deactivators and frothers.

1.4. The use of sodium sulphide as an activator in the flotation of oxide and heavily oxidized sulphide minerals.

Oxide and heavily oxidized sulphide minerals create problems during flotation with sulphhydryl collectors. This is because these minerals have high solubilities which will lead to high consumption of the collector and low hydrophobicity which does not favour bubble attachment during flotation. This problem can be alleviated by first sulphidizing the mineral surface using soluble sulphide before collector addition. Basic knowledge of what the sulphidization treatment does is limited. A number of researchers have pointed out that sulphidization treatment of oxide minerals results in changes in the hydrophobicity of the minerals (5,13,25,29).

In 1933, Rehbinder (37) showed that the treatment of minerals with sodium sulphide leads to major changes in surface properties. The author showed that sulphide ions derived from aqueous solutions of sodium sulphide adsorb on the surface of malachite ($\text{Cu}_2(\text{OH})_2\text{CO}_3$) and sharply decrease its

wettability. Thus with the concentration of sodium sulphide of 1.3×10^{-5} mol/l the surface of malachite becomes hydrophobic (Fig. 6).

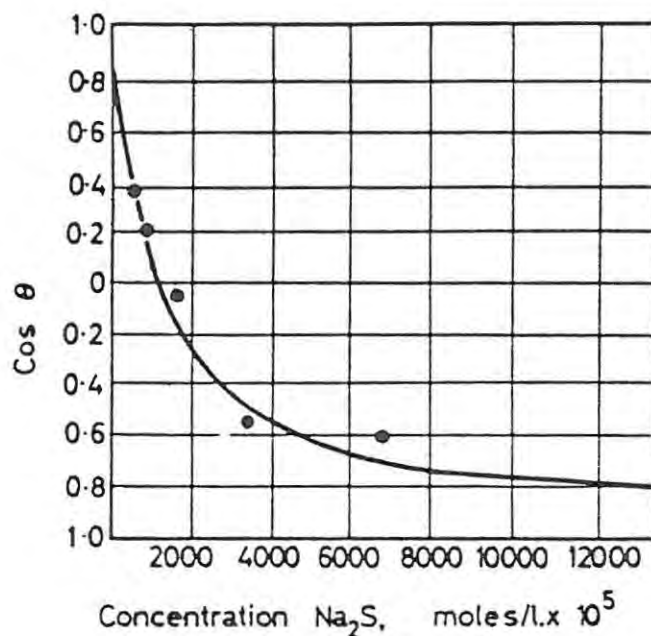


Fig. 6. Effects of sulphidization of the surface of malachite on its wettability (ref 37).

Rey in 1979 (25) reported that the treatment of oxidized zinc minerals with sulphide also led to a change in surface properties. Rey treated both the sulphidized and the unsulphidized oxidized zinc minerals with dithizone. He found that there was adherence of the coloured reaction product to the sulphidized mineral. With the oxidized mineral the colour was only in the bulk solution.

He thereafter examined the surfaces under the microscope. The results obtained were striking. In a slightly ammoniacal solution the oxide mineral dissolved slowly and, if the solution contained dithizone, long streaks of zinc "ions" were seen streaming out of the surface and forming a red precipitate at some distance which never adhered. The addition of a little sodium sulphide sealed the surface with non-porous zinc sulphide. Zinc "ions" were then found to escape only in traces and the red zinc dithizonate precipitate to adhere to the surface. The author suggested that sulphidization changed the more hydrophilic surface to a more hydrophobic one, which then made the adherence of hydrophobic zinc dithizonate possible.

Castro and Bustamante (38) investigated the hydrophobic effects of sodium sulphide on malachite ($\text{Cu}_2(\text{OH})_2\text{CO}_3$) flotation. Their experimental evidence showed that the sulphidized mineral consumed the collector at a faster rate than the natural mineral, and that both natural and sulphidized malachite reacted with considerable amounts of xanthate without reaching final equilibrium concentration. The sulphidized malachite could be floated completely after only very small amounts of xanthate have been consumed whereas natural malachite could not be effectively floated even with a much higher consumption of xanthate. Their flotation results with aqueous emulsions

of amyl dixanthogen showed that malachite is collectable only if it has been previously sulphidized. The same behaviour was observed with aqueous emulsions of n-hexane, cyclohexane and carbontetrachloride which share the characteristic of being non-polar hydrophobic liquids. These results are reproduced in Fig.7 where it can be seen that sulphidization promotes the adhesion and adsorption of the dixanthogen present in the emulsion. It was on this basis that Castro and Bustamante (38) assumed that sulphidization transformed the hydrophilic surface of malachite into a hydrophobic one and that this hydrophobization was only partial, and clearly insufficient to improve floatability by itself.

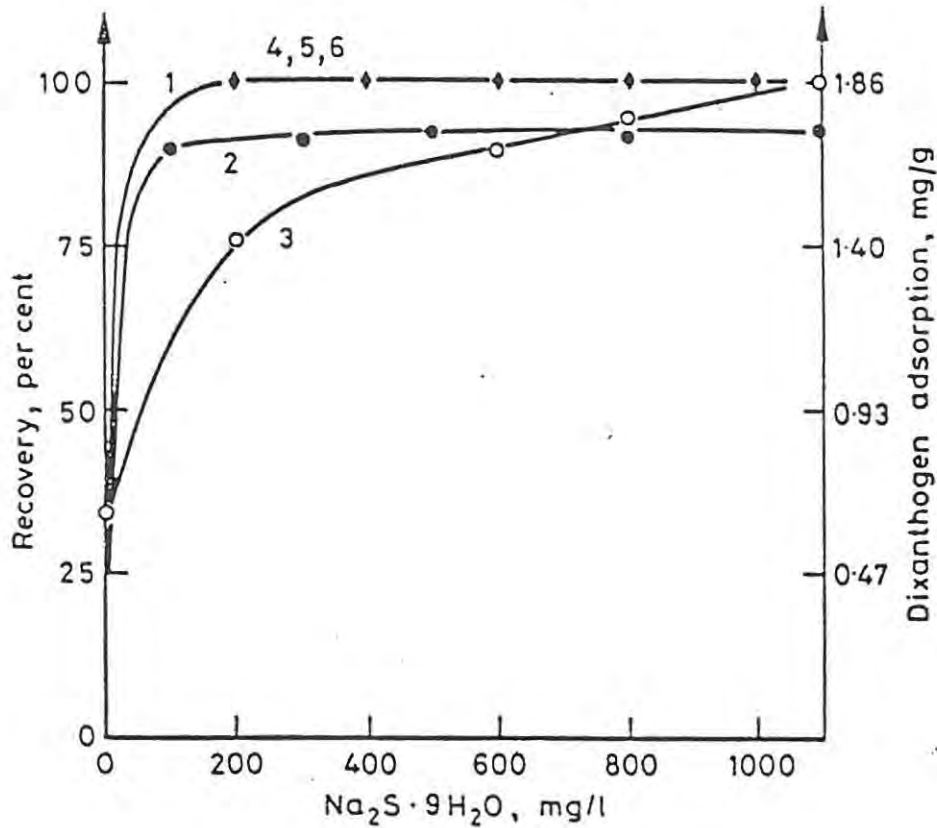
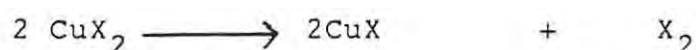


Fig. 7. Effects of Na_2S on adsorption of amyl dixanthogen and on flotation with AmDX, CCl_4 , n-hexane and cyclohexane emulsions and amyl xanthate solutions. Conditioning at pH 8 for 5 min. Curve 1 : flotation with AmDX emulsions : Curve 2 : flotation with 20 mg/l solutions of AmX : Curve 3 : AmDX adsorption : Curves 4,5 and 6 : flotation with CCl_4 , n-hexane and cyclohexane emulsions respectively (from ref 38).

They therefore proposed that flotation was improved by the adsorption of xanthate and dixanthogen on the sulphidized mineral

surface. Dixanthogen was thought to be produced by catalytic oxidation of xanthate by sulphidized particles which acquire semiconductor properties, or as some researchers suggested (39), by the decomposition of cupric xanthate to cuprous xanthate and dixanthogen.



Controversy also exists over the relative role of the species dixanthogen in the enhancement of the floatability of the sulphidized minerals.

Later, Castro et al (40) studied the stabilizing effect of sodium sulphide on the collector coating of chrysocolla. Chrysocolla consumed large amounts of xanthate and particles composed of the reaction products were spontaneously released from the surface of chrysocolla giving rise to a colloidal dispersion. In sulphidized chrysocolla the results showed that this phenomenon is markedly reduced, indicating that sodium sulphide has a stabilizing effect on the collector coating. Although there was high adsorption of xanthate on natural chrysocolla, no floatability of these particles was observed by these authors.

When the particles were sulphidized with small doses of sodium sulphide, flotation recoveries were very high, without appreciable changes in the uptake of xanthate. In separate experiments they found that dixanthogen in the form of an emulsion is a very effective collector for chrysocolla which has been properly sulphidized, whilst unsulphidized chrysocolla is not collected at all.

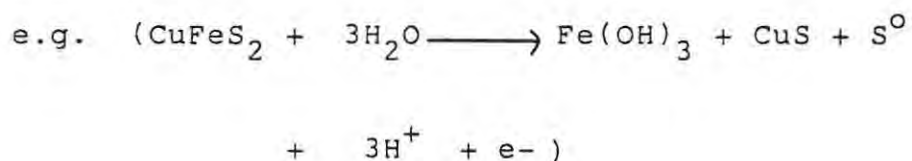
Castro et al considered that the spontaneity of the process of adhesion of dixanthogen droplets to the surface depended on the nature of the surface and hence the sign of the surface free energy term.

$$\Delta G = \gamma_{so} - (\gamma_{sw} + \gamma_{sw})$$

Where γ_{so} , γ_{sw} and γ_{ow} are the surface free energies per unit area of the solid-oil, solid-water and oil-water interfaces respectively. For adhesion to occur, ΔG must have a negative sign. The spontaneous detachment of collector observed by Castro et al was explained by the poor adherence of a hydrophobic colloidal particle to the hydrophilic surface of chrysocolla, and adherence was explained by the hydrophobicity of the surface caused by the reaction of sulphide with the surface. These stabilizing

effects by sodium sulphide, as they suggested, were not sufficient to explain completely the mechanism of hydrophobization.

On the other hand addition of soluble sulphide has been reported as being able to enhance flotation of chalcophyrite without a collector (41, 42). According to Luttrell et al (42) sodium sulphide removes the hydrophilic surface oxidation products such as SO_4^{2-} , $\text{S}_2\text{O}_3^{2-}$, etc from chalcopyrite due to the difference in solubility. Both authors (42, 42) believe that collectorless flotation of chalcopyrite is possible only under oxidizing conditions. They went on to propose that elemental sulphur is formed under oxidizing conditions, which increases surface hydrophobicity.



Sulphidization of malachite and chrysocolla, as discussed, resulted in increased hydrophobicity, but this did not help to reduce the amount of xanthate adsorbed. Instead, the rate of xanthate uptake was even higher on the sulphidized surface

than on the unsulphidized one. This, as Castro et al (38) suggested, is probably due to the catalytic oxidation of xanthate to dixanthogen by a sulphide surface. It should be pointed out that, in the experiments of Castro et al; oxygen was not excluded from the system. Oxygen, as Harris et al (43,44) have noticed in the interaction of chalcopyrite and pyrite with oxygen and xanthate, can also catalyse the reaction between the metal sulphide and xanthate.

Although sulphidization of cerussite produced a hydrophobic surface (13,24), it reduced the amount of xanthate needed for flotation. Marabini et al (26) suggested that sulphidization reduces the solubility of the lead carbonate surface which therefore makes it stable for coating by PbX_2 . For the untreated cerussite, stable adhesion of PbX_2 was not favoured because the solubility of cerussite was greater than that of PbX_2 . Consequently the adhesion of PbX_2 as Marabini et al proposed, is not likely to occur on the dissolving cerussite. In addition the sulphidization causes the surface to be more hydrophobic, thus making it possible for the hydrophobic entity PbX_2 to be more stable than on the hydrophilic cerussite surface.

CHAPTER 2

Experimental

2.1 Preliminary work

2.1.1. General

Investigation of the interaction between oxide minerals and organic reagents has been shown to be complicated by the formation of a metal-reagent complex either as a soluble species in solution or as a dispersed precipitate in the bulk solution. As a result, measurement of the reagent adsorption by the simple measurement of the change in solution concentration of the reagent does not necessarily reflect the adsorption of reagent at the mineral surface. In order to understand the relationship between the amount of reagent adsorbed at the surface and that present in other forms, an analytical technique needs to be developed that distinguishes between different forms of reagent. In this study it was therefore necessary to develop a technique which could distinguish between the free sulphide ions in solution and the bulk precipitate. Techniques selected to measure the free sulphide ion concentration were the methylene blue method (MB) and the sulphide ion selective electrode

(ISE) for sulphide ion determination. (ISE has been used to monitor S^{2-} adsorption during flotation practice (45,47)).

One method of determining the amount of sulphide involved in the bulk precipitate would be to determine the amount of metal ion associated with this form by atomic absorption spectrometry and then, if the ratio of metal ion to sulphide in the precipitate is known, to calculate the amount of sulphide in the bulk precipitate. If this technique is to be used successfully then a knowledge of the ratio of metal ion to sulphide of the various precipitates formed namely CuS and PbS, must be obtained. In addition it must be established that the two methods selected, (MB and ISE) measure only the free sulphide ion concentration and do not also measure the sulphide associated in the bulk precipitate.

~~These~~ methods can then be used to study the adsorption of sulphide on cerussite and CuO with the possibility of distinguishing between the bulk precipitate and that formed on the mineral surface.

2.1.2 Metal ion-soluble sulphide reactions.

The ratio of metal ion to sulphide in the precipitate and the free sulphide concentration was determined by reacting various ratios of Cu^{2+} and Pb^{2+} ions with excess sulphide ions and measuring the residual sulphide concentration with both the MB and the ISE.

A portion of sulphide solution was adjusted to the required pH value (i.e. pH 9 and pH 11) and then titrated with either Cu^{2+} or Pb^{2+} . In the MB method the free sulphide concentration was determined after filtration through a $0.22\mu\text{m}$ filter. Before addition of the metal ions, the solution was deaerated by bubbling N_2 through it. The N_2 flow was maintained throughout the experiment. The ratio of metal ion to sulphide was then determined from the amount of sulphide reacted and the amount of metal ion added in each case. Stock solutions of $1 \times 10^{-2} \text{mol/l}$ Cu^{2+} and Pb^{2+} and $1 \times 10^{-2} \text{mol/l}$ Na_2S in a borax buffer were used.

2.1.3. Sulphide Analysis.

The free sulphide concentration during titration was determined by the ISE and the MB techniques. For the ISE method, the potential of an Orion 94-16 ion selective electrode vs a saturated calomel reference electrode was recorded during the reactions on a 10mV chart recorder. The measured potentials were converted to concentrations in mol/l using standard curves prepared for all pH values under study.

Details of the MB method are as follows (49):
0.5g of N, N-dimethyl-p-phenylene diammonium dichloride (DMPDA) was mixed with 100ml of water in a 500ml volumetric flask. 200ml of 98% sulphuric acid was added immediately with cooling and the solution was then diluted to the final volume (500ml).

1ml of 30% iron (III) chloride was added to the sample solution containing sulphide (between 1×10^{-6} mol/l to 2×10^{-5} mol/l of sulphide) in a 50ml volumetric flask. This was followed by the addition of 2.5ml of DMPDA solution.

The resultant solution was allowed to stand for 90 minutes after mixing. The absorbance of the blue solution produced was measured in a 1cm path length cell using a Bausch and Lomb, spectronic 1001 spectrophotometer at 670nm.

2.2. Detailed Work

2.2.1. Substrate choice

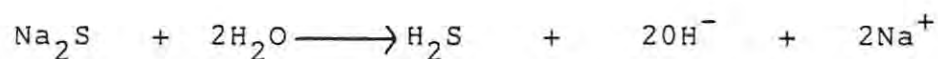
Recrystallized CuO, unlike naturally occurring tenorite and commercially available CuO, was chosen for study because it can be produced

from chemically pure CuO and it can be obtained with well defined smooth surfaces. The smooth surface makes it easy to distinguish the surface precipitate with the aid of a scanning electron microscope. Furthermore, additional complexities arising from impurities and peculiarities of natural minerals could be avoided by using the recrystallized species.

Natural cerussite was chosen because it was difficult to prepare synthetic material of a size suitable for the work to be undertaken. Preparation of chemically pure PbCO_3 by precipitating PbCO_3 from solution and allowing the crystals to grow in a cold place ($1-4^\circ\text{C}$) can lead to the formation of hydroxy cerussite which can have a different chemical behaviour from that of PbCO_3 during sulphidization. The natural cerussite used in this study was obtained in as pure a form as possible. One of the reasons why a lead containing oxide was chosen is the fact that lead occurs in a stable +2 oxidation state, therefore complications created by changes in oxidation state as in most transition elements can be avoided.

2.2.2. Reagent choice and optimum conditions suitable for study.

Sodium sulphide (Na_2S) was chosen for this study because it has been used extensively in the sulphidization process. Knowledge of its reaction with metal ions is well documented in literature. Soluble sulphides are easily oxidized by the presence of oxygen in solution to form sulphoxides species. As a result sulphide solutions were prepared using deaerated water. There is a large increase in alkalinity in the presence of sulphide as is evident from the hydrolysis and dissociation reaction that occur when Na_2S is dissolved in water.



Consequently the sulphide solutions were prepared in a heavily buffered solution in order to make it possible to control the pH value. At pH values below 7, sulphide in solution is present mainly as H_2S which can be lost as H_2S gas. Therefore all adsorption experiments were conducted at pH values greater than 9 where only negligibly small concentrations of H_2S are present. Fig. 8 shows the mole fractions of H_2S , HS^- and S^{2-} calculated to be present at equilibrium as a function of pH (45).

2.2.3. Experimental material and methods

2.2.3.1. Material and Reagents

2.2.3.1.1. Materials

Copper (II) oxide was recrystallized using the method described by Bryson (7). An analytical grade copper (II) oxide powder was mixed in equimolar proportions with sodium carbonate and then melted in a platinum crucible heated in a furnace. The melt was kept at $900^\circ C$ for about 20 hours and then cooled slowly. The copper (II) oxide crystals produced were repeatedly washed with water to remove all traces of sodium carbonate. Batch samples of oxide (70g) each, produced were mixed and a mean surface area of

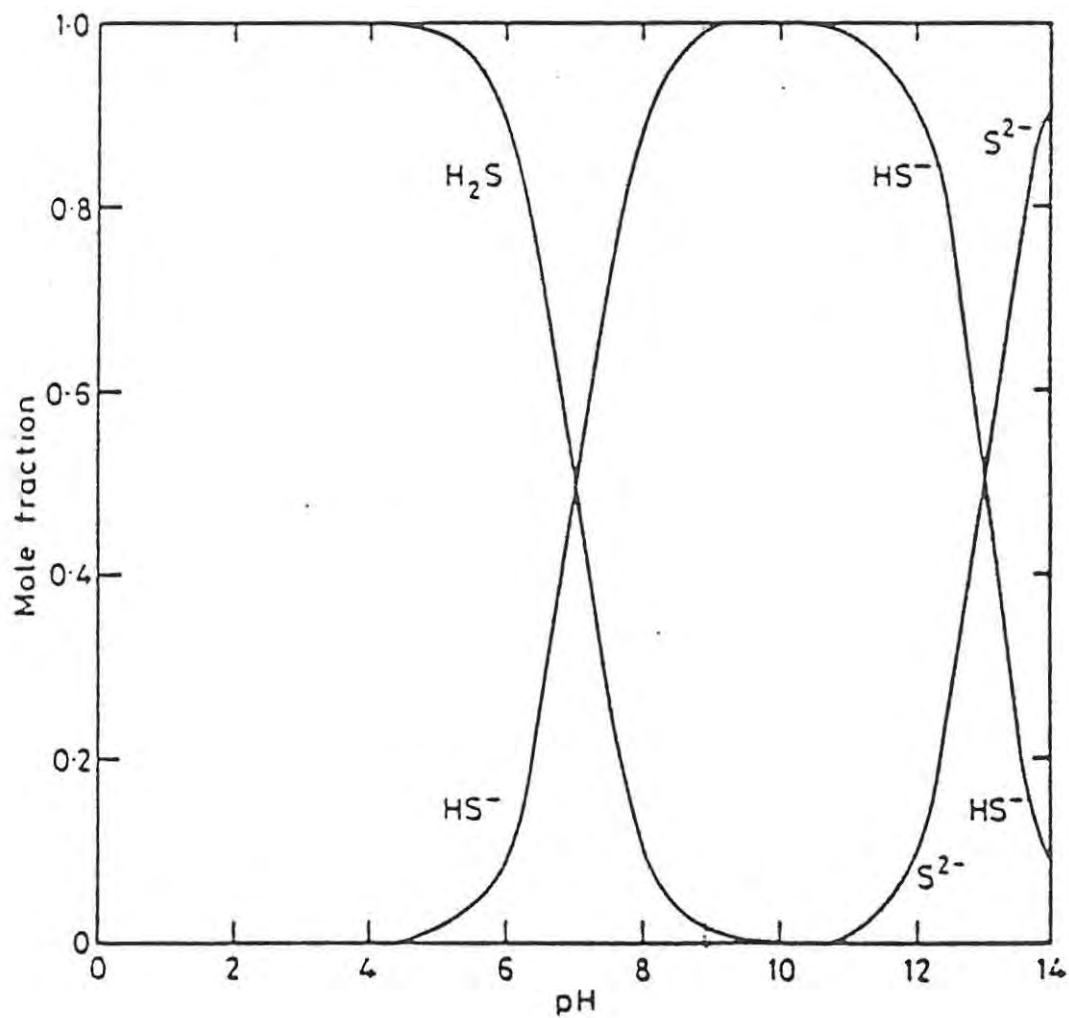


Fig. 8. Proportion of total sulphide present as S^{2-} , HS^- and H_2S in aqueous solution as function of pH.

(from ref 45)

0.21 m²/g was obtained.

Cerussite was obtained from Tsumeb,, Namibia. It was hand sorted, and then ground using an agate mortar and pestle. The size fraction between 38-106 μm was collected and then washed in an ultrasonic bath in order to remove any fine particles that are loosely attached to the bigger ones. No impurities were detected when the sample was analysed using X-Ray diffractometry. The specific surface area was found to be 0.02m²/g.

The specific surface areas was determined by the standard krypton Brunauer, Emmett and Teller (B.E.T.) method at the Council for Mineral Technology, Randburg. South Africa.

2.2.3.1.2. Reagents

Na₂S 2H₂O , analytical grade was used in all experiments. The starch used is a modified potato starch, Flocgel 100, with an average relative molecular mass of 1.9x10⁷.

Nonionic surfactant Triton X-100 is a polydisperse compound which is an octylphenol with an average 9.5 oxyethylene units per molecule. It has an average molecular mass of 600.

Gum arabic used was obtained from Merck. Its molecular mass is approximately 4x10⁵. Gum arabic consists of a back bone chain of 1 to 3 linked galactose

units with side chains at the C6 position. Carboxylic groups of uronic acids are distributed along the chain, the gum also contain some Ca^{2+} , Mg^{2+} and K^+ .

The following stock solutions were prepared: 2.5×10^{-3} mol/l of Ca^{2+} and 4×10^{-3} mol/l of Mg^{2+} from Merck CaCl_2 and $\text{MgCl}_2 \cdot 2\text{H}_2\text{O}$ respectively, and 1g/l of gum arabic, starch and Triton X-100. Sodium sulphide solutions were prepared in a 1×10^{-4} mol/l borax buffer solution. The pH of a solution containing sodium sulphide was found to range between 9 and 9.5 depending on the concentration of sulphide. The concentration of sodium sulphide used in this study ranged between 1×10^{-4} mol/l and 1×10^{-2} mol/l and that of gum arabic, starch and Triton X-100 were maintained at 50ppm. 2×10^{-3} mol/l of Mg^{2+} (50ppm) and 1.25×10^{-3} mol/l Ca^{2+} , (50ppm) were also used. HClO_4 and NaOH were used for pH adjustments. All solutions were prepared using deaerated water.

2.2.3.2. Solubility of copper (II) oxide and cerussite.

Determination of the solubility of copper (II) oxide at various pH values was carried out by conditioning 1g of recrystallized copper (II) oxide in a 100ml buffered solution for 60 minutes. In the case of cerussite 0.5g solid sample was conditioned in a 50ml buffered solution for 30 minutes. The amount of metal ion released was measured by atomic absorption spectrometry (AAS) after a portion of the solution (without filtering) was acidified and diluted to the required volume.

2.2.3.3. Sulphide - mineral reactions

The sulphidization experiments were conducted in a 180cm³ five-necked round-bottom flask. The apparatus is shown in Fig. 9. It was designed so that the reaction could be carried out under nitrogen atmosphere, and so that the abstraction of the sulphide could be followed continuously.

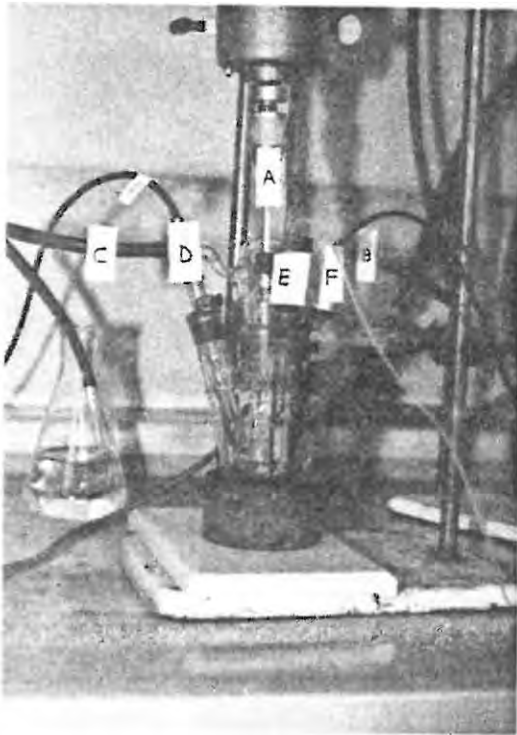


Fig. 9a. Apparatus used
for sulphidization

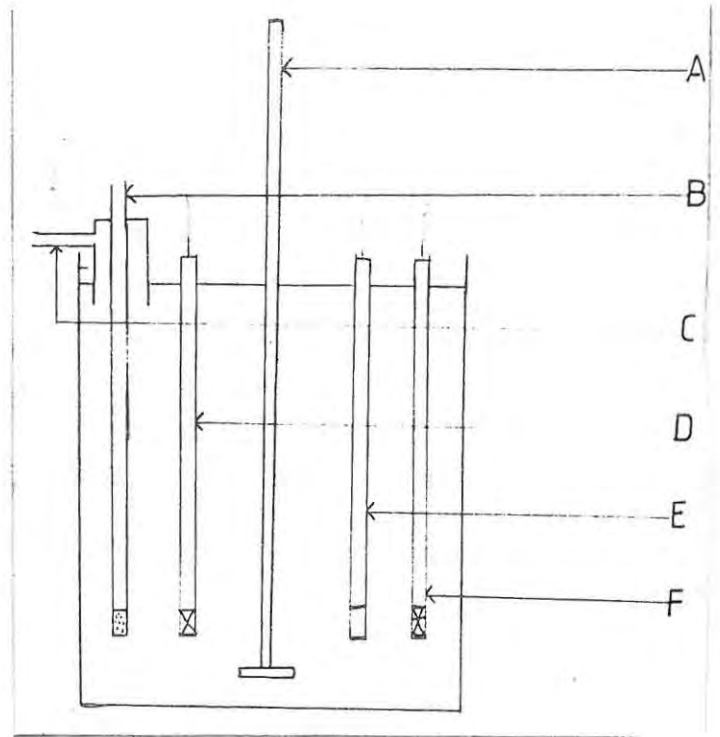


Fig. 10b. Schematic diagram
of the apparatus
used for sulphidization.

A = Glass stirrer attached to a stirrer motor and it passes through a rubber seal.

B = Nitrogen gas inlet (N_2 is flushed through the solution and is released from the solution through the outlet C).

D = Glass electrode attached to a pH meter.

E = Calomel electrode.

F = Sulphide ion selective electrode ISE.

A rubber seal is placed around each electrode to ensure that the system is air tight. The sulphide solution was introduced to the reaction vessel after it was flushed with N_2 continuously. After the pH has been adjusted to the required value, the ISE and the calomel electrode were placed into the solution. The solid was quickly introduced to the reaction vessel through D. The solid was kept suspended in the solution using a glass stirrer (A) attached to a stirrer motor and a controller. For all experiments a speed of 700rpm was used. This process was repeated in the presence of 50ppm Mg^{2+} , Ca^{2+} , starch and gum arabic at various pH values.

When the MB has to be used for sulphide analysis, in the presence of Triton X-100 the calomel and ion selective electrodes were replaced by a quickfit glass stopper and a rubber septum. A sample needed for analysis was drawn from the solution using a syringe.

2.2.3.4. Sulphide Analysis

In most kinetic experiments, sulphide concentration was monitored by measuring the potential of sulphide containing solution using an Orion 94-16 sulphide ion selective electrode ISE.

The change in potential during sulphidization was followed on a Philips (PM 1800) recorder. The MB method was used for sulphide analysis for kinetic experiments conducted in the presence of 50ppm Triton X-100. The bulk precipitate during CuO-sulphide interaction was determined indirectly by measuring the amount of copper present in solution using AAS. In the case of $PbCO_3$ - sulphide interaction, the bulk precipitate was measured using a MB method. (The methods for determining bulk precipitate were adopted after the techniques had been developed : see section 3.1 and 3.2)

2.2.3.5. Starch analysis

The amount of starch adsorbed was determined by measurement of the difference in the starch concentration in solution before and after contacting with the solid for 45 minutes by use of the phenol-sulphuric acid method proposed by Dubois et al (50). The method involved pipetting 2ml of aliquot portions of both the standard and sample solutions (concentration range 0-100ppm) into a pill vial. This was followed by the addition of 0.5ml of 5% phenol solution.

Thereafter, 5ml of concentrated H_2SO_4 was added quickly using a graduated pipette. The contents were mixed and allowed to stand for 10 minutes. The sample vials were then placed in a waterbath at 25 - 30°C for a further 10 minutes. The orange colour developed was read at 470nm using a spectrophotometer.

2.2.3.6. Determination of CO_3^{2-}

The method used was based on that developed by Basset et al (51). The amount of carbonate released during sulphidization was determined after complete adsorption of sulphide by cerussite at pH 11. The residual solution was filtered through a 0.22 μm filter paper and the total alkali (carbonate and hydroxide) was determined by titration with 1×10^{-2} mol/l HCl using methyl orange as indicator. In a second portion of solution the carbonate was precipitated with a slight excess of barium chloride solution, without filtering, the solution was titrated with 1×10^{-2} mol/l HCl using phenolphthalein as indicator. The latter titration gives the hydroxide content, and by subtracting this from the first titration, the volume of acid required for the carbonate was obtained, and hence the concentration of carbonate.

2.2.3.7. Xanthate-sulphidized mineral interaction

Reactions of xanthate with the sulphidized mineral were carried out using the apparatus shown in Fig. 10. After the mineral has been sulphidized, the calomel and the ion selective electrode were quickly replaced by a quickfit glass stopper and a rubber septum. The solution was then flushed with nitrogen gas for 15 minutes to ensure that there was a minimum amount of oxygen present. (Oxygen is undesirable during xanthate/mineral interaction because it can catalyse the reaction between the metal sulphide species adsorbed and xanthate, and it can oxidize xanthate to dixanthogen (43,44)). In this investigation it was desirable that only the reaction between xanthate and the soluble metal ion should occur. After allowing the particles to settle, the residual sulphide solution was drawn out of the vessel through a rubber septum using a syringe. The solid sample was washed several times with deaerated water from the separating funnel (F). After washing the sample, a clamp on the rubber tube (G) was closed. The rubber tube was then disconnected at a point where it was attached to the funnel. Xanthate solution was added to the funnel (F), and then flushed with N_2 gas for 15 minutes before the rubber tube (G) was reconnected to the funnel and the clamp opened.

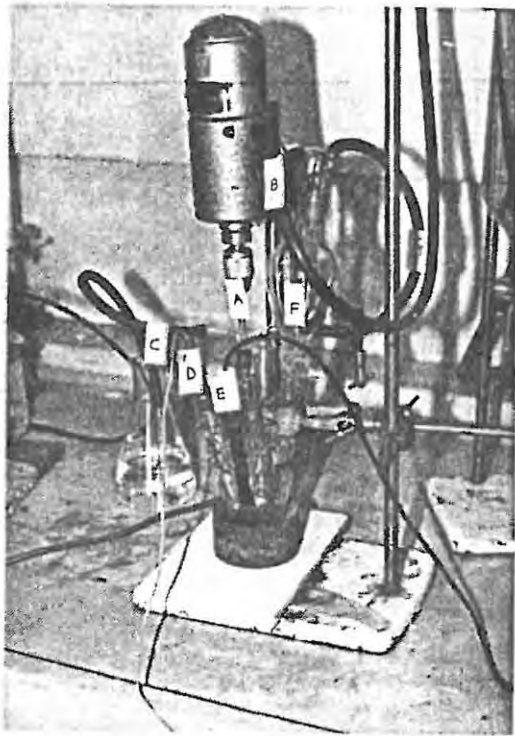


Fig. 10a. Apparatus used for xanthate-sulphidized mineral interaction.

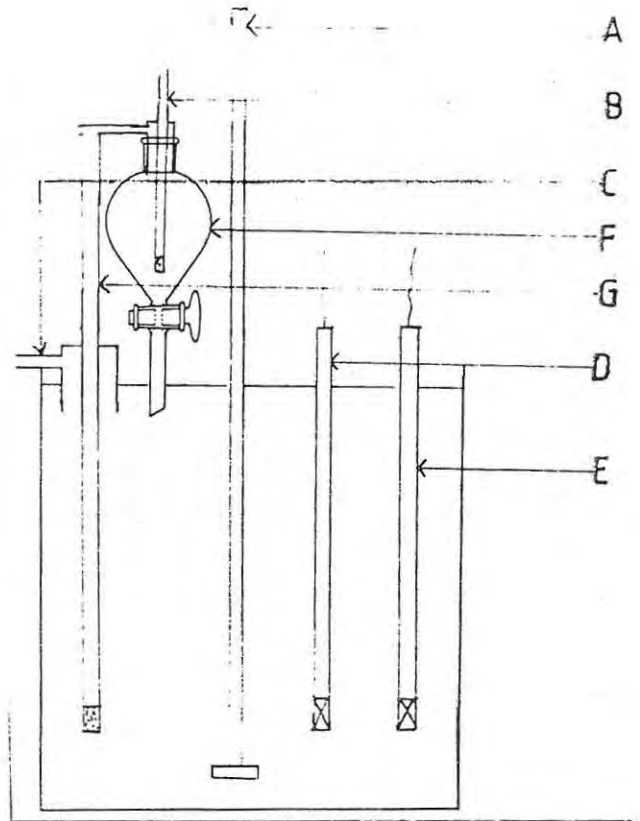


Fig.10b. Schematic diagram of the apparatus.

A = Glass stirrer attached to a stirrer motor and it passes through a rubber seal.

B = Nitrogen gas inlet (Nitrogen passes through the solution in the separating funnel (F) to the solution in the main reaction vessel via the rubber tubing (G). Nitrogen comes out of the main reaction vessel through the rubber tube (C).

D = Calomel electrode

E = Ion selective electrode

A 100ml solution of xanthate (amyl xanthate) was then added to the reaction vessel. Samples were conditioned with xanthate for 20 minutes during which time a stream of nitrogen gas was passed through the solution. The amount of xanthate adsorbed was determined by measuring a change in xanthate concentration by spectrophotometric determination at 300nm.

2.2.3.8 Scanning electron microscope and electron microprobe studies.

The structure of the metal sulphide precipitates adsorbed on the oxide mineral were studied using a Jeol model 260 scanning electron microscope with the assistance of the Rhodes University Electron Microscrope unit. The electron microprobe analysis facility (Jeol model 240) was used to confirm that the adsorbed species was a metal sulphide.

CHAPTER 3

Results and Discussion

3.1. Preliminary work.

3.1.1. Results

The overall results obtained when Cu^{2+} reacted with sulphide indicated that Cu^{2+} reacts with sulphide at a ratio of sulphide to copper greater than one when the sulphide concentration is in excess. The experimental results are given in Fig.11, which shows the relationship that exists after reaction with sulphide at each stage of addition of copper solution at pH 9 and 11. It can be seen that Cu^{2+} did not react with sulphide in a constant proportion of sulphide/copper = 1. The ratio of sulphide/copper = 1 was, however, obtained when the equivalent point was reached. This behaviour was observed when both the ISE and MB methods were used for sulphide analysis. The amount of sulphide reacted was found to be slightly lower when the MB method was used for sulphide analysis than when the ISE was employed. (MB was employed on solution filtered by $0.22\mu\text{m}$ filter paper).

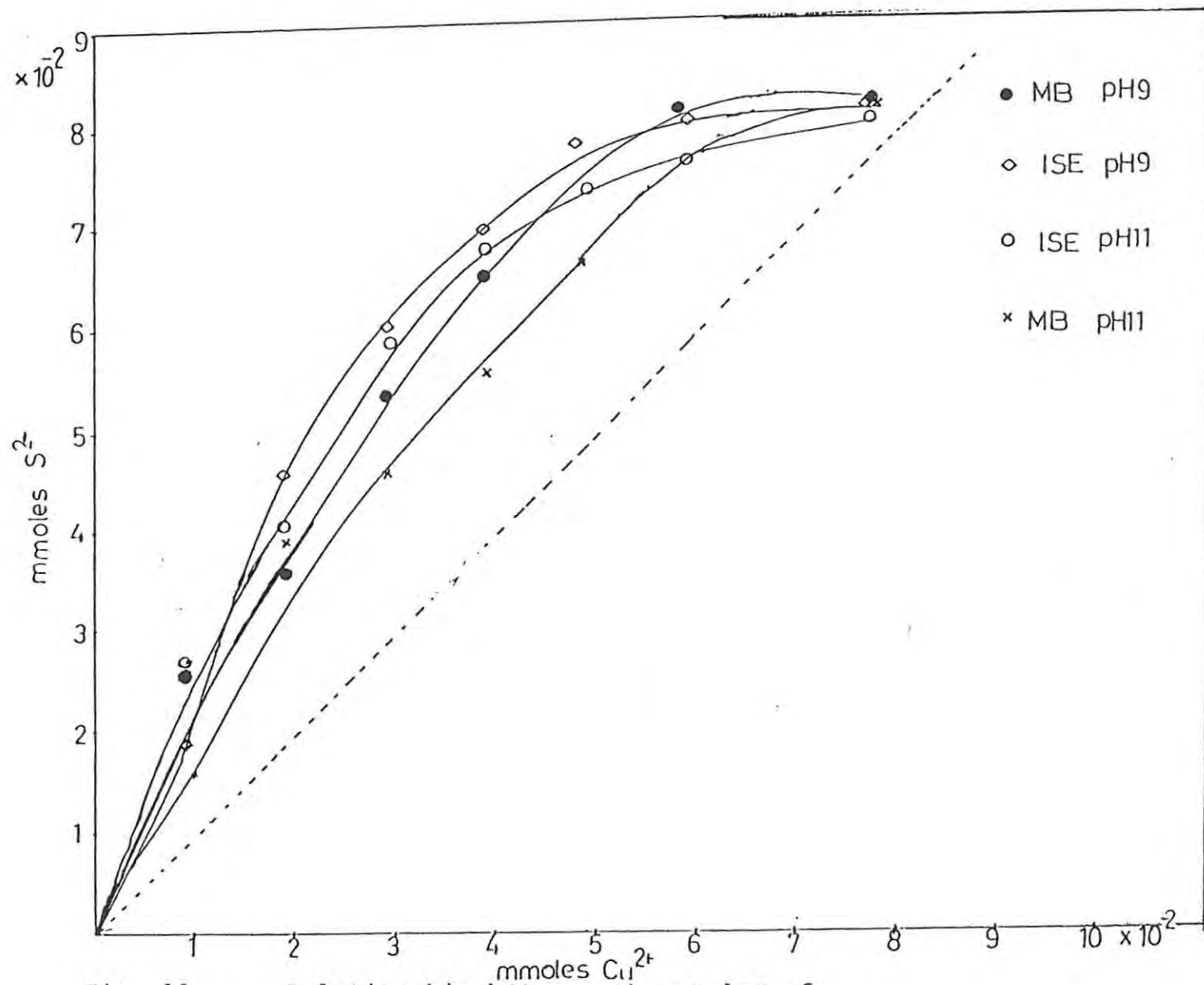


Fig. 11. Relationship between the mmoles of sulphide reacted and the mmoles of copper added at pH 9 and 11. $[\text{Cu}^{2+}] = 1 \times 10^{-2} \text{ mol/l}$, $[\text{S}^{2-}] = 1 \times 10^{-3} \text{ mol/l}$. Sulphide was determined by the MB and ISE.

Copper/sulphide reactions gave a brown colour attributable to what was apparently a suspension of very fine colloidal particles which could not be separated by filtration (0.22 μ m filter paper) but which was normally found to flocculate after about six hours, but more readily at high pH and after addition of NaCl and MgCl₂. The UV spectrum of the filtered solution showed a continuous increase in optical density for wavelengths lower than 350nm. This may be due to the scattering of light caused by colloidal particles present in the system(58).

Results of copper/sulphide interaction at pH 9 and 11 were found to be unaltered by the presence of 100ppm gum arabic and starch, i.e. results given in Fig. 11 remain unchanged in the presence of these compounds.

Experiments which were conducted in the presence of Triton X-100 showed that ISE gave a low response to changes in sulphide concentration after the metal ions had been added. It was, however, found that Triton X-100 did not interfere with sulphide determination when the MB method was used.

The fact that the reaction of Cu²⁺ with sulphide produced a stoichiometric ratio sulphide/copper greater than 1 before the equivalent point was reached, was thought to be the result of the reaction

of Cu^{2+} with sulphide in a ratio of 1 : 1, and the adsorption of some sulphide ions on the metal-sulphide species produced. In an attempt to obtain a ratio of sulphide/copper = 1, the methylene blue method was modified by increasing the acid concentration needed for the preparation of the DMPDA solution by 50%. The higher acid concentration has the effect of releasing the sulphide adsorbed on the CuS precipitate, and possibly, dissolving the CuS precipitate. The results obtained are shown in Fig. 12. As can be seen a sulphide copper ratio greater than one occurs only after the addition of 3×10^{-3} mmoles of Cu^{2+} .

Titration conducted using lead confirmed that lead always reacts with sulphide in a ratio of 1 : 1 i.e. when both the MB and ISE were used. In addition results obtained indicated that the ratio of sulphide : lead is not affected by the presence of starch and gum arabic, and changes in pH (Fig. 13). Experiments which were conducted in the presence of Triton X-100, however, showed that ISE gave a low response to changes in the sulphide concentration. It was again observed that Triton X-100 did not interfere with sulphide determination when the MB method was used. However, if the solution is not filtered the acid conditions in the MB method dissolve the bulk PbS formed and the free sulphide value obtained includes the sulphide associated with the bulk precipitate.

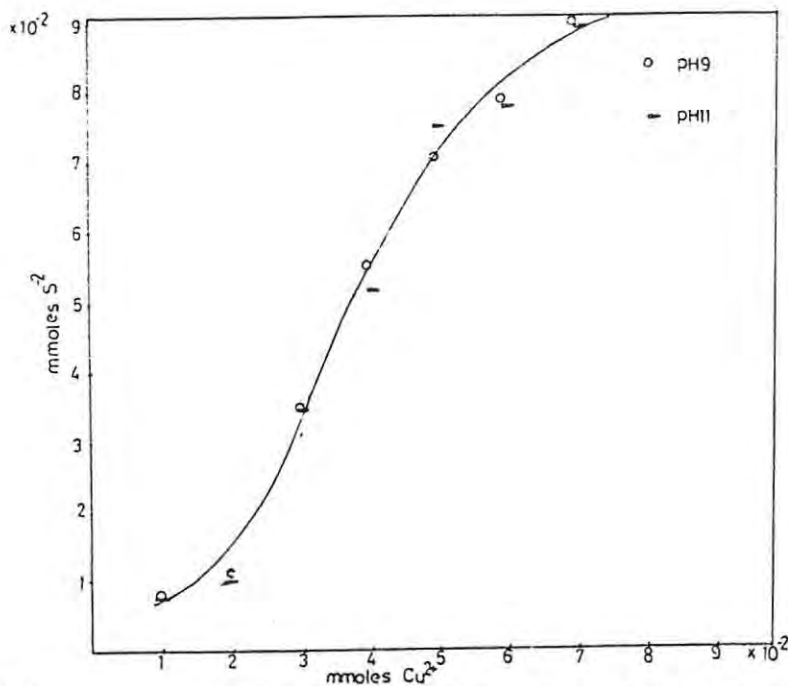


Fig. 12. Relationship between mmoles of sulphide reacted and the mmoles of copper added. $[\text{Cu}^{2+}] = 1 \times 10^{-2} \text{ mol/l}$, $[\text{S}^{2-}] = 1 \times 10^{-3} \text{ mol/l}$. Sulphide was determined by the MB after its modification.

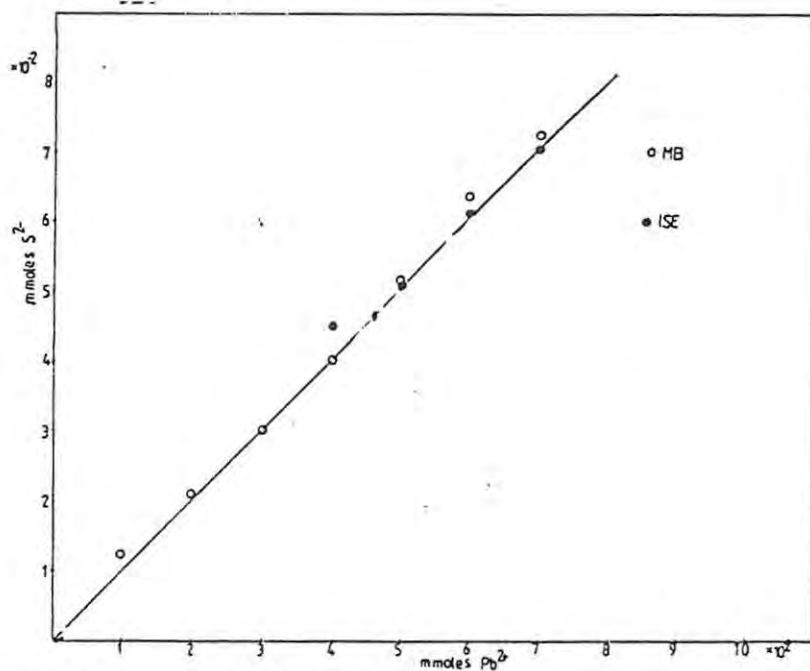
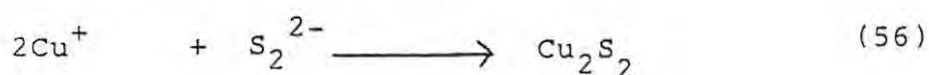


Fig. 13. Relationship between the mmoles of sulphide reacted and the mmoles of lead added $[\text{Pb}^{2+}] = 1 \times 10^{-2} \text{ mol/l}$, $[\text{S}^{2-}] = 1 \times 10^{-3} \text{ mol/l}$. MB was carried out on a filtered solution.

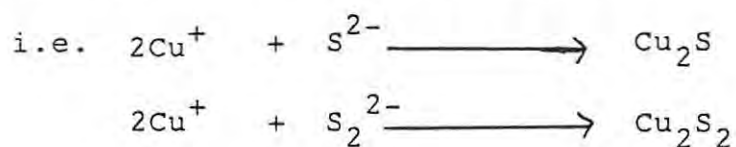
3.1.2 Discussion

Copper-sulphide reactions do not necessarily follow the simple stoichiometry $\text{Cu}^{2+} + \text{S}^{2-} \rightarrow \text{CuS}$.

Evidence from literature (52-55) suggests that copper favours a +1 oxidation state in the presence of sulphide. Consequently the overall reaction between copper and sulphide can probably occur by a series of oxidation reduction steps to give Cu_2S_2 i.e.



This can be explained according to the hard and soft acid base theory (HSAB). According to the HSAB theory, Cu^+ is a soft acid, and S^{2-} and S_2^{2-} are soft bases (57). The reaction between Cu^+ and S^{2-} or S_2^{2-} is favoured.



because it will give stable products. Furthermore this enhanced stability may be ascribed to 'back-donation' (55) of electrons from the filled d-orbitals of the cation to the empty d-orbitals of the sulphide ion.

This back donation is particularly important if the cation has a low formal charge and if it is large in size like Cu^+ . In the presence of reducing agents, which stabilize S^{2-} , Cu^+ will react with sulphide to form Cu_2S .

The evidence provided for the interaction of Cu^+ with soluble sulphide indicated that Cu^{2+} does not react with S^{2-} in a ratio of 1 : 1 especially when the concentration of copper is lower than that of sulphide. Soto et al (58) observed a similar departure from the actual copper:sulphide ratio of 1 and considered that CuS was the main product of the reaction between sulphide ions and Cu^{2+} (in fact when the precipitates were examined by X-Ray diffractometry, a CuS structure was found), and that the nuclei of CuS did not combine with one another to form large particles in the presence of excess sulphide ions in solution. Adsorption of excess sulphide stabilized the colloidal particles and hence prevented crystal growth. Since the nuclei were small (less than $0.22\mu\text{m}$) a substantial number of the structural unit could absorb light giving rise to the absorption peak at 1100nm. The authors also observed the increase in optical density with a decrease in wavelength i.e. for wavelengths lower than 400nm. This, was thought to be due to the scattering of light caused by colloidal particles present. A similar behaviour was noted in this present study.

The evidence provided in Fig. 11 indicates that the techniques developed can be used for studying sulphide adsorption on CuO with a possibility of distinguishing between free sulphide and the bulk precipitate. It has been established that the interaction of copper with sulphide does not give a constant ratio of sulphide/copper = 1 and that the ratio depends on the free sulphide concentration. Measurement of the residual sulphide concentration using MB, and Cu^{2+} concentration using AAS, can make it possible to estimate the amount of sulphide associated with the bulk precipitate using Fig.11. However, in most experiments conducted here the residual sulphide concentration was very low and was in most cases less than 1×10^{-5} mol/l. Under these conditions it could be reasonably assumed that the ratio of copper to sulphide is close to 1 : 1.

In most CuO/sulphide interaction experiments results reported in section 3.2 where 1×10^{-4} mol/l Na_2S was used, the amount of Cu^{2+} associated with CuS could not be determined because it was below the detection limits (less than 2×10^{-7} mol/l). Hence the bulk precipitate could not be estimated but was assumed to be negligible compared to the amount of sulphide adsorbed on the particles. Consequently in experiments conducted using 1×10^{-4} mol/l sulphide, the ISE values alone were

used to determine the extent of reaction.

The results obtained using this electrode were in agreement with results obtained when the MB was used.

When a concentration of 1×10^{-3} mol/l sulphide was used for sulphidization, the bulk precipitate was always found to be less than 10% of the amount of sulphide adsorbed. Thus in the experiments where 1×10^{-3} mol/l sulphide was used the MB was used for sulphide analysis (the ISE does not work well at high sulphide concentration). This method was also used for all experiments conducted in the presence of Triton X-100 because this surfactant interferes with sulphide determination by the ISE technique. In the case of sulphide/cerussite interaction experiments, the ISE was used for residual sulphide concentration measurements and the MB was used to determine the bulk and residual concentration. This is because the colour forming reagent (DMPDA) used in this technique is prepared in an acid and is able to dissolve PbS. The bulk precipitate was calculated by obtaining the difference between results obtained by ISE and those obtained by MB on an unfiltered solution.

3.2. CuO Interactions

3.2.1. Solubility of CuO

The solubility of recrystallized CuO after contact with aqueous buffer solution for one hour was determined by measuring the Cu^{2+} concentration by AAS after a portion of the sample solution was acidified and diluted to the required volume. After one hour it was assumed that dissolution of the mineral approaches equilibrium. The results illustrated in Fig. 14 are higher than the theoretical values reported by Baes et al (59), Attia (60) and the experimental values reported by Bryson (7). This may be due to the fact that, in this study, the solid sample had a surface area of $0.21 \text{ m}^2/\text{g}$ as opposed to $0.07 \text{ m}^2/\text{g}$ reported by Bryson. Results calculated by Baes et al are reproduced in Fig 15. It can be seen from these results that the concentration of copper in solution is slightly higher at pH 9 than at pH 10 although the actual position of the minimum is uncertain. Experimental results obtained in this investigation show that the solubility increases with pH from pH 9 to 12. Although the solubility of CuO was high under the conditions of this study, the shape of the curve is similar to that presented in Fig. 15.

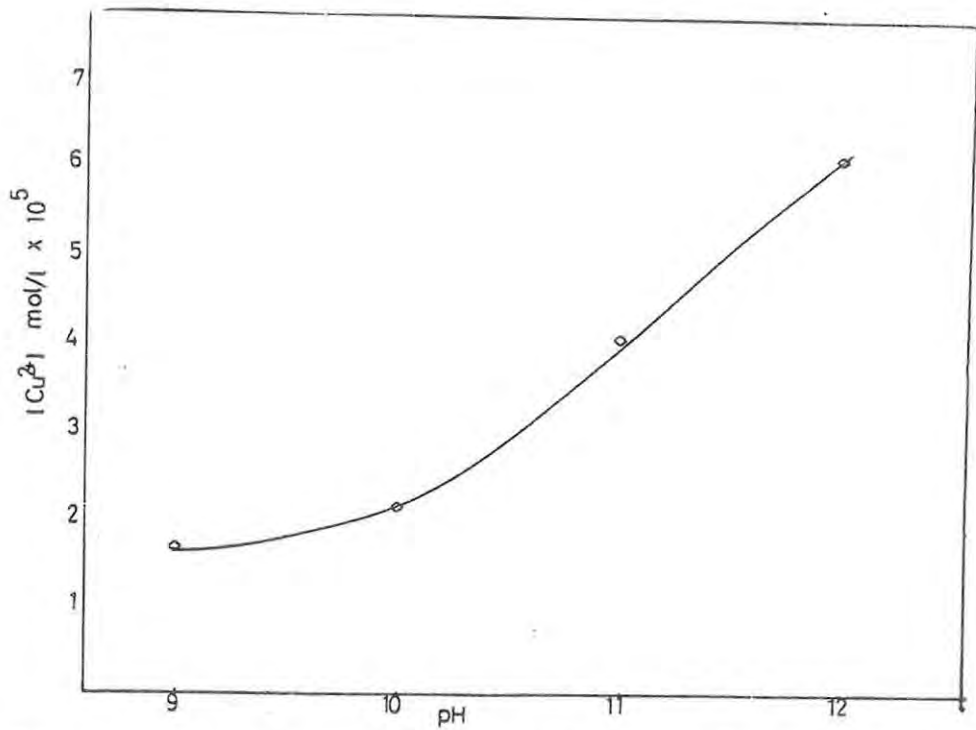


Fig. 14. The solubility of lg CuO after 1 hour conditioning in a borax buffer solution.

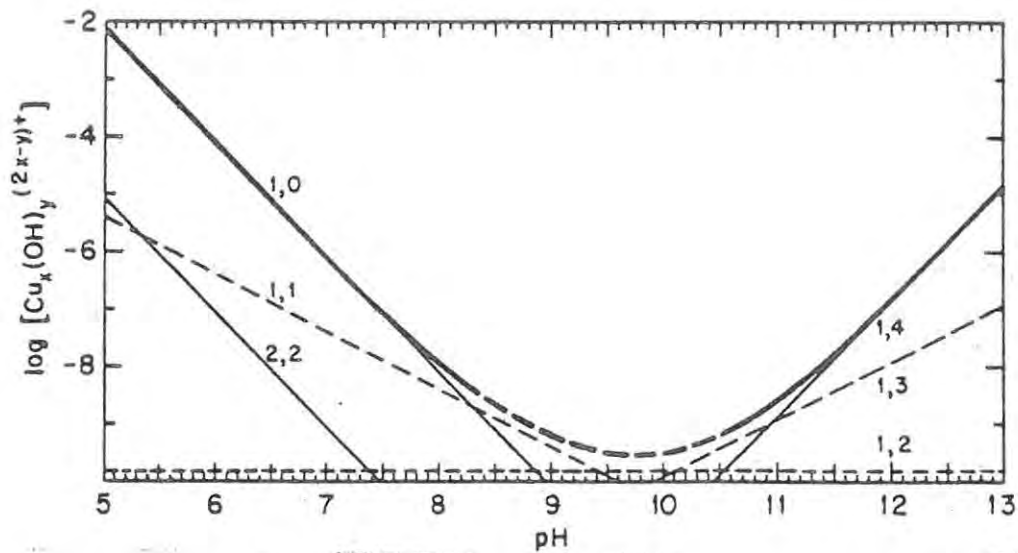
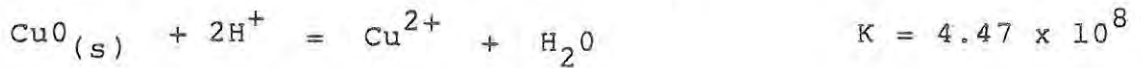
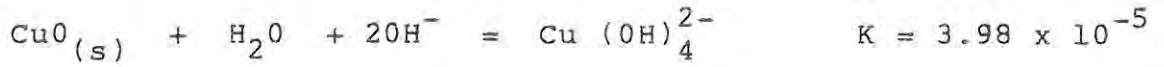
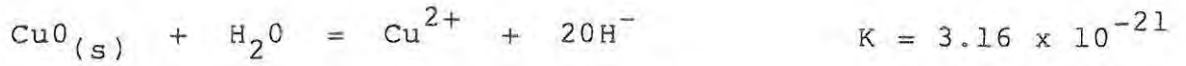
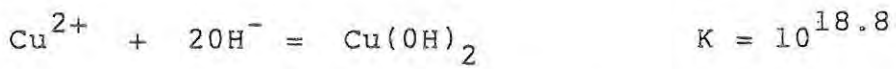
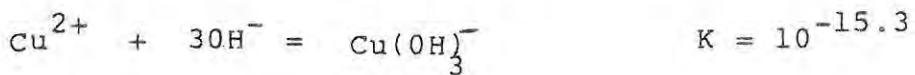
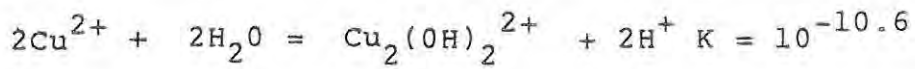
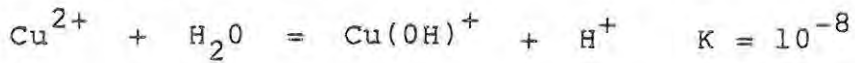


Figure.15. Distribution of hydrolysis products (x, y) at $I = 1\text{m}$ and 25°C in solutions saturated with CuO. The heavy curve is the total concentration of copper (II) the minimum is dashed because of the uncertainty with which the $\text{Cu}(\text{OH})_2$ and $\text{Cu}(\text{OH})_3^-$ species are known (ref 59).

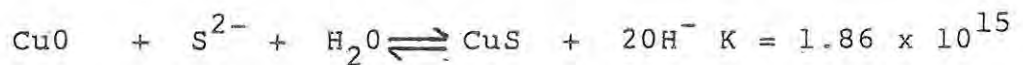
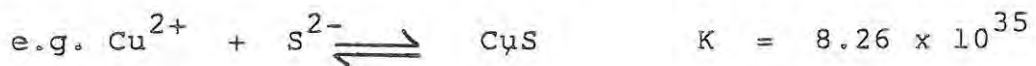
Dissolution of tenorite (CuO) can be governed by the following reactions (60).



The Cu^{2+} released can also undergo a number of hydrolysis steps :



The relative proportion of each species depends on the pH value of the solution. It is expected that the form of the copper-hydroxy species can as well affect the manner of sulphide uptake on the mineral surface.



3.2.2. Kinetics of sulphide uptake on CuO.

The rate of sulphide abstraction when 1×10^{-4} mol/l sulphide was used, was followed using an ISE.

The results were confirmed using the MB method.

The MB method was also used for sulphide analysis

when CuO particles were conditioned in the

1×10^{-3} mol/l sulphide.

The results of the rate of sulphide uptake on CuO after conditioning with 1×10^{-4} mol/l sulphide are shown in Fig. 16. The rate decreased with an increase in pH i.e. from pH 9 to 11. As can be seen from the figure, the rate, however, increased again at pH 12. It is expected that the rate of sulphide uptake should be influenced by the mineral solubility, but comparing the results given in Fig. 16 with those given in Fig. 14, for the solubility of CuO, it can be seen that the rate of sulphide uptake is not simply related to the mineral solubility except possibly at pH 12. At pH 10 and 11 the rate of sulphide uptake decreases with an increase in mineral solubility. This tends to suggest that other factors might be playing an important role. Semilogarithmic plots of the concentration of sulphide against time were reasonably linear under various pH values considered (Fig. 17).

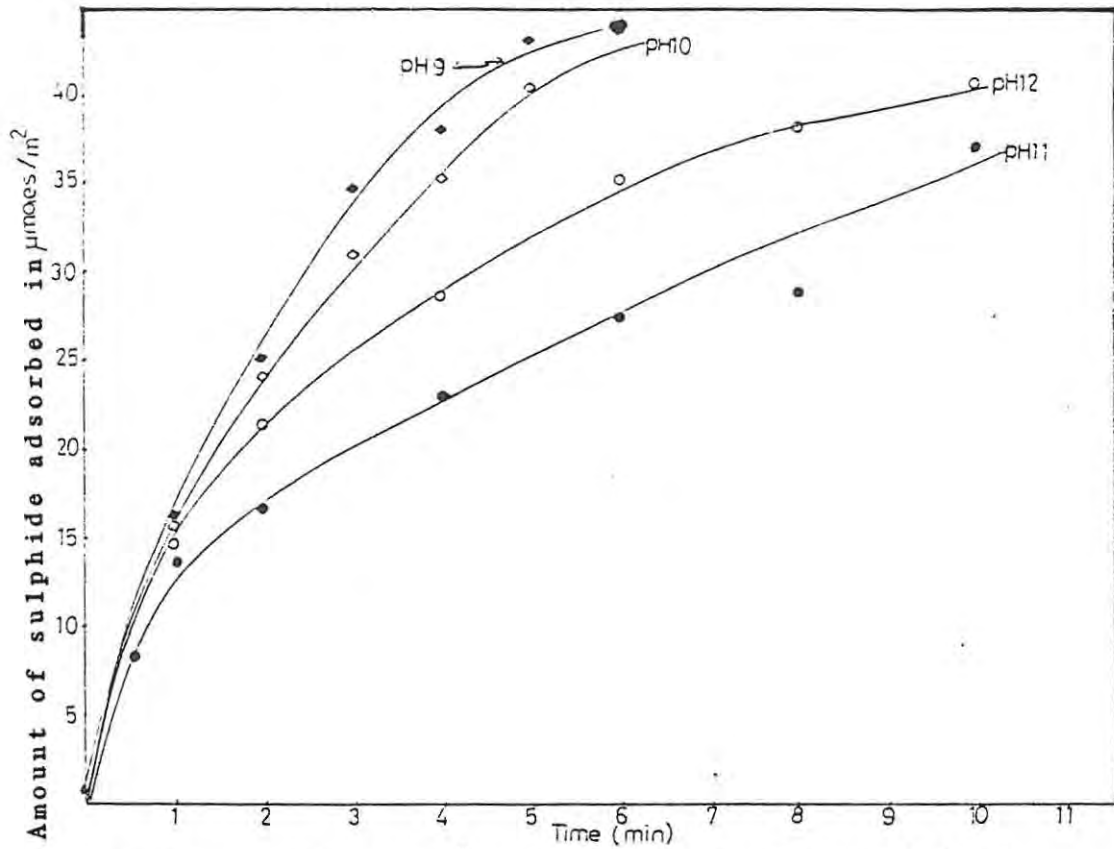


Figure.16. Kinetics of sulphide uptake on CuO at various pH values, 1×10^{-4} mol/l sulphide was used.

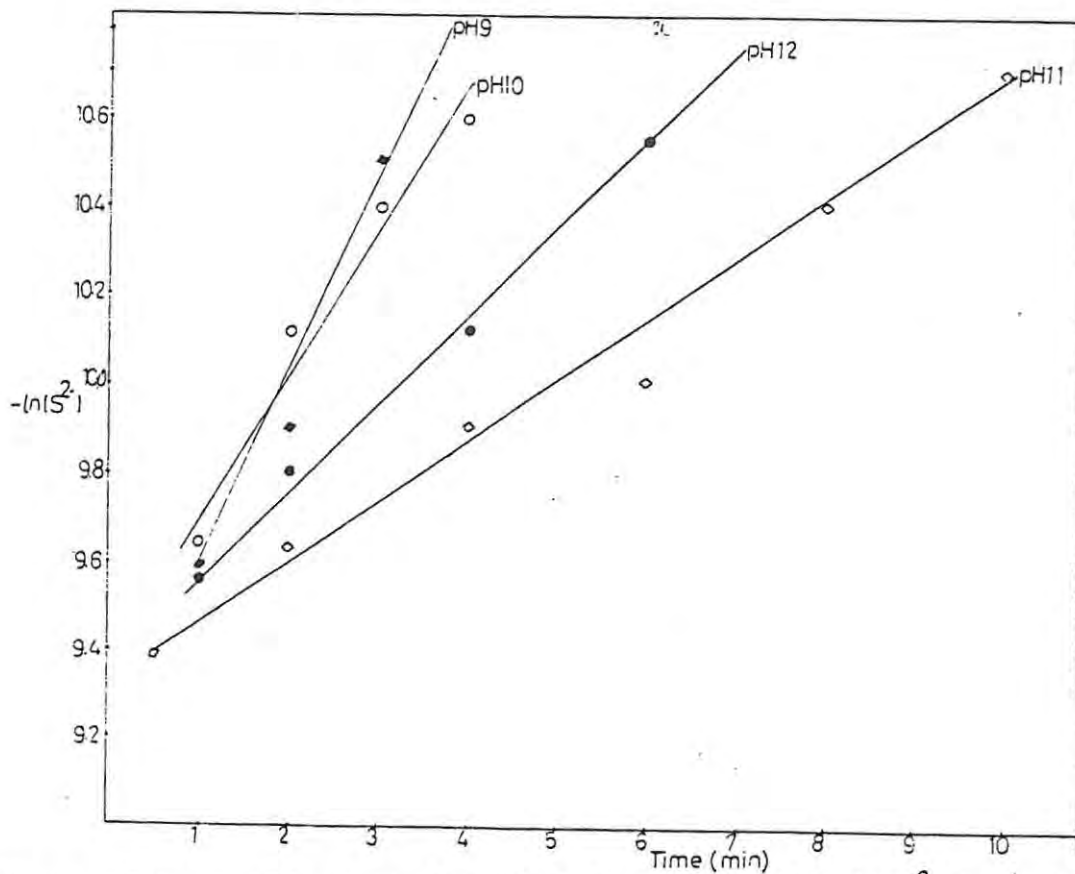


Figure.17. First order plot for sulphide interaction with CuO. Initials $[S^{2-}] = 1 \times 10^{-4}$ mol/l.

The rate of sulphide uptake when CuO particles were conditioned with 1×10^{-3} mol/l sulphide (Fig.18) seemed to have been more influenced by the mineral solubility in that the minimum rate of uptake was obtained at pH 10. Semilogarithmic plots of the concentration of sulphide against time were also linear. If the reaction was a true first order reaction it would be expected that the rate constant would be independent of the initial sulphide concentration. However this is not the case when the rate constants are compared for the initial concentrations of 1×10^{-4} mol/l and 1×10^{-3} mol/l sulphide. Consequently the extent of the reaction can best be expressed as reaction velocities rather than rate constants. The variation of these reaction velocities with pH are shown in Fig.19.

The bulk precipitate results obtained after sulphidization using 1×10^{-3} mol/l sulphide are given in Fig. 20. As can be seen, the bulk precipitate was less than 8% of the initial sulphide concentration used and did not vary significantly over the pH range examined.

Copper(II) oxide particles produced after sulphidization when 1×10^{-4} mol/l sulphide was used, were viewed under the scanning electron microscope (micrograph 1).

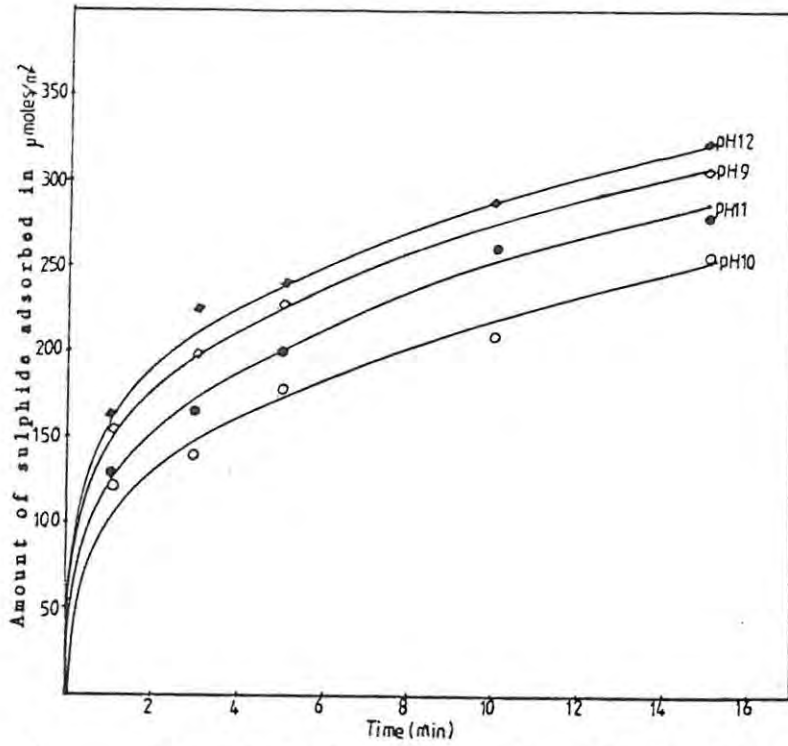


Figure.18. Kinetics of sulphide uptake on CuO at various pH values. 1×10^{-3} mol/l sulphide was used.

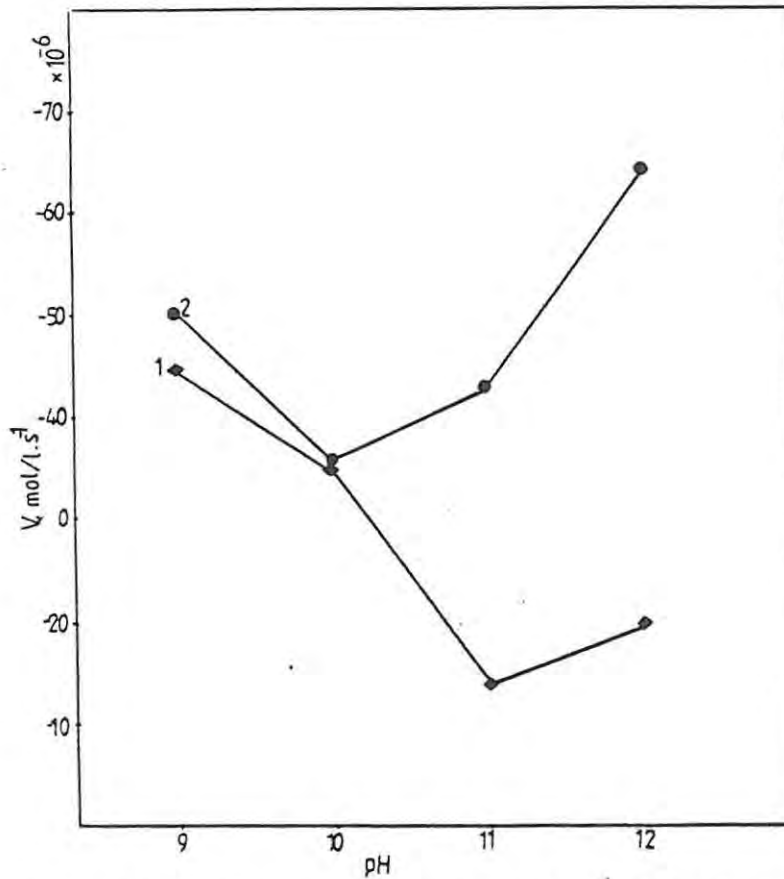
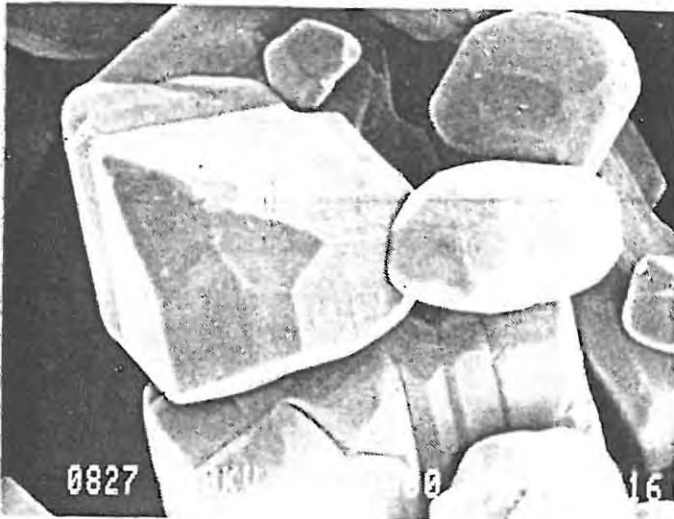


Figure.19. Variation with pH of the reaction velocities.
 1) after conditioning CuO with 1×10^{-4} mol/l sulphide.
 2) after conditioning CuO with 1×10^{-3} mol/l sulphide.

As can be seen from the micrograph very few crystallites of CuS can be identified on the surface. This was partly because the sulphide concentration used is very low and in fact the maximum possible sulphide adsorption is only equivalent to 2 monolayers. This was calculated on the assumption that one molecule of HS^- can occupy 10 \AA^2 (29). The micrograph shown here is for a sample that was treated with 1×10^{-4} mol/l sulphide at pH 9. The same feature were also observed for samples treated at higher pH values. When the sulphide concentration was increased tenfold (1×10^{-3} mol/l sulphide) the sulphidized particles produced showed a non-uniform coverage of the CuO particles by sulphide (micrographs 2 and 3 for sulphidization conducted at pH 9 and 10 respectively).

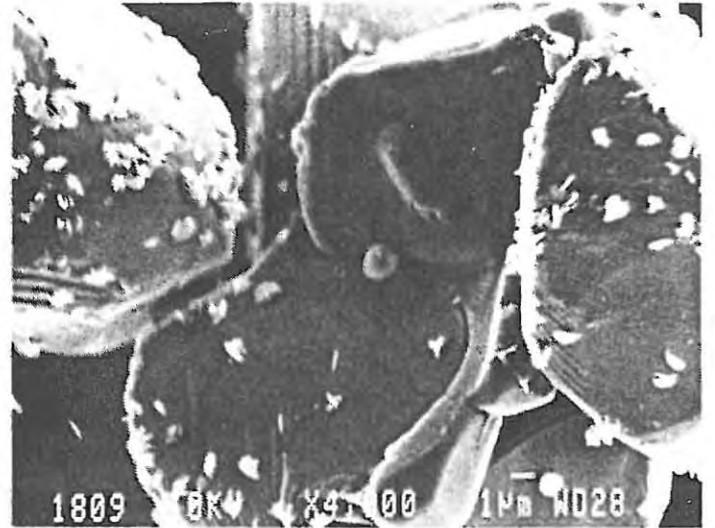
3.2.3. Kinetics of sulphide uptake on CuO in the presence of Ca^{2+} and Mg^{2+} .

The rate of sulphide uptake on CuO was found to be affected by the presence of both Ca^{2+} and Mg^{2+} . The rate was reduced by the presence of Ca^{2+} or Mg^{2+} (Fig. 21 and Fig. 22 respectively) when 1×10^{-4} mol/l sulphide was used.



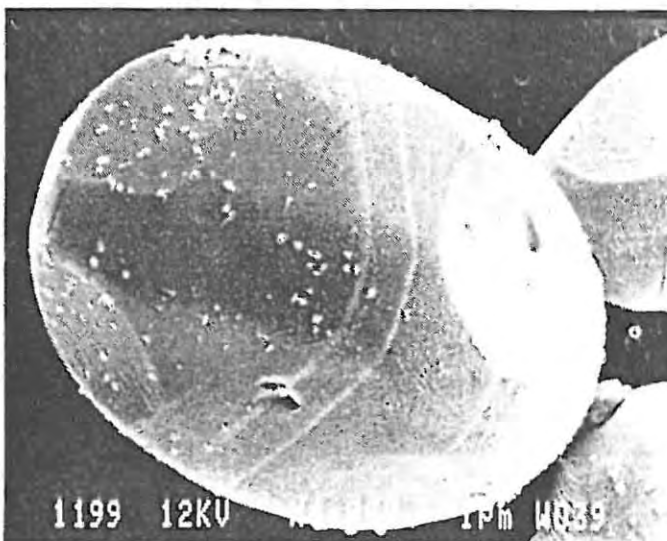
Micrograph.1.

CuO conditioned with 1×10^{-4} mol/l sulphide at pH 9.



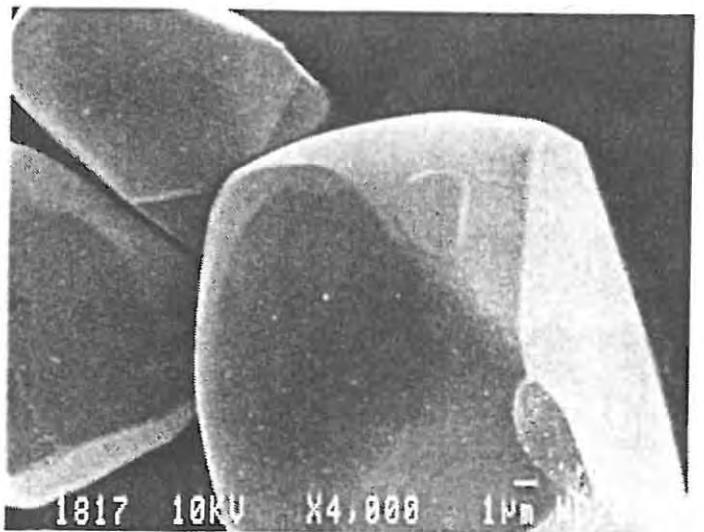
Micrograph.2.

CuO conditioned with 1×10^{-3} mol/l sulphide at pH 9.



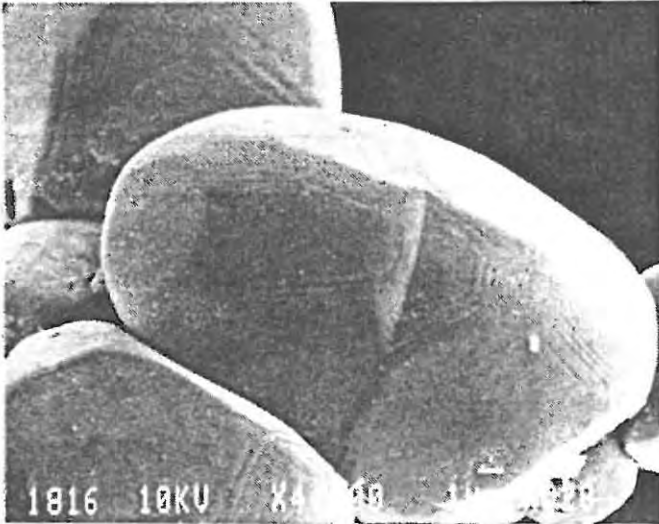
Micrograph.3.

CuO conditioned with 1×10^{-3} mol/l sulphide at pH 10.



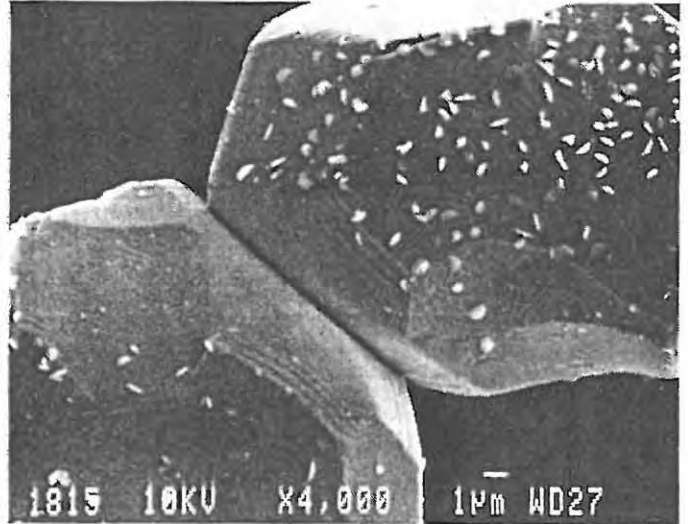
Micrograph.4.

CuO conditioned with 1×10^{-4} mol/l sulphide at pH 9 in the presence of 1.25×10^{-3} mol/l Ca^{2+} .



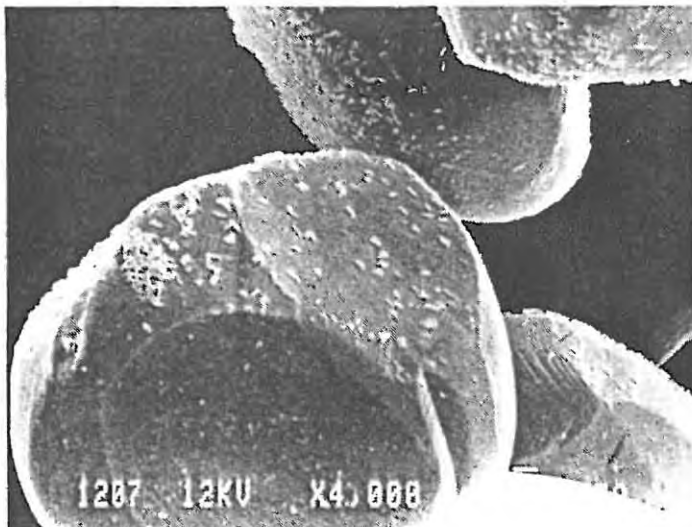
Micrograph.5.

CuO conditioned with 1×10^{-4} mol/l sulphide at pH 9 in the presence of 2.06×10^{-3} mol/l Mg^{2+}



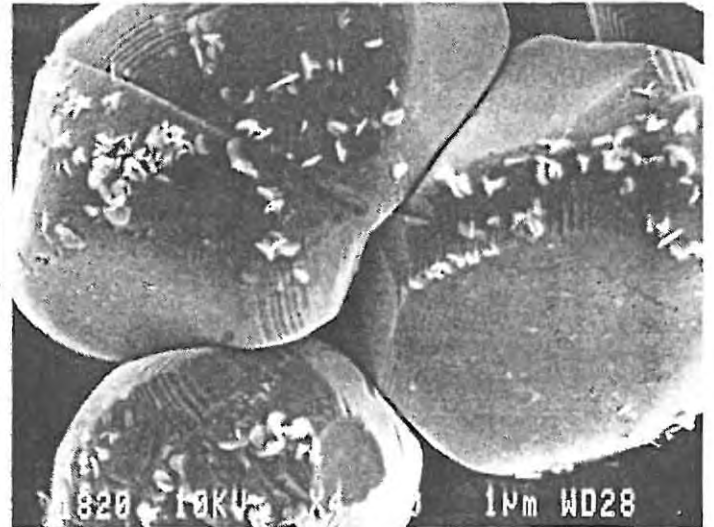
Micrograph.6.

CuO conditioned with 1×10^{-3} mol/l sulphide at pH 9 in the presence of 1.25×10^{-3} mol/l Ca^{2+} .



Micrograph.7.

CuO conditioned with 1×10^{-3} mol/l sulphide at pH 9 in the presence of 2.06×10^{-3} mol/l Mg^{2+} .



Micrograph.8.

CuO conditioned with 1×10^{-3} mol/l sulphide at pH 10 in the presence of 1.25 mol/l Ca^{2+} .

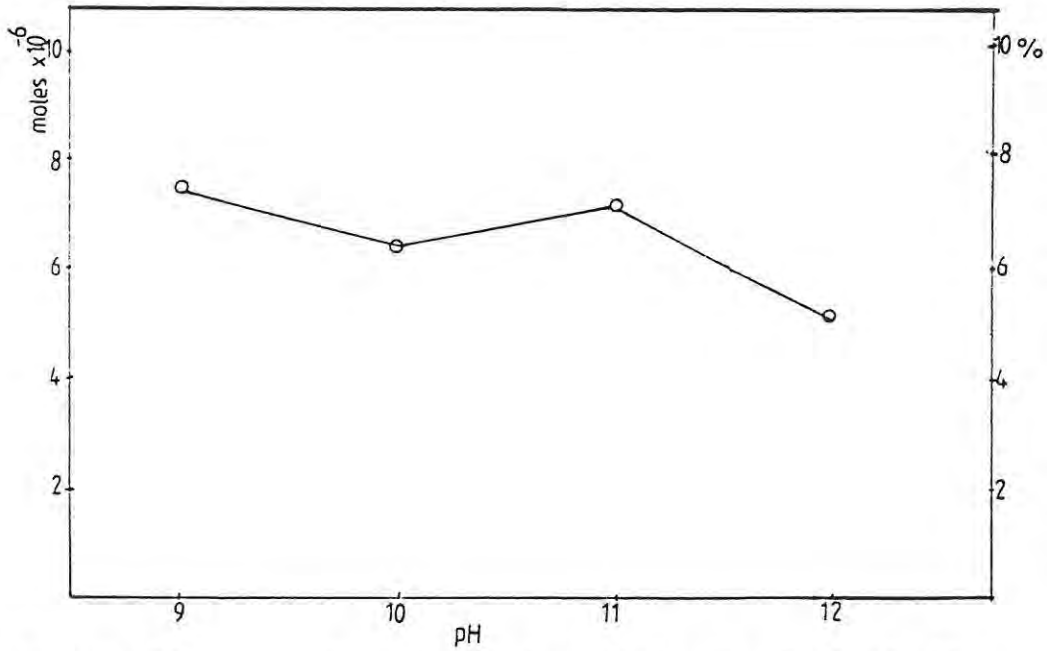


Figure.20. The variation with pH of the bulk precipitate after sulphidization using 1×10^{-3} mol/l sulphide. The bulk precipitate is also represented as % of initial concentration.

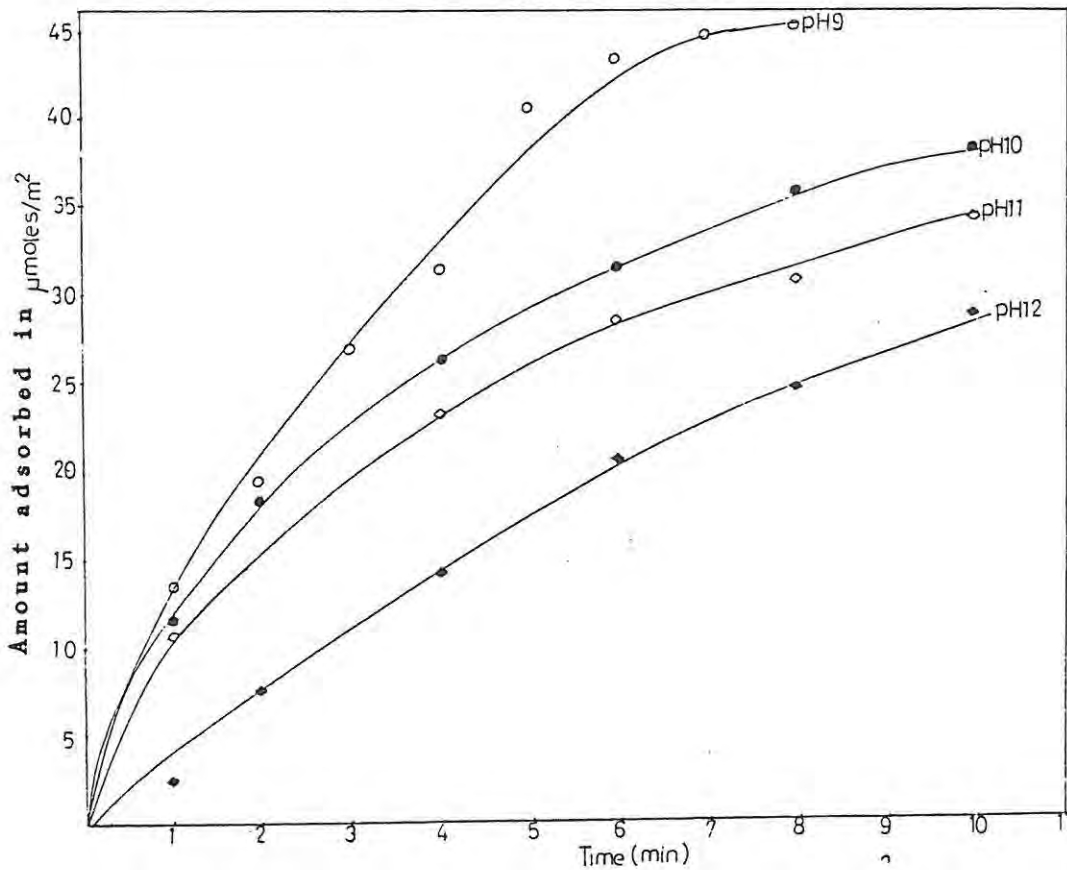


Figure.21. Kinetics of sulphide uptake on CuO in the presence 1.25×10^{-3} mol/l Ca^{2+} at various pH values. 1×10^{-4} mol/l sulphide was used.

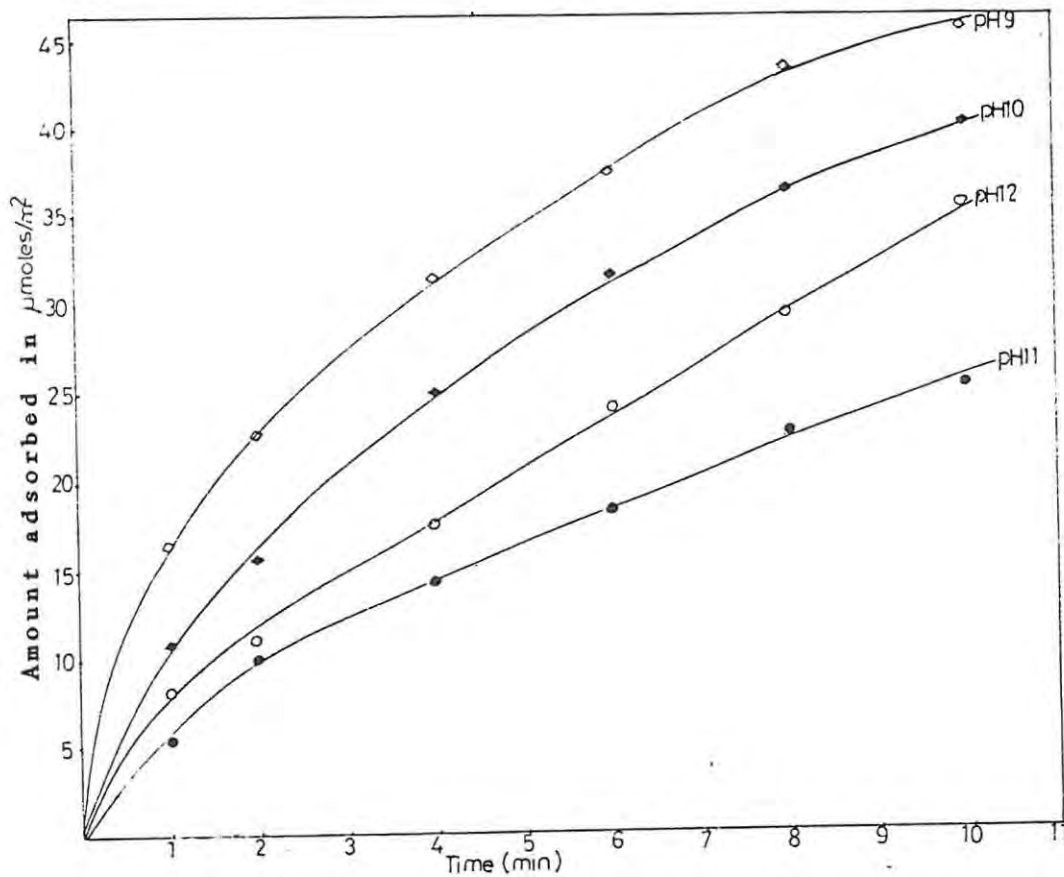


Figure.22. Kinetics uptake on CuO in the presence of $2.06 \times 10^{-3} \text{ mol/l Mg}^{2+}$ at various pH $1 \times 10^{-4} \text{ mol/l}$ sulphide was used.

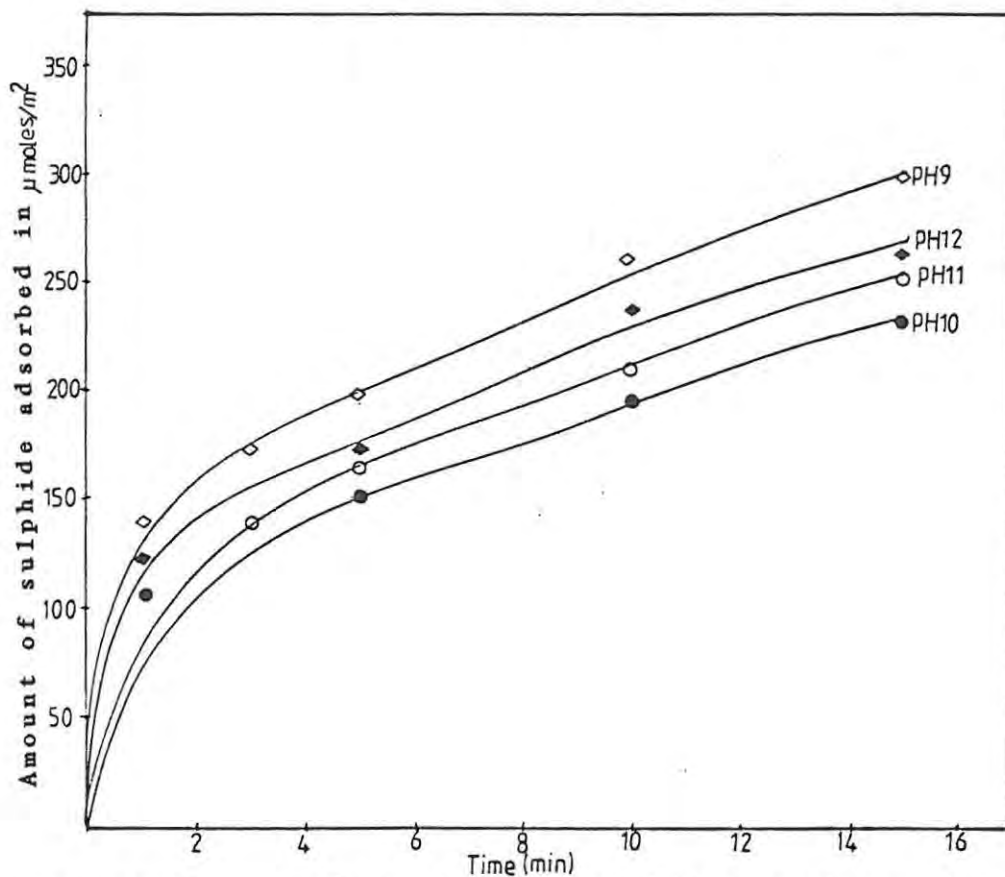


Figure.23. Kinetics of sulphide uptake on CuO in the presence of $1.25 \times 10^{-3} \text{ mol/l Ca}^{2+}$ at various pH values. $1 \times 10^{-3} \text{ mol/l}$ sulphide was used.

The rate of sulphide uptake was slightly reduced by the presence of these metal ions when 1×10^{-3} mol/l sulphide was used (Fig.23 and 24).

Semilogarithmic plots of the concentration of sulphide against time for experiments conducted in the presence of Ca^{2+} or Mg^{2+} were reasonably linear under various pH values considered. The variation in reaction velocities with pH are shown in Fig.25. In the presence of Ca^{2+} the rate was found to decrease as the pH was increased at 1×10^{-4} mol/l sulphide. Similar trends were observed in the presence of Mg^{2+} except that the rate was higher at pH 12 than pH 11. At the higher sulphide concentration of 1×10^{-3} mol/l the Ca^{2+} and Mg^{2+} ions had little effect on the rate of sulphide adsorption.

The bulk precipitate results obtained after sulphidization using 1×10^{-3} mol/l sulphide in the presence of these metal ions are given in Fig.26. The amount of bulk precipitate formed in the presence of Ca^{2+} ions was only reduced at pH 12. However, in the presence of Mg^{2+} ions the amount of bulk precipitate was reduced at all pH values (Cf Fig.20.)

Copper (II) oxide particles produced after sulphidization using 1×10^{-4} mol/l sulphide, showed very few crystallites of CuS on the

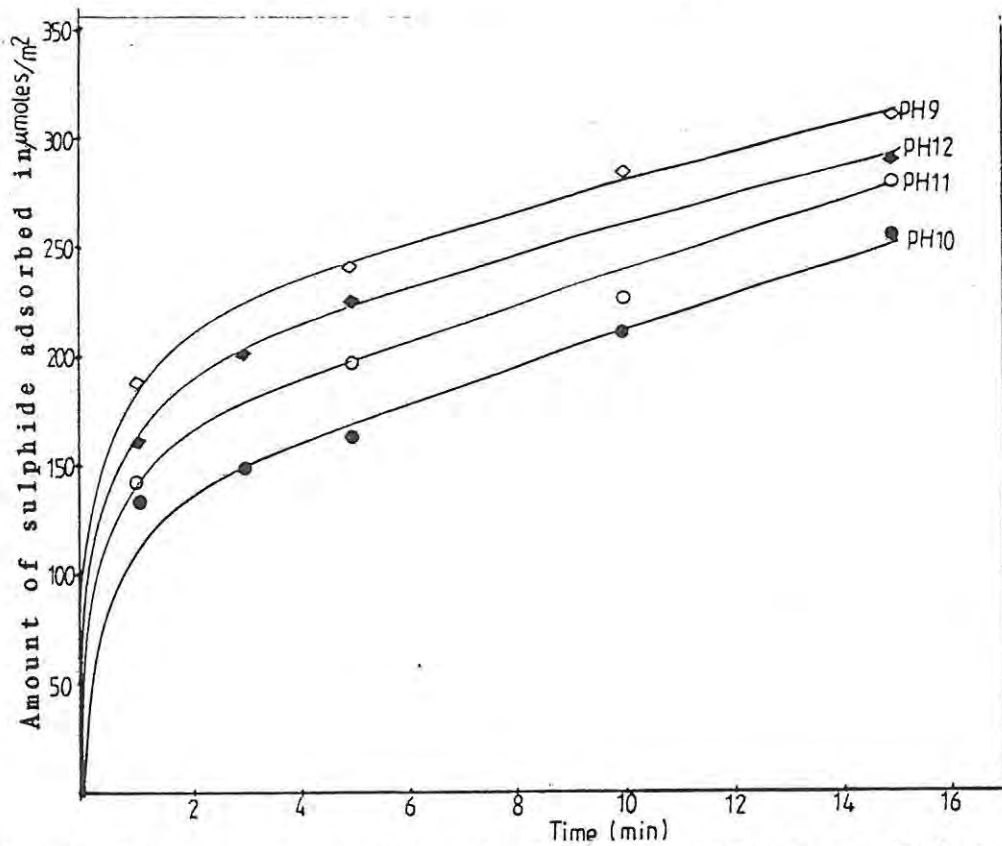


Figure.24. Kinetics of sulphide uptake on CuO in the presence of $2.06 \times 10^{-3} \text{ mol/l Mg}^{2+}$ at various pH values. $1 \times 10^{-3} \text{ mol/l}$ sulphide was used.

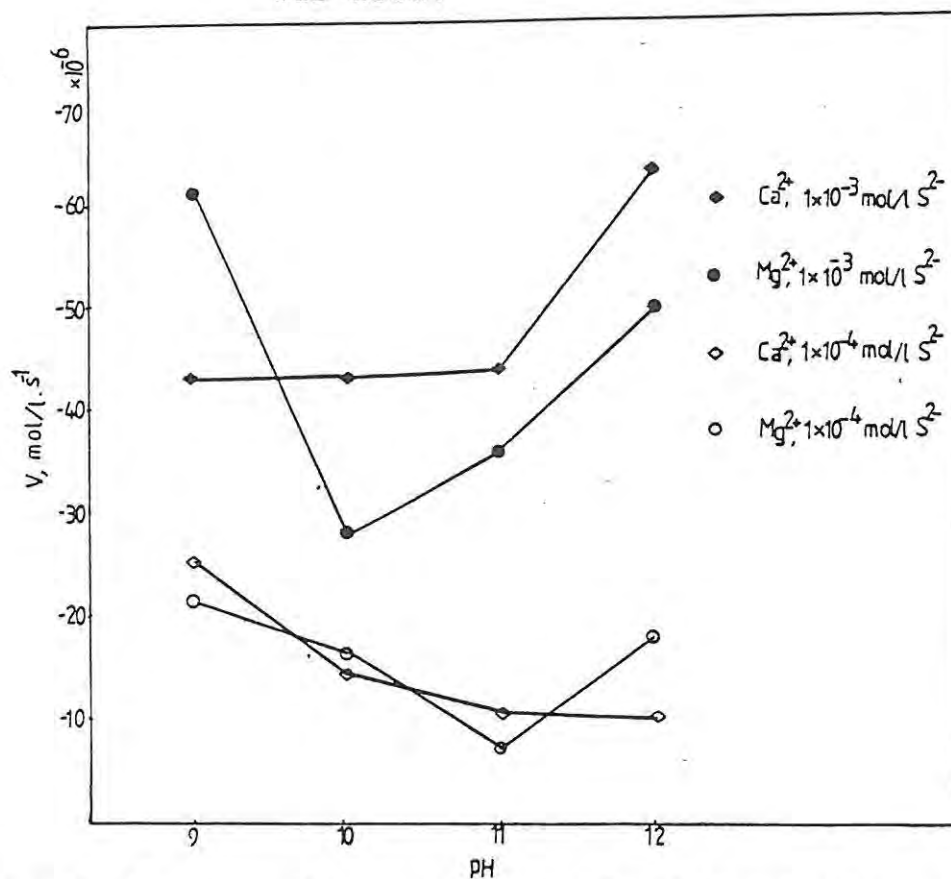


Figure.25. Variation with pH of the reaction velocities after sulphidization in the presence of $1.25 \times 10^{-3} \text{ mol/l Ca}^{2+}$ and $2.06 \times 10^{-3} \text{ mol/l Mg}^{2+}$.

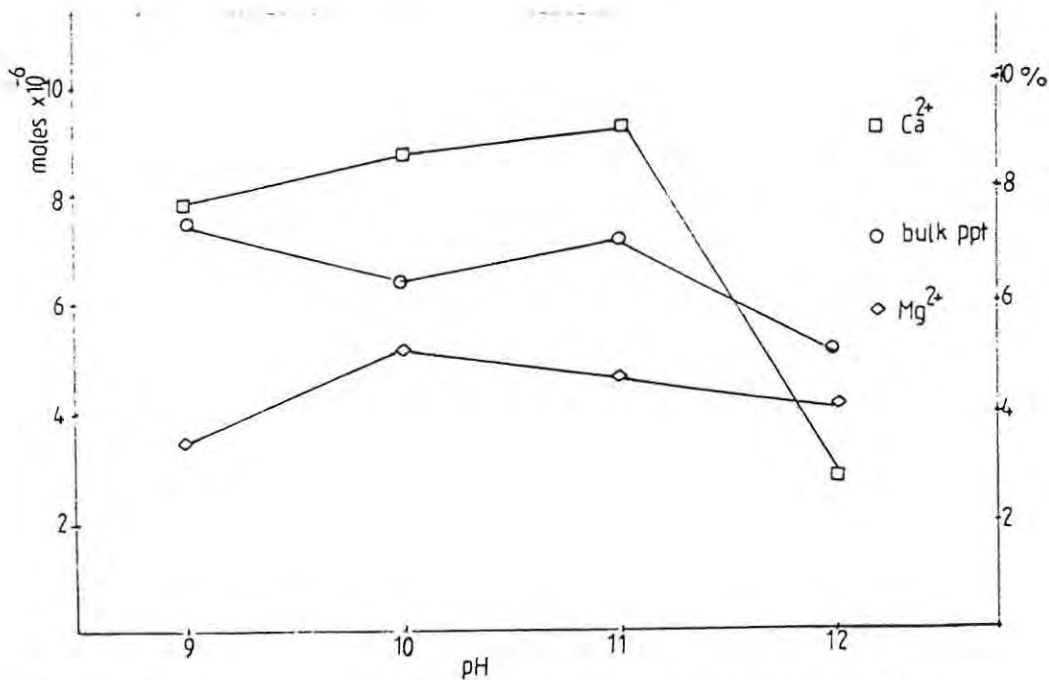


Figure.26. Variation with pH, of the bulk precipitate after sulphidization in the presence of Ca^{2+} and Mg^{2+} using 1×10^{-3} mol/l sulphide. The bulk precipitate is also represented as % of the initial sulphide concentration.

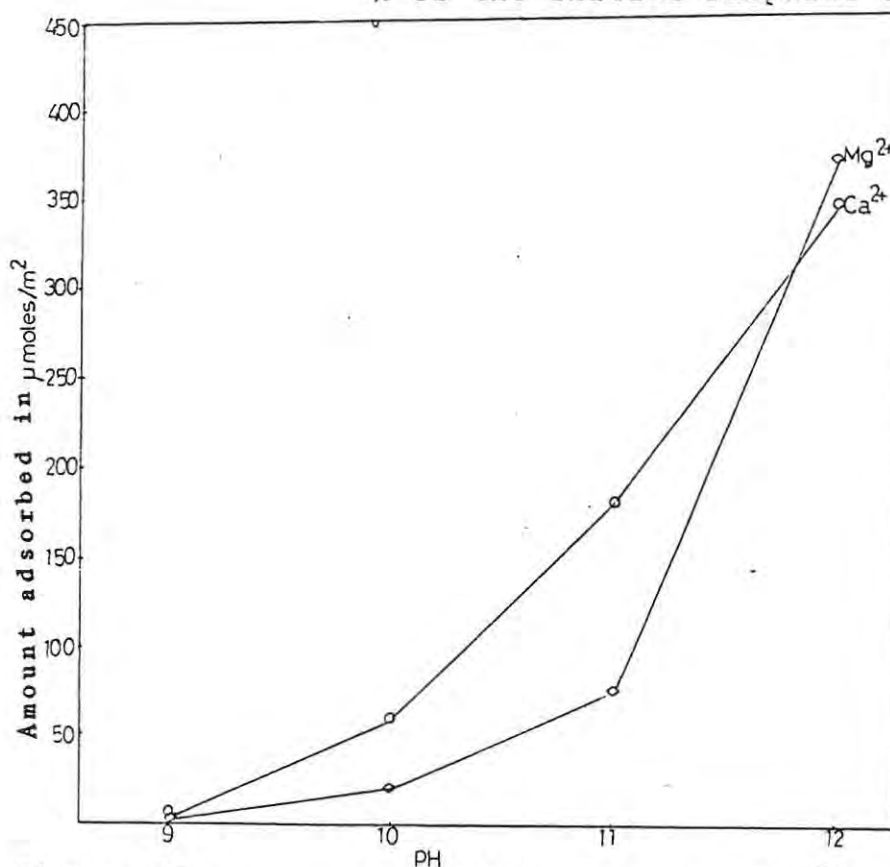
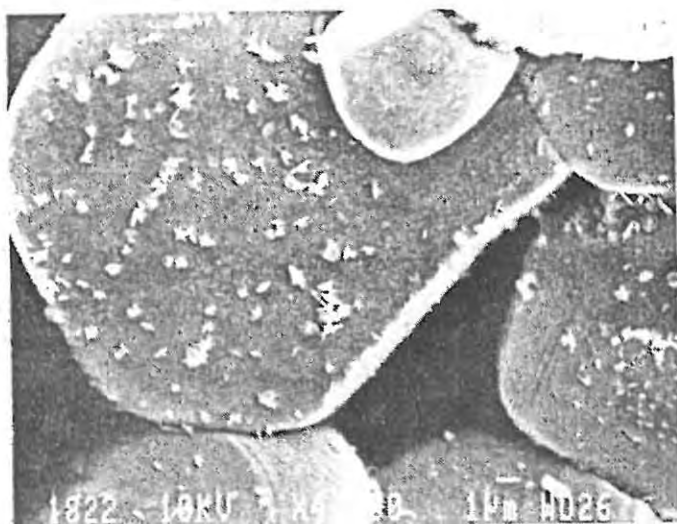


Figure.27. Variation with pH of Ca^{2+} and Mg^{2+} uptake on CuO after 1 hour conditioning with 1.25×10^{-3} mol/l Ca^{2+} and 2.06×10^{-3} mol/l Mg^{2+} .

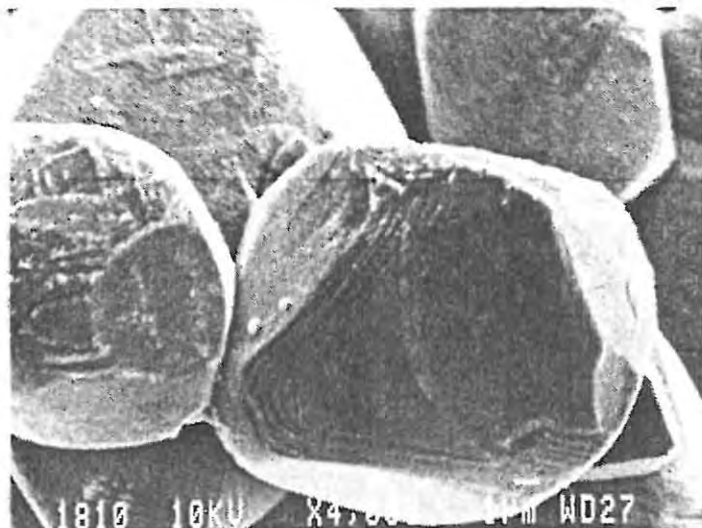
surface when viewed under the scanning electron microscope (micrographs 4 and 5). The particles produced when CuO was sulphidized using 1×10^{-3} mol/l sulphide showed a non-uniform coverage by sulphide (micrographs 6 and 7 for sulphidization at pH 9 and micrographs 8 and 9 for sulphidization at pH 10). The formation of the small crystallites does not appear to be influenced by the presence of Ca^{2+} and Mg^{2+} ions.

Experimental evidence given in Fig. 27 for the adsorption of Ca^{2+} or Mg^{2+} on CuO showed that the amount of Ca^{2+} and Mg^{2+} adsorbed increased with an increase in pH value. This suggests that the reduction in rate can be caused by the presence of calcium or magnesium species present on the oxide surface. A further consideration of the adsorption results given in Fig. 27 indicate that adsorption of these metal ions, for example at pH 10, is higher than the $7 \mu\text{mol}/\text{m}^2$ which is equivalent to one monolayer if the metal ion adsorbed is considered to be in the form of first hydroxy species (the monolayer value was calculated on the assumption that Mg^{2+} and Ca^{2+} molecules occupies 5 \AA^2). Part of the overall high uptake of these metal ions may be due to the formation of their respective carbonates because the mineral CuO was recrystallized by heating in the presence of Na_2CO_3 and the



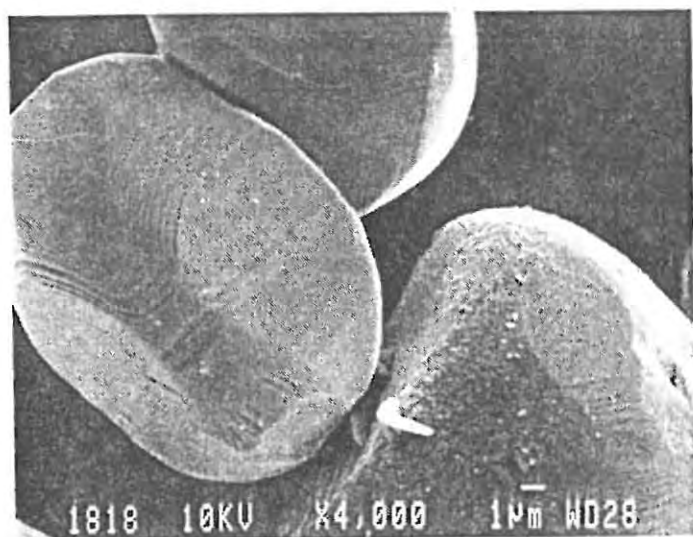
Micrograph.9.

CuO conditioned with 1×10^{-3} mol/l sulphide at pH 10 in the presence of 2.06×10^{-3} mol/l Mg^{2+} .



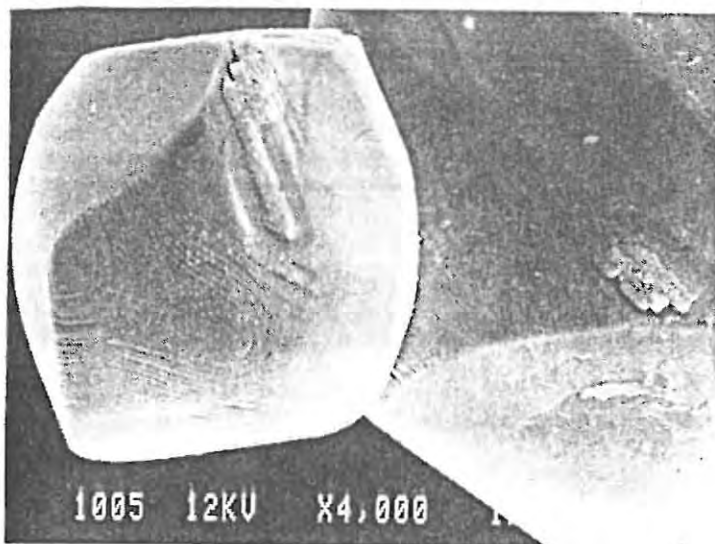
Micrograph.10.

CuO conditioned with 1×10^{-4} mol/l sulphide at pH 9 in the presence of 50ppm starch.



Micrograph.11.

CuO conditioned with 1×10^{-4} mol/l sulphide at pH 9 in the presence of 50ppm gum arabic.



Micrograph.12.

CuO conditioned with 1×10^{-4} mol/l sulphide at pH 9 in the presence of 50ppm Triton X-100.

possibility of having traces of CO_3^{2-} after washing cannot be ruled out. The solubility product of MgCO_3 ($K_{sp} = 10^{-7.5}$ (61)) and CaCO_3 ($K_{sp} = 10^{-7.5}$ (61)) decreases with an increase in pH. However, it must be remembered that these adsorptions were carried out in the absence of sulphide and the presence of sulphide ions may significantly reduce the amount adsorbed.

3.2.4. Kinetics of sulphide uptake on CuO in the presence of starch, gum arabic and Triton X-100.

Fig. 28, 29 and 30 show how the consumption of sulphide varies with time in the presence of 50 ppm of starch, gum arabic and Triton X-100 at pH values between 9 and 12 when CuO particles are conditioned with 1×10^{-4} mol/l sulphide.

Linear semilogarithmic plots of the concentration of sulphide against time were obtained at all pH values in the presence of starch and gum arabic. However, in the presence of Triton X-100 linear plots were not obtained since, as can be seen in Fig. 30, the reaction of sulphide appeared to cease after approximately 2 minutes of reaction (Fig. 30). This suggests that the Triton X-100 adsorbs very strongly on the CuO.

The effect on the rate of sulphide uptake on CuO when 1×10^{-3} mol/l sulphide was used in the

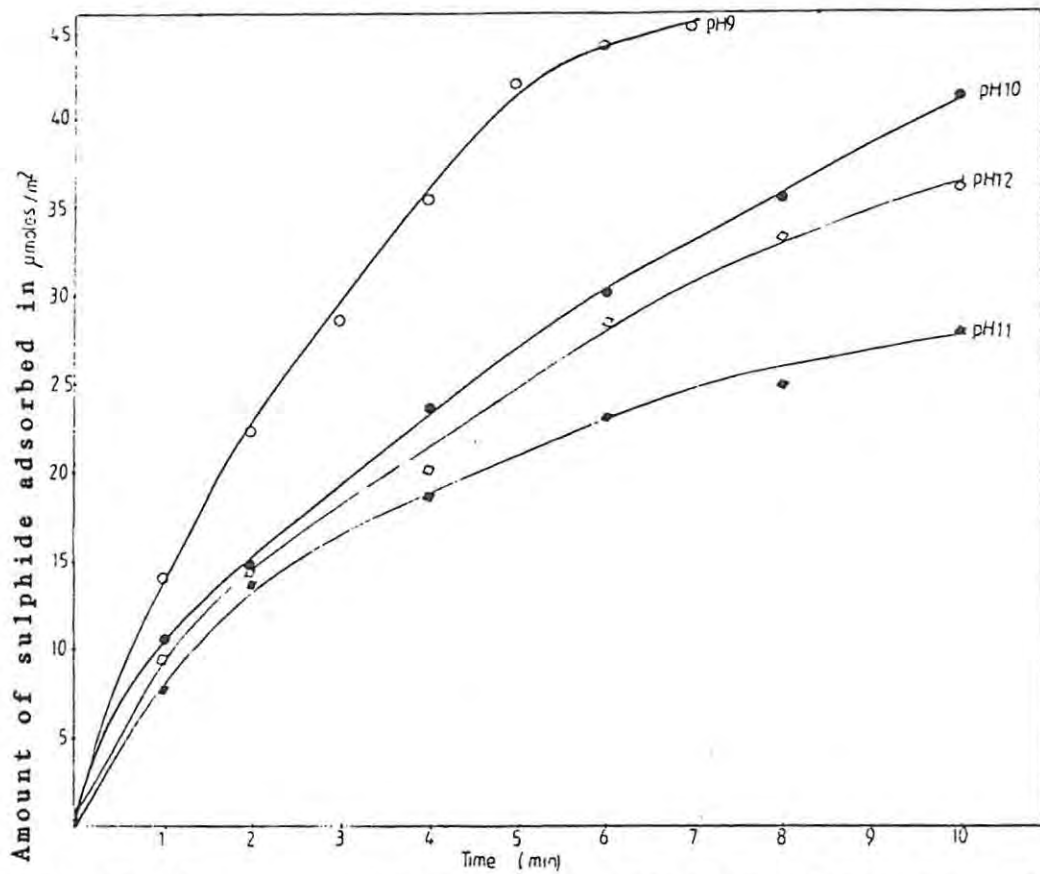


Figure.28. Kinetics of sulphide uptake on CuO in the presence of 50ppm starch. Initial $[\text{S}^{2-}] = 1 \times 10^{-4} \text{ mol/l}$.

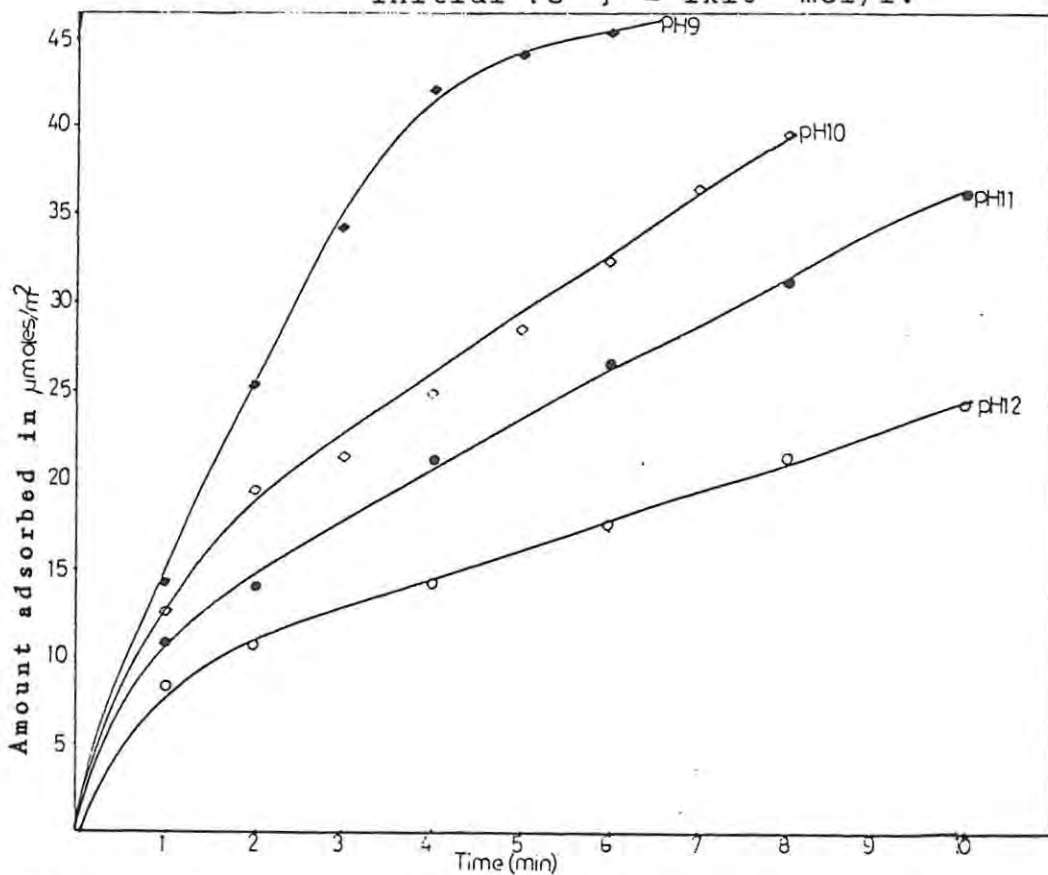


Figure.29. Kinetics of sulphide uptake on CuO in the presence of 50ppm gum arabic. Initial $[\text{S}^{2-}] = 1 \times 10^{-4} \text{ mol/l}$.

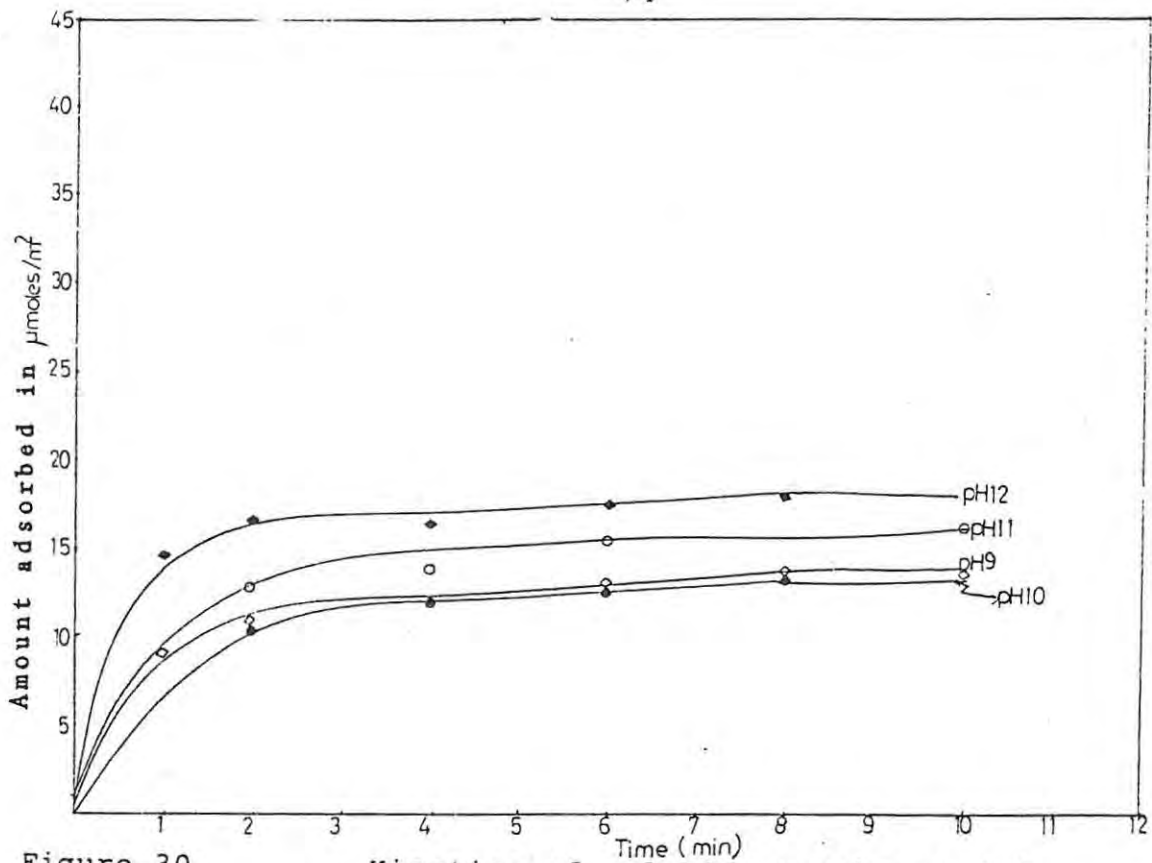


Figure.30. Kinetics of sulphide uptake on CuO
in the presence of 50ppm Triton X-100.
Initial $[S^{2-}] = 1 \times 10^{-4}$ mol/l.

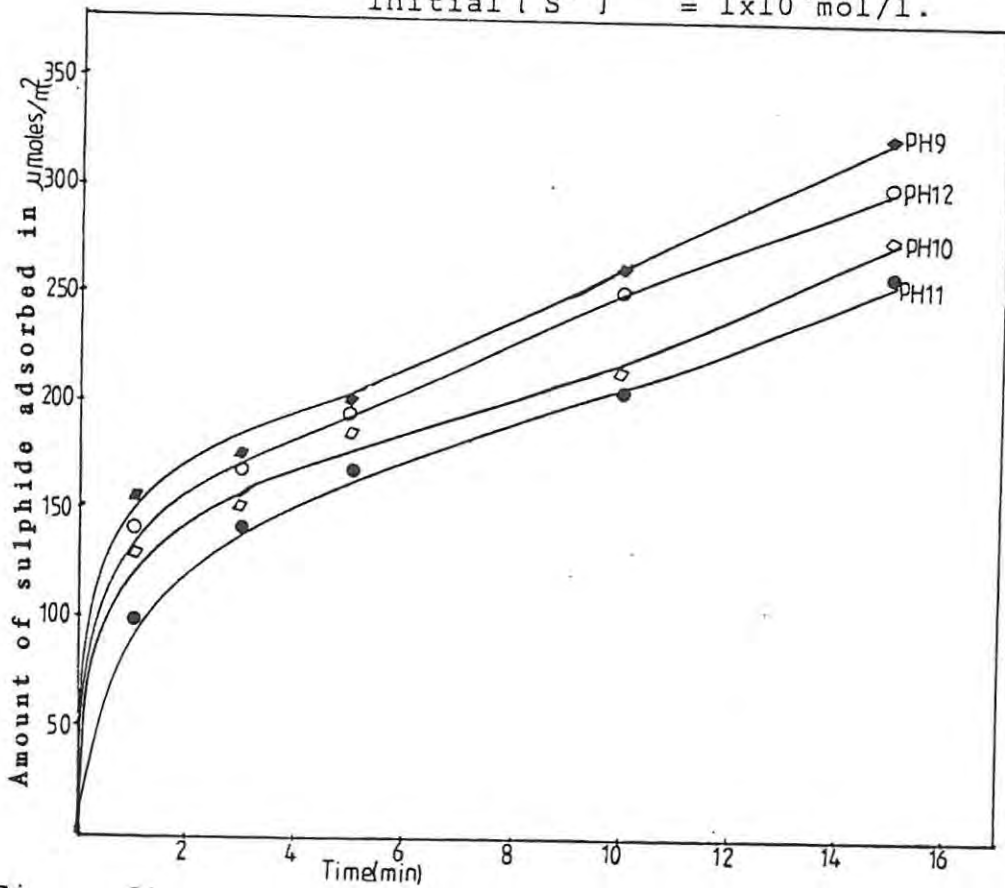


Figure.31. Kinetics of sulphide uptake on CuO in
the presence of 50ppm starch.
 1×10^{-3} mol/l sulphide was used.

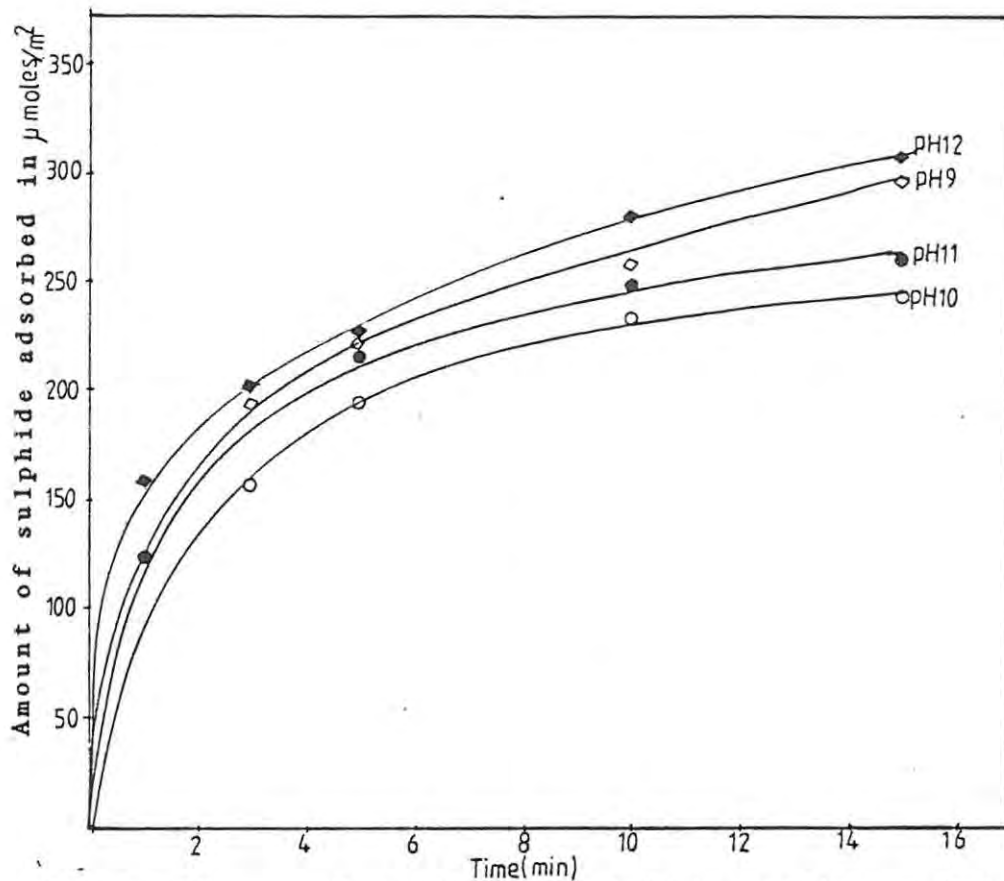


Figure.32. Kinetics of sulphide uptake on CuO in the presence of 50ppm gum arabic. 1×10^{-3} mol/l sulphide was used.

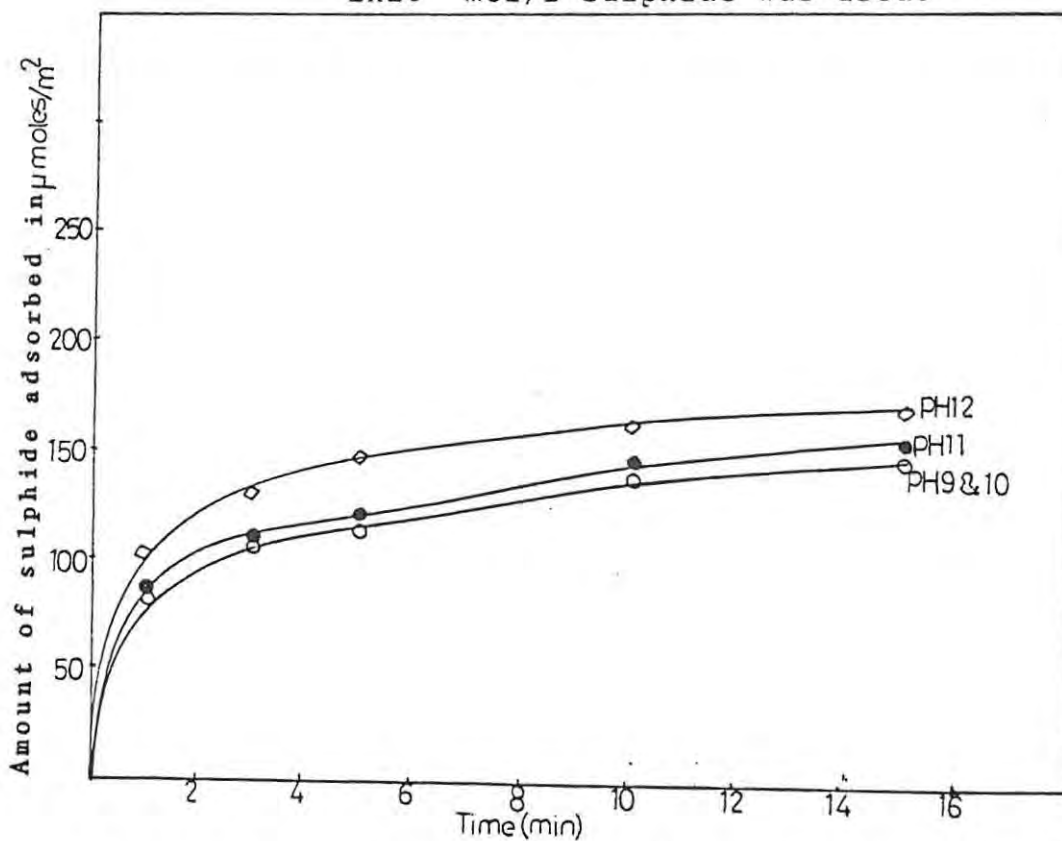


Figure.33. Kinetics of sulphide uptake on CuO in the presence of 50ppm Triton X-100. 1×10^{-3} mol/l sulphide was used.

presence of starch, gum arabic and Triton X-100 are shown respectively in Figs. 31, 32 and 33. Again, linear semilogarithmic plots of the concentration of sulphide against time were obtained at all pH values for starch and gum arabic. In the case of Triton X-100 the plots were also reasonably linear since the reaction, although very much slower, was continuous throughout the duration of the experiment. The variation of the reaction velocities with pH are shown in Fig. 34 for both low and high sulphide concentrations. It should be noted that the reaction velocities could not be established for Triton X-100 at 1×10^{-4} mol/l sulphide. In the presence of starch, the rate of sulphide uptake is significantly reduced at all pH values compared to sulphide alone. At pH 12, the rate of sulphide abstraction was higher than that obtained at pH 11. In the presence of gum arabic, the rate at pH 9 was enhanced while that at pH 10 was markedly reduced. At pH 11 there was very little change and at pH 12 the rate of adsorption was very low (less than pH 11). In the presence of gum arabic, the rate at pH 9 was enhanced while that at pH 10 was markedly reduced. At pH 11 there was very little change and at pH 12 the rate of adsorption was very low (less than pH 11).

The rates of sulphide uptake on CuO in the presence of starch and gum arabic when 1×10^{-3} mol/l sulphide was used, are also shown in Fig. 34.

It can be seen from these curves that the rate of sulphide uptake is not significantly affected by the presence of these polymers. However, in the presence of Triton X-100 the rate of reaction is markedly reduced probably at the lower pH values.

The results for bulk precipitate obtained when solid samples were conditioned with sulphide (1×10^{-3} mol/l) in the presence of starch, Triton X-100 and gum arabic are shown in Fig. 35 only in the case of Triton X-100 was the amount of bulk precipitate reduced. The amount of bulk precipitate formed in the presence of gum arabic and starch was greater than found with sulphide alone. However, the amounts were always less than 10% of the sulphide present.

SEM results for CuO particles sulphidized when using 1×10^{-4} mol/l showed few copper sulphide crystallites that were adsorbed on the surface (micrographs 10, 11 and 12). Samples produced after conditioning with 1×10^{-3} mol/l sulphide in the presence of starch and gum arabic showed a non-uniform coverage of CuO surface by sulphide when viewed under the SEM (micrographs 13 and 14 for pH 9, and 15 and 16 for pH 10).

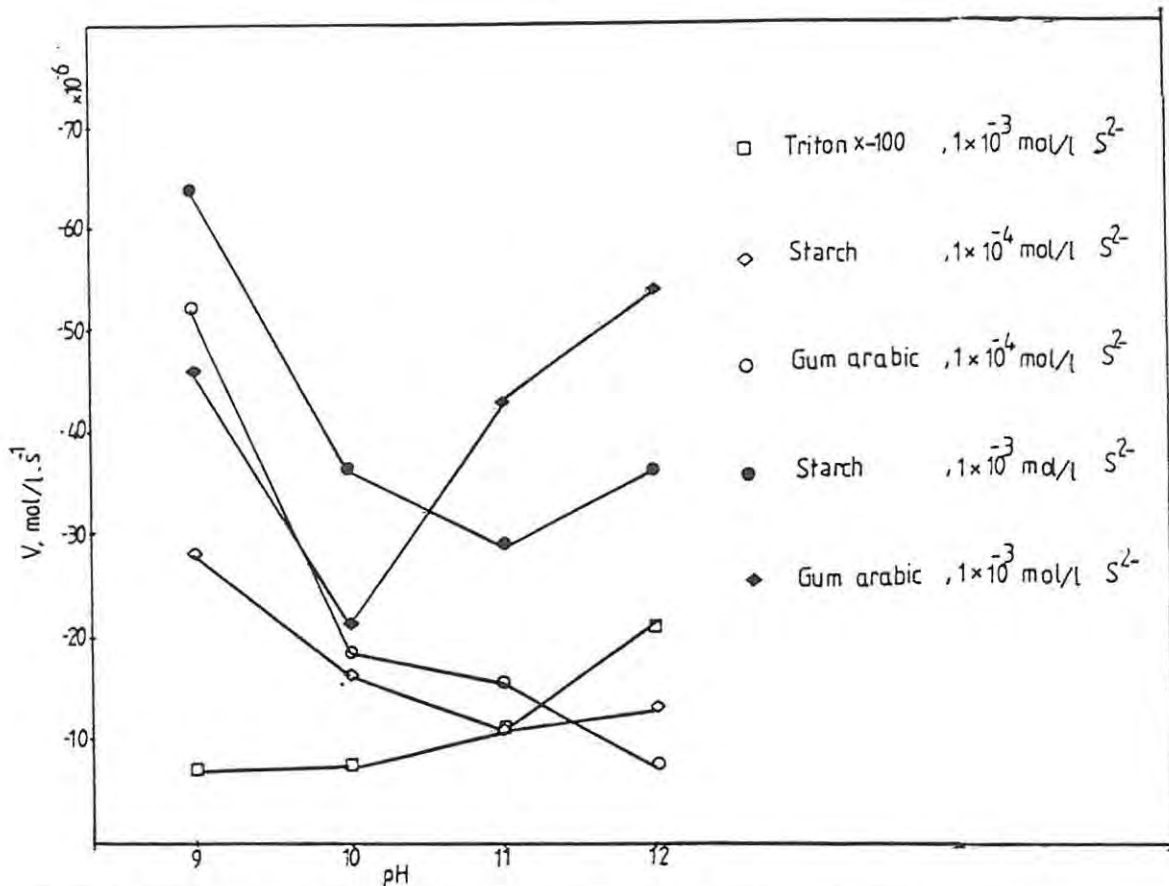


Figure.34. Variation with pH of the reaction velocities after sulphidization in the presence of 50ppm starch, gum arabic and Triton X-100.

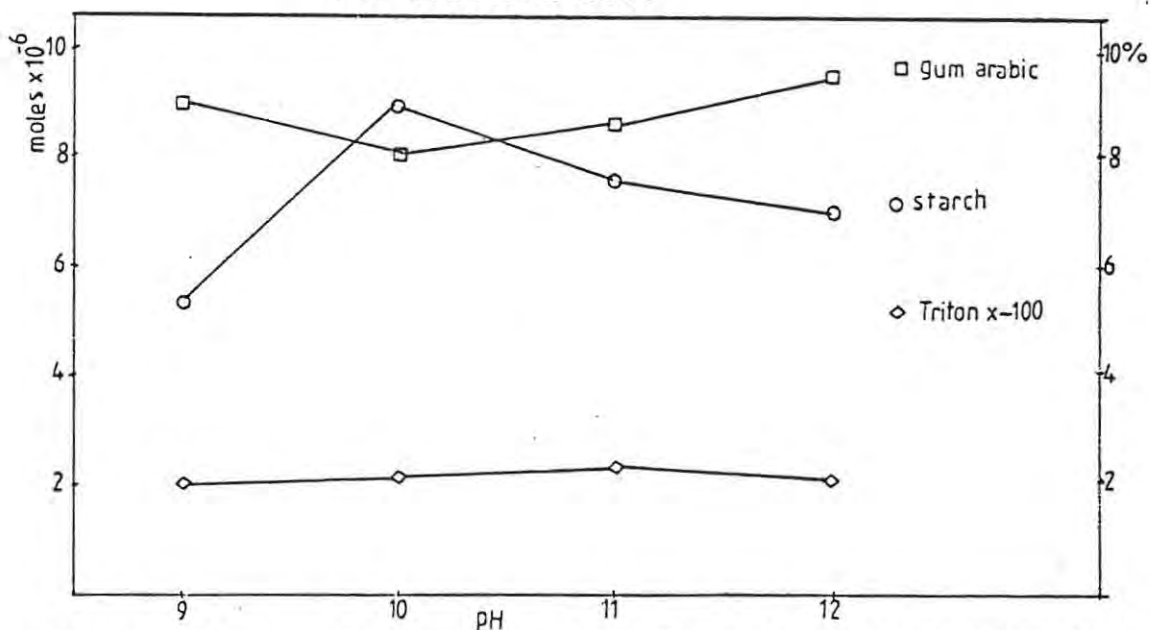
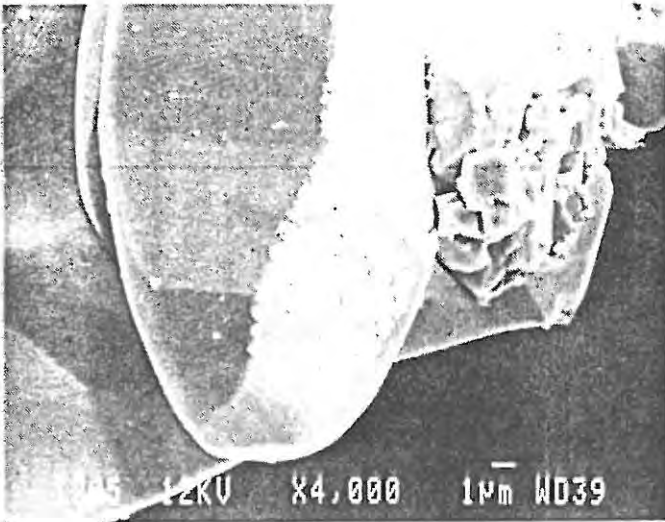


Figure.35. Variation with pH of the bulk precipitate after sulphidization in the presence of 50ppm starch, gum arabic and Triton X-100 using 1×10^{-3} mol/l sulphide. The bulk precipitate is also represented as % of the initial sulphide concentration.



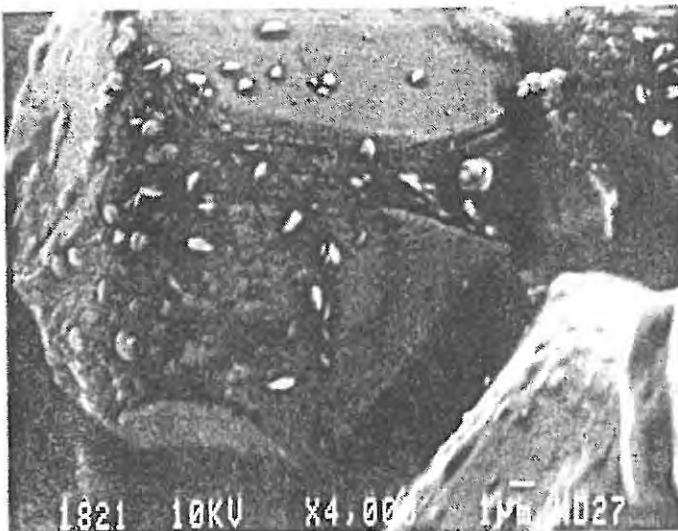
Micrograph.13.

CuO conditioned with 1×10^{-3} mol/l sulphide at pH 9 in the presence of 50ppm gum arabic.



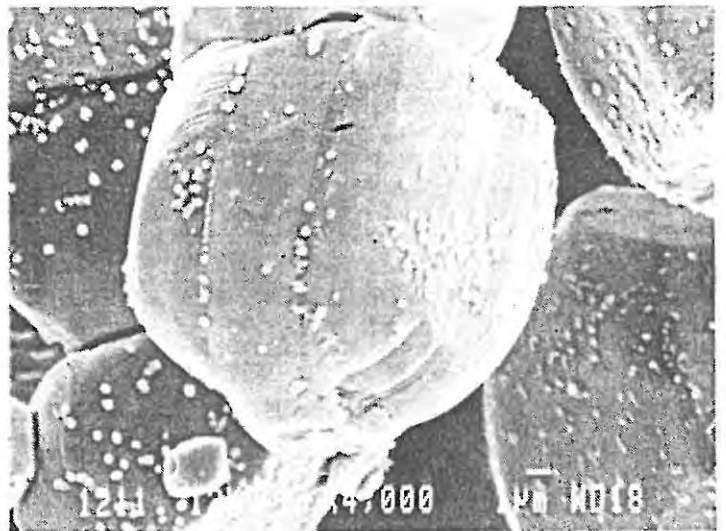
Micrograph.14.

CuO conditioned with 1×10^{-3} mol/l sulphide at pH 9 in the presence of 50ppm gum arabic.



Micrograph.15.

CuO conditioned with 1×10^{-3} mol/l sulphide at pH 10 in the presence of 50ppm starch.



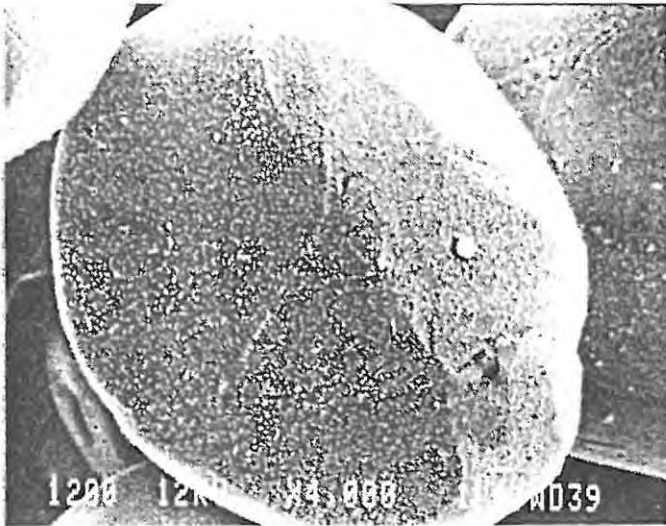
Micrograph.16.

CuO conditioned with 1×10^{-3} mol/l sulphide at pH 10 in the presence of 50ppm gum arabic.

Samples conditioned in the presence of Triton X-100, however, showed smaller CuS precipitate particles absorbed on the surface than those observed in the presence of starch and gum arabic (micrograph 17 for pH 9 and micrograph 18 for pH 10).

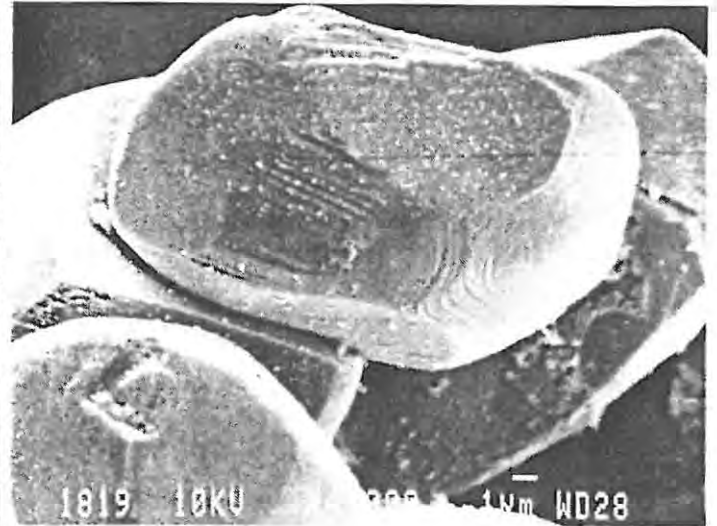
3.2.5. Reaction of xanthate with CuO sulphidized at pH 11.

In these reactions care was taken to prevent oxygen from entering the system before the sulphidized mineral was reacted with oxygen free xanthate. Results shown in Fig. 36 indicate that xanthate uptake was reduced when surface coverage by the sulphide was increased until a minimum value in the xanthate adsorbed was reached when a sample having approximately $1800 \mu\text{mol}/\text{m}^2$ sulphide adsorbed was used. At this point, xanthate uptake started to increase with an increase in sulphidization level. The various conditions under which xanthate experiments were conducted are shown in Table 1.



Micrograph.17.

CuO conditioned with 1×10^{-3} mol/l sulphide at pH 9 in the presence of 50ppm Triton X-100.



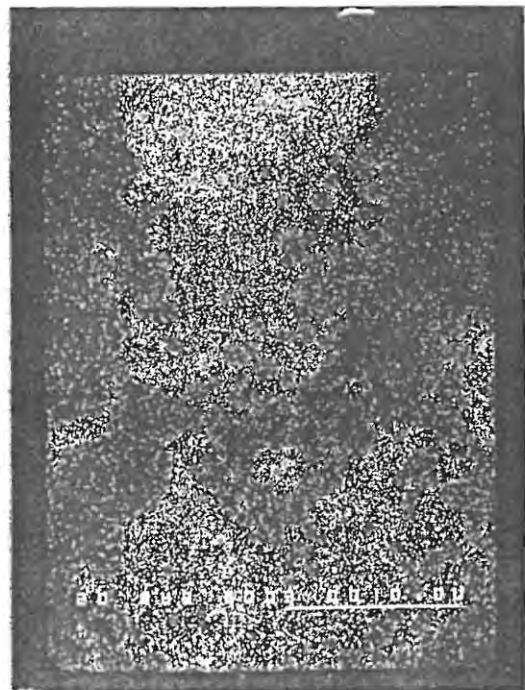
Micrograph.18.

CuO conditioned with 1×10^{-3} mol/l sulphide at pH 10 in the presence of 50ppm Triton X-100.



Micrograph.19.

CuO sulphidized with 1×10^{-3} mol/l sulphide at pH 12.



Micrograph.20.

X-Ray image for sulphur for micrograph 19.

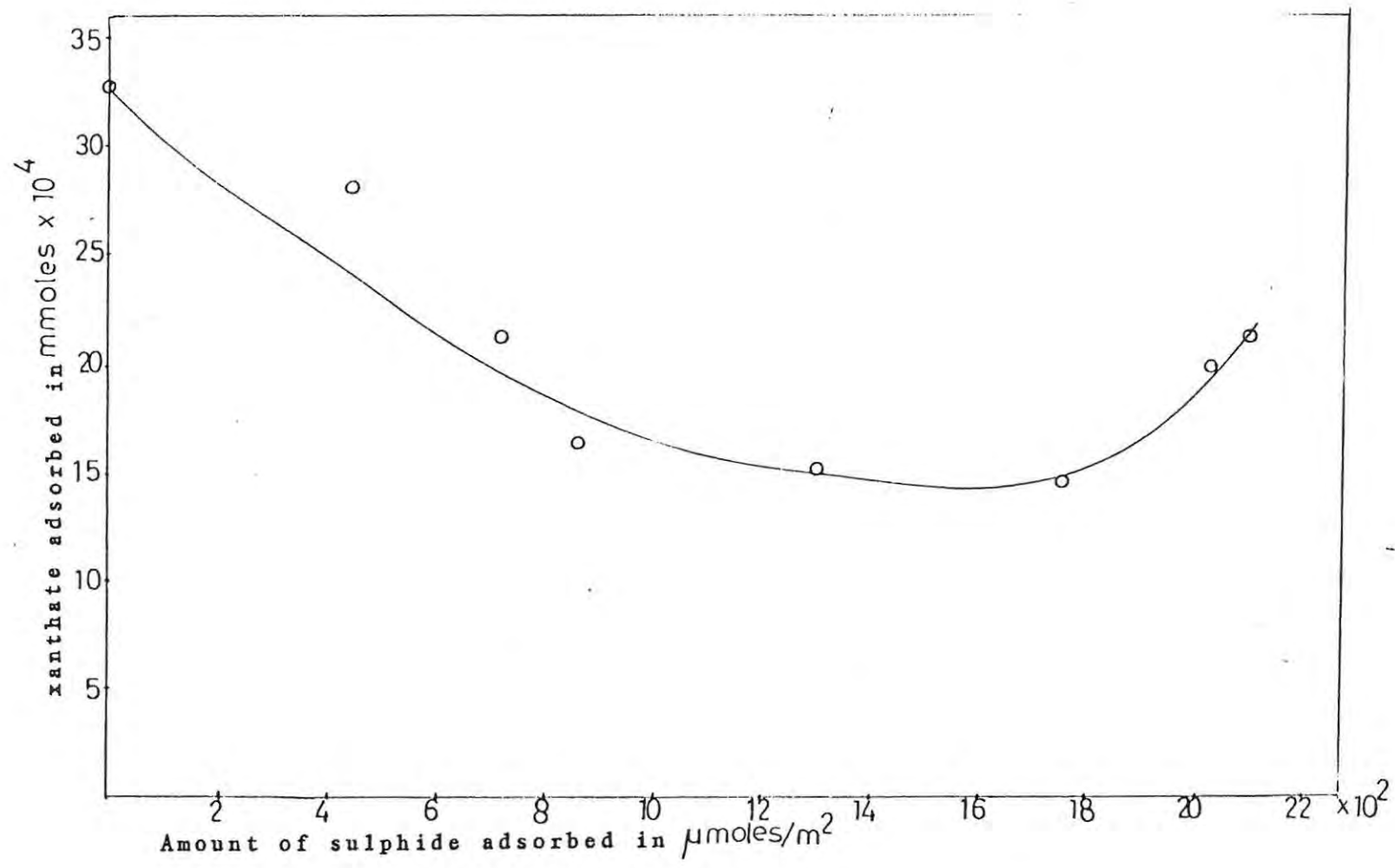


Figure.36. Variation in xanthate uptake on CuO with sulphidization level.

Table 1 Conditions under which xanthate experiments were conducted at pH 11 of sulphidization and pH 9 of xanthate reaction. 1g CuO with a surface area of $0.1\text{m}^2/\text{g}$ was used.

Initial $[\text{S}^{2-}] \times 10^{-4}$ in mol/l	$[\text{S}^{2-}]$ after 45 minutes	Amount of sulphide adsorbed $\mu\text{mol}/\text{m}^2$	Initial $[\text{X}^-]$ in mol/l $\times 10^{-5}$	Amount of xanthate adsorbed in mmoles $\times 10^{-4}$
0	-	-	5	32.68
4.55	0.0	455.00	5	28.32
7.28	0.0	760.00	5	21.09
9.11	5×10^{-5}	860.00	5	16.30
13.65	5.5×10^{-5}	1309.70	5	15.22
18.20	5.5×10^{-5}	1759.80	5	15.09
22.75	2.35×10^{-4}	2034.90	5	20.29
27.30	6.4×10^{-4}	2095.10	5	21.21

3.2.6 Discussion

Interesting facts that emerge from this work are that the rate of sulphide uptake on copper (II) oxide when 1×10^{-4} mol/l sulphide was used decreases as the pH value is increased from 9 to 11 and increases at pH 12 (Fig. 19), and that the rate is reduced (pH values greater than 9) by the presence of Ca^{2+} , Mg^{2+} , starch, gum arabic and Triton X-100 (Figs. 25 and 34). At higher sulphide concentration of 1×10^{-3} mol/l the rate of sulphide uptake increased with an increase in pH from pH 10 to 12 (Fig. 19). At this sulphide concentration, the rate was marginally reduced by the presence of Ca^{2+} , Mg^{2+} , starch, gum arabic (pH greater than 9) and Triton X-100. (Figs. 25 and 34.) Another finding was that CuO particles after sulphidization in the absence or presence of these compounds were found to have a non-uniform coverage by sulphide when 1×10^{-3} mol/l sulphide was used.

The decrease in rate of sulphide uptake as the pH is increased from 9 to 11 when 1×10^{-4} mol/l sulphide concentration was used (Fig. 19), cannot be explained by the mineral solubility curves (Figs. 14 and 15). The solubility levels obtained after one hour equilibration do not give an indication of the rate of release of Cu^{2+} ions at any particular pH value. It is not known if this rate can be directly related to the final equilibrium Cu^{2+} concentration.

It seems likely that the rate of sulphide uptake at these pH values is influenced by the sulphide concentration. If this is the case then a variation in reaction rates with pH would depend on the relevant sulphide species present at that particular pH value. The higher reaction rates at pH 9 and 10 therefore suggest that the HS^- ion, rather than S^{2-} ion, may be more important in the adsorption process. However, a variation in pH will strongly influence the soluble copper species present at the CuO surface. At lower pH values (pH 9 and 10) the $\text{Cu}(\text{OH})^+$ species is expected to predominate whereas at higher pH values the $\text{Cu}(\text{OH})_3^-$ and $\text{Cu}(\text{OH})_4^{2-}$ species are likely to be present. These species in turn may influence the rate and extent of sulphide reaction.

On the other hand, at a high sulphide concentration (1×10^{-3} mol/l) experimental results showed that the minimum sulphide adsorption was observed at pH 10. It seems likely that at this higher sulphide level sulphide uptake is influenced more by the mineral solubility rather than the diffusion of sulphide ion to the mineral particle surface.

The reduction in rate of sulphide uptake in the presence of Ca^{2+} , and Mg^{2+} may be due to the adsorption the oxide surface of either $\text{Mg}(\text{OH})^+$,

Mg(OH)_2 or Ca(OH)^+ (Fig. 27). In general, adsorption of a positive multivalent ion only occurs very readily onto a negative surface when the lower charged hydroxylated species (M(OH)^{n+}) are present in solution. The explanation given for this by Healy (62) involves the hydration energy of the adsorbate species. For a highly charged parent ion the energy involved in removing the secondary hydration sheath, to allow the ion to penetrate to the inner Helmholtz plane is so large that the overall value of ΔG of adsorption is positive and hence adsorption does not occur. Only when the charge has been reduced by hydroxylation is the net free energy on adsorption negative. It can be seen that in the presence of Ca^{2+} reduction in sulphide adsorption at pH 12 is greater than that observed in the presence Mg^{2+} (Figs. 21 and 22). This could be due to the predominance of Ca(OH)^+ at pH 12 (Fig. 37) which adsorb more strongly than Mg(OH)_2 (Fig. 38). The solid Mg(OH)_2 can coat the mineral surface by a heterocoagulation process or alternatively the formation of CaCO_3 and MgCO_3 on the surface may possibly occur at this high pH value. The effect of Ca^{2+} and Mg^{2+} on sulphide adsorption when 1×10^{-3} mol/l sulphide was used is less than that observed when 1×10^{-4} mol/l sulphide was used.

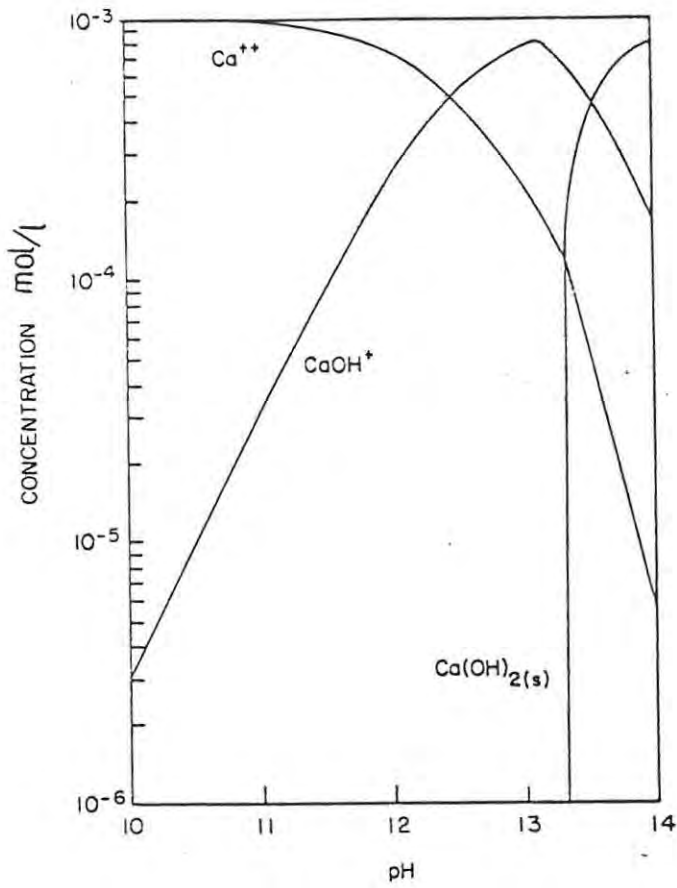


Figure.37. Logarithmic concentration diagram for $1 \times 10^{-3} \text{ M Ca}^{2+}$ Equilibrium data from ref (20).

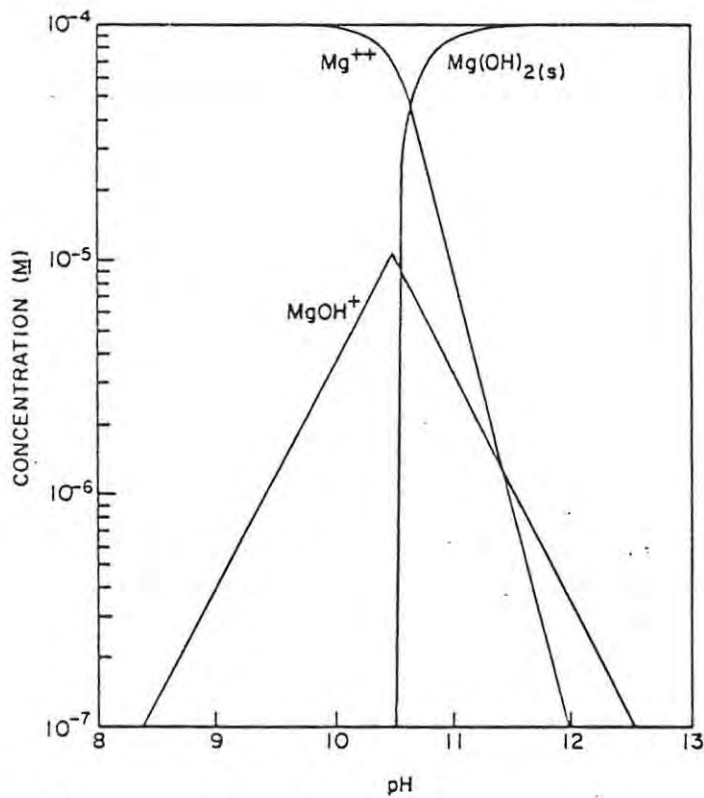


Figure.38. Logarithmic concentration diagram for $1 \times 10^{-4} \text{ M Mg}^{2+}$ Equilibrium data from ref (20).

Sulphide uptake was also reduced by the presence of starch and gum arabic (Figs. 28, 29, 31 and 32). This is likely to be caused by the adsorption of these polymers on the surface which can change the manner of sulphide adsorption and hence reduce the rate of sulphide uptake. For example about 3mg/m^2 of starch was found to be adsorbed on the surface at all pH values considered. According to Steenberg and Harris (63), adsorption of starch on most oxide and sulphide minerals occurs via a physisorption type process, hence adsorption of starch onto most oxides is likely to be unspecific. Gum arabic with its strong dispersing action had a greater effect on sulphide adsorption at pH 12 (Fig. 29), i.e. when 1×10^{-4} mol/l was used. When 1×10^{-3} mol/l sulphide was used gum arabic offered an overall reduction of sulphide uptake (Fig.32).

Triton X-100 also produced an effective reduction of rate of sulphide uptake (Figs. 30 and 33). In the presence of this polymer the rate of sulphide uptake seems to be influenced by the mineral solubility. The fact that the rate at pH 9 is low (where surface active $\text{Cu}(\text{OH})^+$ predominates) may also indicate the effectiveness of this polymer towards blocking the surface by slowing down the diffusion of sulphide to the surface.

Gao Yueying et al (64) and Levitz et al (65,66) have proposed mechanisms by which Triton X-100 adsorbs onto oxide-water interface. Gao Yueying et al suggested that adsorption of Triton X-100 is of a double layer type. The molecules in the first layer were presumed to be attached to their oxide surface by their oxyethelene chains such that their hydrocarbon chains were exposed to the medium. The molecules of the second layer were postulated to adsorb on the first layer but in the opposite orientation with the oxyethelene chain directed towards the adsorption medium. On the other hand Levitz et al have suggested that the adsorbed phase is an assembly of aggregates very similar to regular micelles, which when closed packing is about to be reached, coalesce into a continuous phase of a morphology which still has to be determined.

If such a continuous phase is to be found on CuO, the rate of sulphide uptake in the presence of this layer is expected to be reduced (Figs.30 and 33).

Semilogarithmic plots of the concentration of sulphide against time were linear for all experiments conducted except in the presence of Triton X-100

when 1×10^{-4} mol/l sulphide was used. Semilogarithmic plots tend to suggest that the reaction between sulphide and the surface is controlled by the transport of sulphide to the oxide surface, and this is further influenced by the initial sulphide concentration (Figs. 19, 26 and 34).

SEM results obtained after sulphidization of CuO using 1×10^{-3} mol/l sulphide between pH 9 and 12 showed a non-uniform surface coverage by CuS (micrographs 2 and 3). This was also observed when sulphidization was conducted in the presence of Mg^{2+} , Ca^{2+} , starch and gum arabic (micrographs 6 to 9 and 13 to 16). The electron microprobe analysis confirmed the presence of sulphide on the surface (micrographs 19 and 20). The white 'spots' in micrograph 20 show the X-Ray image of sulphur present on the CuO surface. It can be seen from micrographs 19 and 20 that where there are more clusters of CuS precipitate on the surface, there is also a high density of white 'spots'.

The presence of copper sulphide precipitates on the surface tend to support the postulation made that sulphide adsorption on CuO occurs mainly via the initial dissolution of oxide mineral which is then followed by copper-sulphide complex formation in solution and precipitation of this copper-sulphide species on the surface.

Samples that were conditioned in the presence of Triton X-100 showed small crystallites of copper sulphide adsorbed (micrographs 17 and 18). In the presence of Triton X-100 the rate of mineral dissolution is low. Thus under these conditions one can expect bigger crystals of copper sulphide to be formed on the surface. Rubio (67, 68), however, reported that nonionic surfactants, namely, polyethelene oxides flocculate most sulphide minerals suspensions. The same author also reported that oxide minerals can be flocculated after sulphidization. Since Triton X-100 is a nonionic surfactant, it can flocculate most of the copper sulphide colloidal particles. Therefore a high rate of precipitation is expected to occur which will result in the formation of small copper sulphide crystals on the oxide surface.

Results for the interaction of xanthate with sulphidized CuO (Fig. 36) indicate that reduction of xanthate adsorption is caused by the presence of sulphide on the surface. It is not understood why xanthate uptake increased with an increase in the sulphidization level beyond $1759.80 \mu\text{mol}/\text{m}^2$.

3.3 Cerussite Interaction

3.3.1. Solubility of cerussite

The first part of this investigation involved the determination of the solubility of cerussite at pH values between 9 and 12 as with copper (II) oxide, knowledge of the solubility of cerussite is important because it can affect the manner in which sulphide ions are removed from solution during sulphidization. The concentration of lead in an aqueous solution after contact with cerussite for 30 minutes was measured at various pH values by AAS. The results as illustrated in Fig.39 showed that the amount of Pb^{2+} released increased rapidly from pH 9 to pH 12. This indicates that solubility of the mineral or rate of mineral dissolution is dependent on the pH of the solution. At pH 11 and 12 the solution turned 'milky' indicating the presence of $Pb(OH)_2$ in suspension. It should be noted, however, that the surface composition of $PbCO_3(s)$ changes with pH. This composition - pH dependence, can have an effect on the rate of mineral dissolution and on the form of metal ion species released.

It has been established (24) that if cerussite is placed in water at pH values below 7.3, $PbCO_3(s)$ is the predominant species.

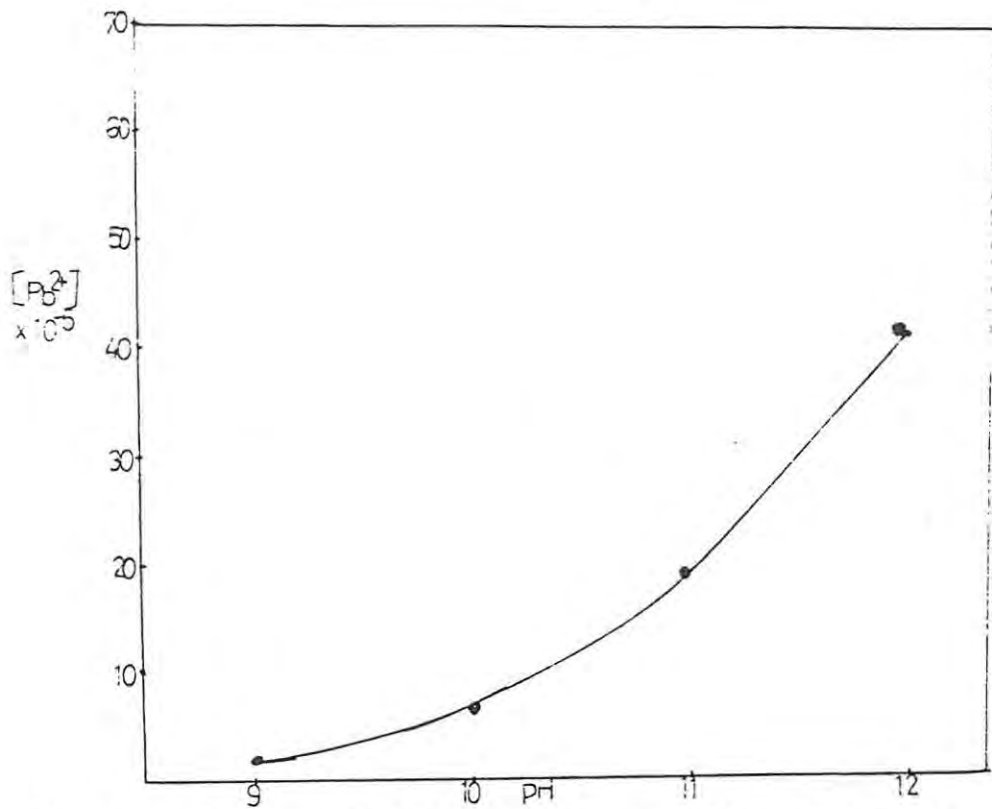


Figure.39. Solubility of cerussite after 30 minutes of conditioning.

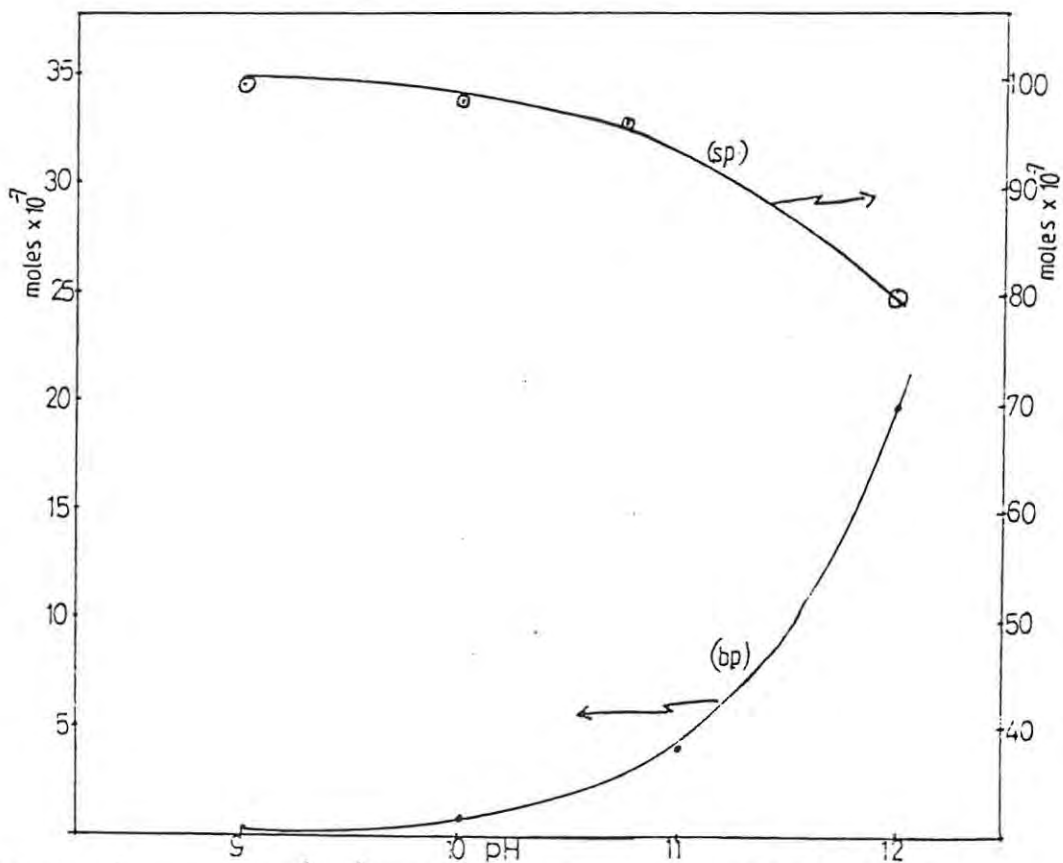
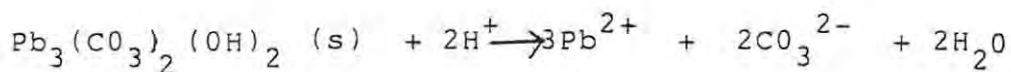


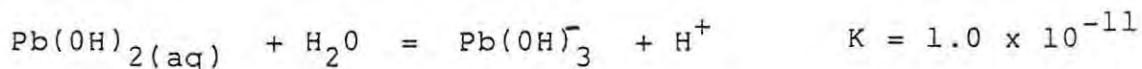
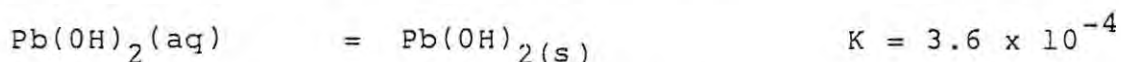
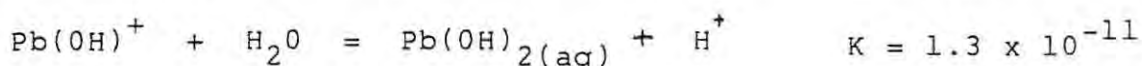
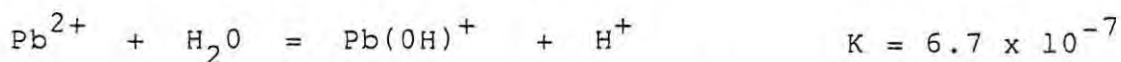
Figure.40. Comparison of bulk precipitate (bp) and the surface precipitate (sp) measured after complete reaction of sulphide with cerussite surface, concentration of sulphide used = 1×10^{-4} mol/l.

Whereas between pH 7.3 and 12.5 the $\text{Pb}_3(\text{CO}_3)_2(\text{OH})_2$ (s) or hydrocerussite is dominant with its solution equilibria being governed by the following reaction:



$$K = 1.6 \times 10^{-19}$$

Even if the equilibrium is not attained, the surface region will comprise a certain amount of the hydrocerussite. The Pb^{2+} produced by dissolution can be hydrolysed according to the following equilibria:



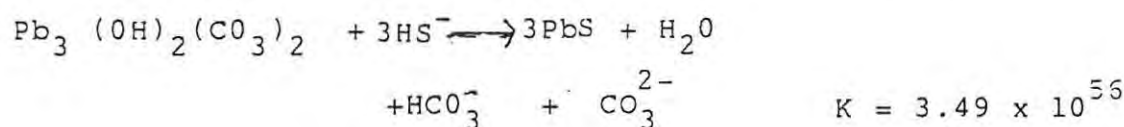
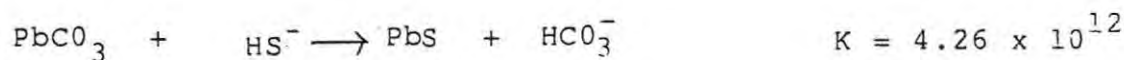
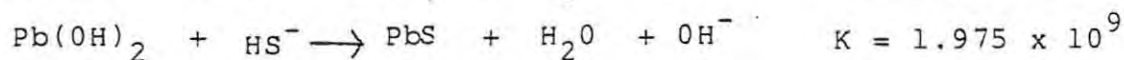
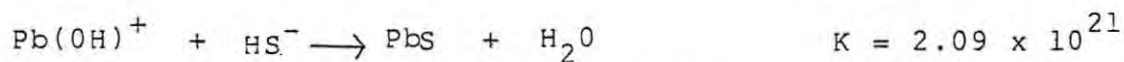
The predominance of each hydroxy species depends on the pH value of the solution. Table II presents the concentration of various lead ion species as a function of pH (this data was obtained from ref. (69)).

TABLE II. Concentration of various species of Pb^{++} as a function of pH for an addition of 1×10^{-4} mol / l Pb^{++} to water from ref 69.

pH	Species			
	Pb^{++}	$Pb(OH)^+$	$Pb(OH)_2(aq)$	$HPbO_2^-$
4	1.0×10^{-4}	6.7×10^{-7}	8.4×10^{-14}	1.0×10^{-20}
5	9.4×10^{-5}	6.0×10^{-6}	7.1×10^{-12}	8.5×10^{-18}
6	6.0×10^{-5}	4.0×10^{-5}	4.7×10^{-10}	5.7×10^{-15}
7	1.3×10^{-5}	8.7×10^{-5}	1.0×10^{-8}	1.2×10^{-12}
8	1.5×10^{-6}	9.8×10^{-5}	1.2×10^{-7}	1.4×10^{-10}
9	1.5×10^{-7}	9.9×10^{-5}	1.0×10^{-6}	1.2×10^{-8}
10	1.3×10^{-8}	8.8×10^{-5}	1.0×10^{-5}	1.3×10^{-6}
11	4.2×10^{-10}	2.8×10^{-5}	3.3×10^{-5}	3.9×10^{-5}
12	9.7×10^{-13}	6.5×10^{-7}	7.7×10^{-6}	9.3×10^{-5}
13	1.0×10^{-15}	7.0×10^{-9}	8.3×10^{-7}	1.0×10^{-4}

It is expected that the form of the hydroxy species can affect the manner of sulphide uptake on the mineral because of differences in the free energy of formation and hence equilibrium constants.

Equilibrium constants were calculated according to data obtained from ref. 70.



Furthermore, the surface active $\text{Pb}(\text{OH})^+$ would tend to favour the formation of a surface precipitation of PbS whereas the soluble $\text{Pb}(\text{OH})_3^-$ (aq) and $\text{Pb}(\text{OH})_2$ will favour bulk precipitation.

3.3.2. Kinetics of sulphide uptake on cerussite.

The rate of sulphide uptake was followed by measuring the residual concentration using an ISE. In order to distinguish between the bulk and surface precipitates, the MB method was used to measure the bulk precipitate and the residual sulphide concentration (sample solutions were not filtered). The amount of bulk precipitate obtained by finding the difference in results by the MB and ISE methods is shown in Fig. 40. From Fig. 40, it can be seen that the amount of bulk precipitate is very low when compared to the amount of surface precipitate between pH 9 and 11. Only at pH 12 does the bulk precipitate become significant. Therefore it can be assumed that measurements of the residual concentration after sulphidization between pH 9 and 11 could be used to reflect the rate of sulphide adsorption on the mineral surface.

The rates of sulphide uptake at varying pH values are shown in Fig. 41. The results show that the rate of sulphide uptake is pH dependent, and increased with an increase in pH. At pH 9 for example, the sulphide uptake only reaches completion after 5 minutes, whereas at pH 12 the reaction rate is so high that it cannot be determined. At pH 9 the low rate of sulphide uptake corresponds to the low mineral solubility (Fig.39); Conversely the rate of sulphide uptake is high at pH 12 where mineral solubility is high. Using the data presented in Fig. 41 for experiments conducted at pH 9 and 10, $\ln[S^{2-}]$ was plotted against reaction time and a linear relationship was found which accords with first order kinetics (Fig.42). The data for higher pH values could not be plotted in the same way because the reaction rate was too high.

A change in the colour of cerussite particles was noticed during sulphidization. Cerussite particles showed a colour change from white to black (Fig. 43), and the colour intensity decreased with an increase in pH of sulphidization. At pH 9 and 10 the colour changed from white to black (A to C Fig. 43) and at pH 11 and 12 the colour changed from white to light brown. (A to B Fig. 43).

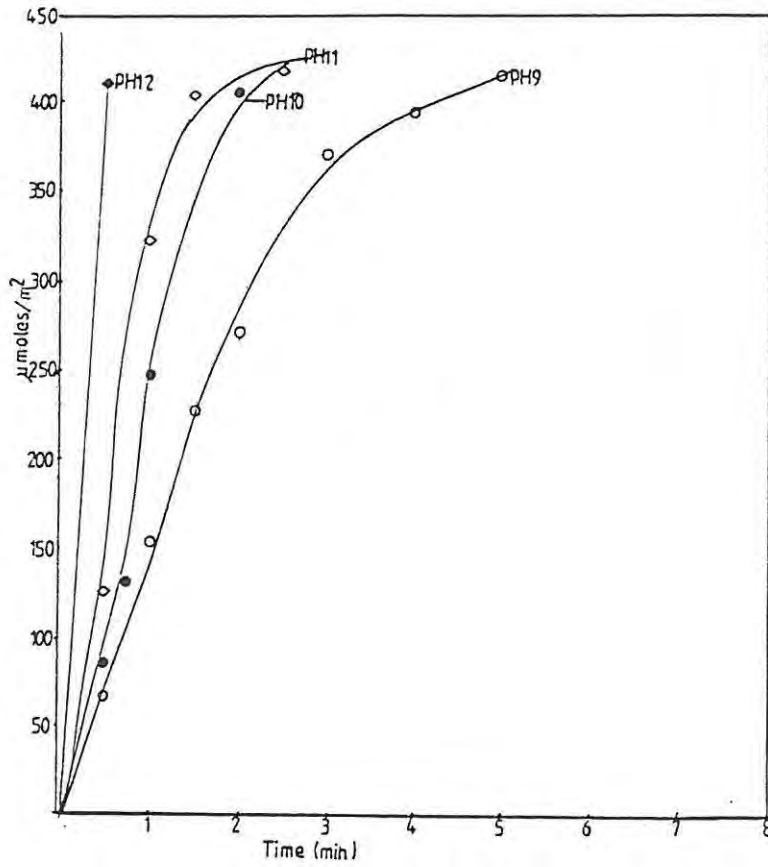


Figure.41. Kinetics of sulphide uptake on cerussite
concentration of sulphide used = 1×10^{-4} mol/l.

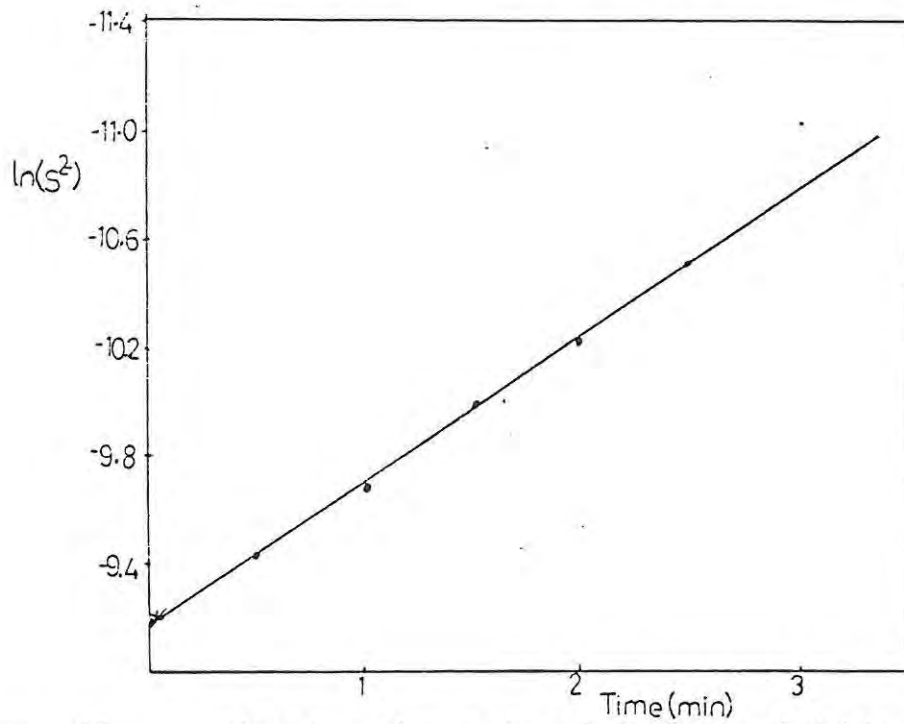


Figure.42. First order rate plot for sulphide
interaction with cerussite.

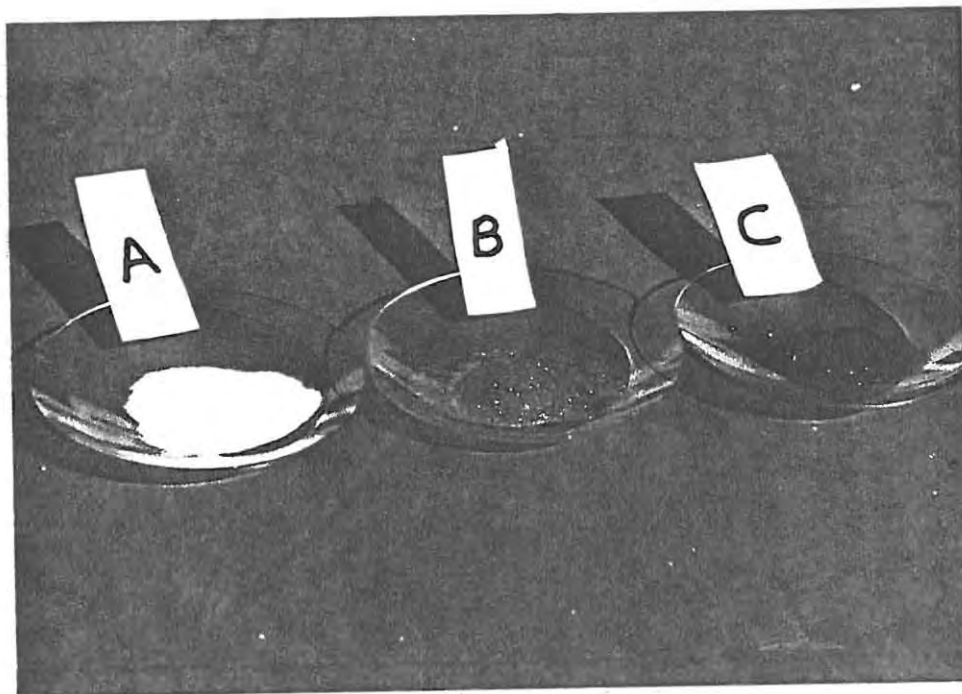
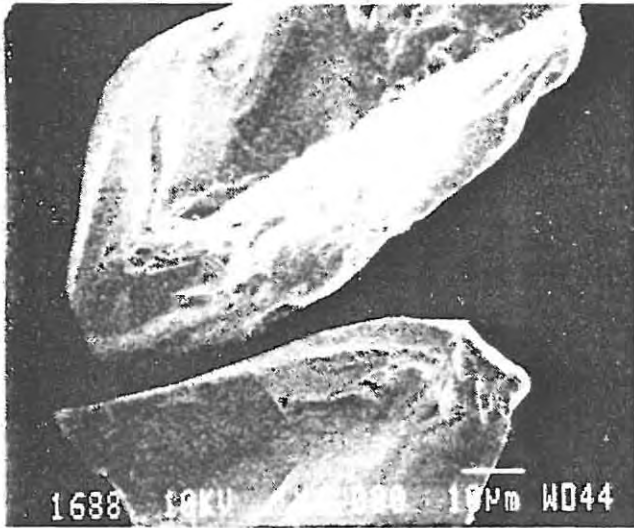


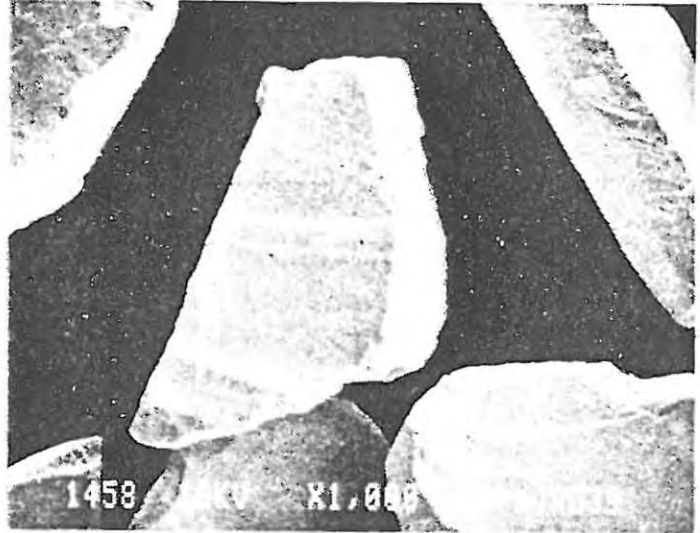
Fig. 43 : Cerussite particles produced after sulphidization under various conditions.
A = untreated cerussite, B and C = Treated cerussite.

Upon examining these sulphidized cerussite particles under the scanning electron microscope, a few crystallites of PbS could be seen on the mineral surface for samples treated at pH 9 and 10 (micrograph 21). This can be interpreted as the formation of a uniform coverage of cerussite particles by sulphide. (Micrograph 22 is for untreated cerussite). The electron microprobe analysis facility confirmed



Micrograph.21.

Cerussite conditioned with
 1×10^{-4} mol/l sulphide at pH 9.



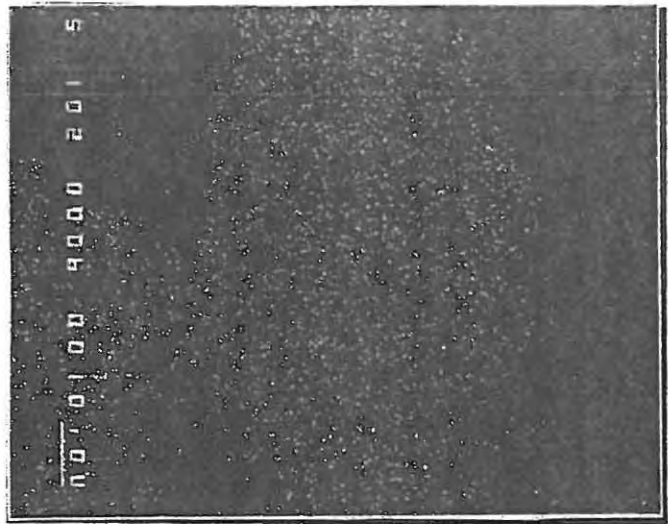
Micrograph.22.

Untreated cerussite particles.



Micrograph.23.

Cerussite conditioned with 1×10^{-4} mol/l
 sulphide at pH 10 (4000 x
 magnification).



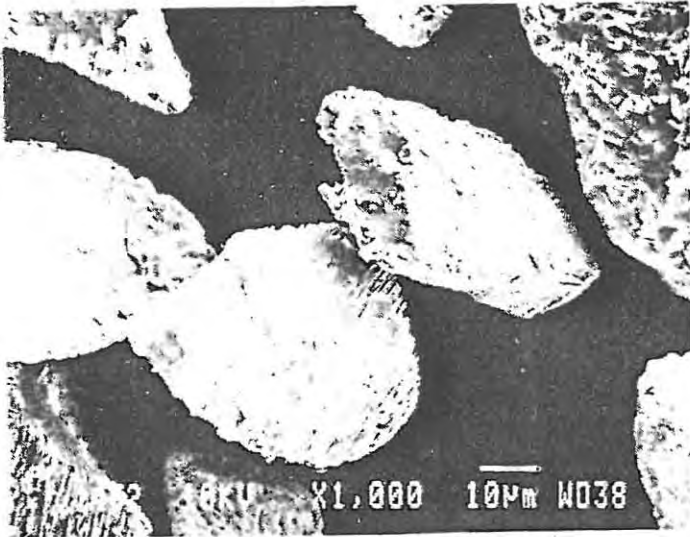
Micrograph.24.

X-Ray image for sulphur for
 micrograph 23 (4000 x magnification).

the presence of sulphide on the surface (cf micrographs 23 and 24). The white 'spots' in micrograph 24 show the X-Ray image of sulphur present on the cerussite surface. However, samples that were sulphidized at pH 11 and 12 exhibited a non-uniform surface coverage (micrographs 25 and 26). Electron microprobe results also confirmed the presence of sulphide on the surface (See micrographs 27 and 28).

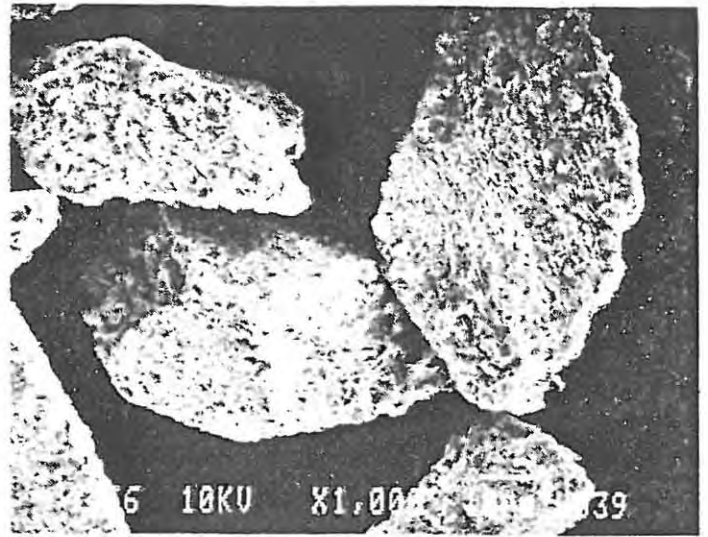
3.3.3. Kinetics of sulphide uptake on cerussite in the presence of Mg^{2+} and Ca^{2+} .

Experiments conducted in the presence of $2.06 \times 10^{-3} \text{ mol/l } Mg^{2+}$ and $1.25 \times 10^{-3} \text{ mol/l } Ca^{2+}$ showed that the rate of sulphide uptake is affected by the presence of these metal ions. Fig. 44 illustrates the rate of sulphide uptake between pH 9 and 12 in the presence of $2.06 \times 10^{-3} \text{ mol/l } Mg^{2+}$. The overall trend in the rate of sulphide uptake at these pH values is higher than that shown in Fig. 41. The kinetic data displayed in Fig. 44 for experiments conducted at pH 9 were also plotted according to the first order kinetics and the results are shown in Fig. 46, curve 1. As shown in the figure, a plot of $\ln [\text{sulphide}]$ vs time gave a linear relationship. On the other hand, the rate of sulphide uptake on cerussite in the presence of $1.25 \times 10^{-3} \text{ mol/l } Ca^{2+}$ for



Micrograph.25.

Cerussite conditioned with 1×10^{-4} mol/l sulphide at pH 11.



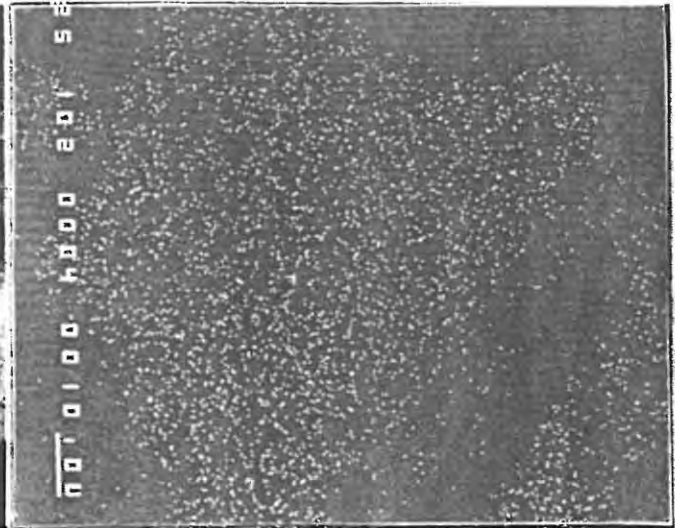
Micrograph.26.

Cerussite conditioned with 1×10^{-4} mol/l sulphide at pH 12.



Micrograph.27.

Cerussite conditioned with 1×10^{-4} mol/l sulphide at pH 11 (4000 x magnification).



Micrograph.28.

X-Ray image for sulphur, for micrograph 27 (4000 x magnification).

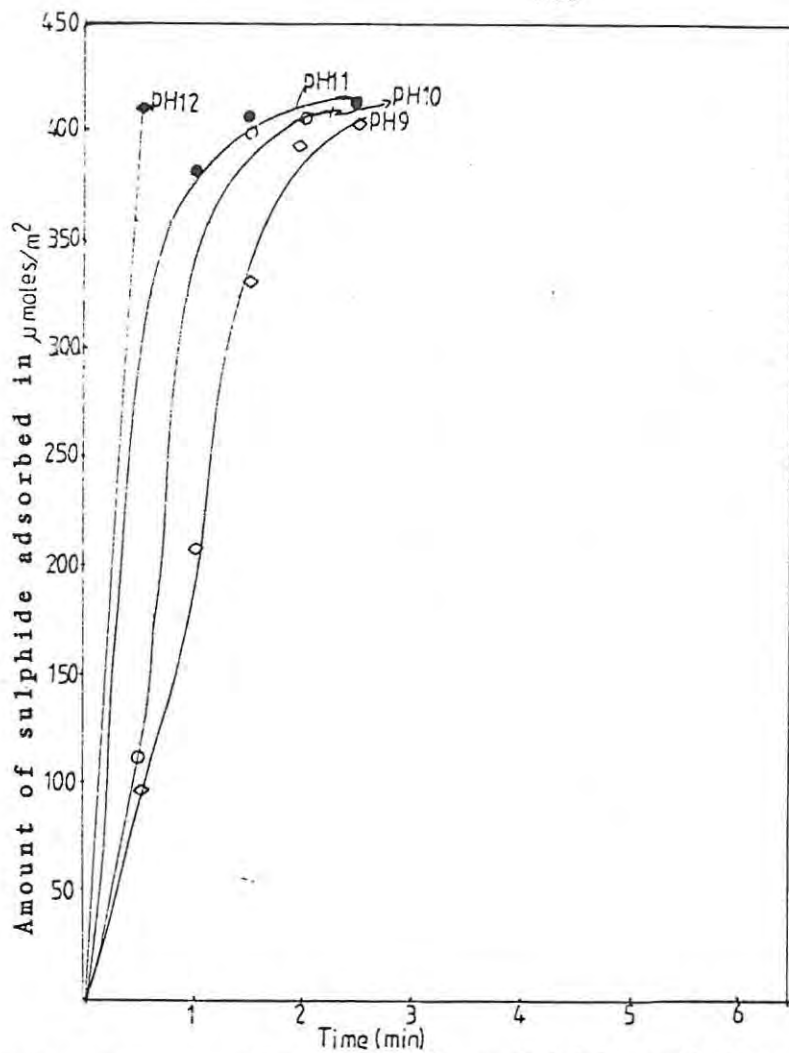


Figure.44. Kinetics of sulphide uptake in the presence of $2.06 \times 10^{-3} \text{ mol/l Mg}^{2+}$.
Concentration = $1 \times 10^{-4} \text{ mol/l}$ sulphide was used.

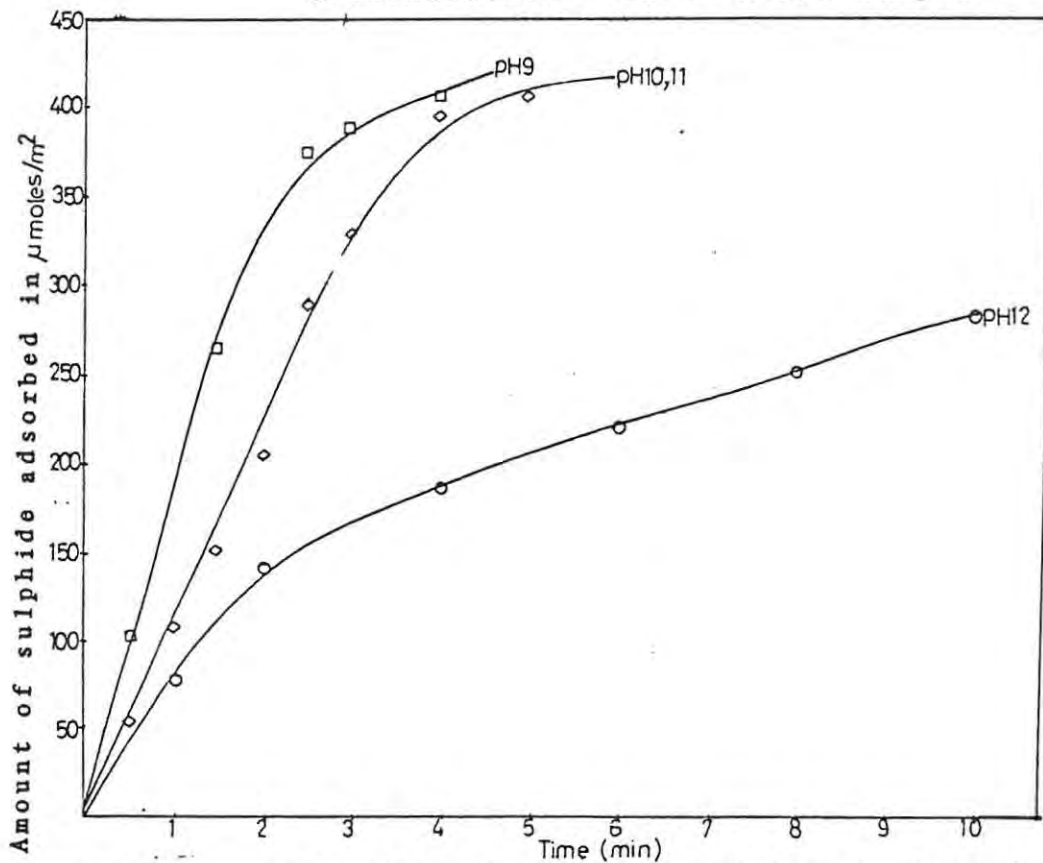


Figure.45. Kinetics of sulphide uptake on cerussite in the presence of $1.25 \times 10^{-3} \text{ mol/l Ca}^{2+}$.

all pH values (except pH 9) studied was relatively low when compared with cases described above. Results shown in Fig. 45 were also replotted according to the first order rate equation. (Fig.46). The rate of sulphide uptake was also found to decrease with an increase in Ca^{2+} concentration at pH 11 (Fig.47). The proportion of bulk precipitate measured after sulphidization in the presence of Ca^{2+} was found to increase with an increase in pH of sulphidization but it was lower than that obtained when sulphidization was conducted in the absence of Ca^{2+} (Fig.48).

Since the rate of sulphide uptake on cerussite was found to be reduced by the presence of Ca^{2+} , it was considered necessary to study the solubility of cerussite under these conditions. The amount of Pb^{2+} released in the presence of $1.25 \times 10^{-3} \text{ mol/l}$ Ca^{2+} ions was found to be lower than that shown in Fig. 39. The results illustrated in Fig. 49 show these differences. Furthermore, the amount of Ca^{2+} adsorbed during sulphidization was determined. This was done in an attempt to establish whether calcium (probably in the form of CaCO_3) is responsible for the reduction in rate. The amount of Ca^{2+} adsorbed was found to increase with increasing pH of sulphidization. Similarly, the amount of Mg^{2+} adsorbed was

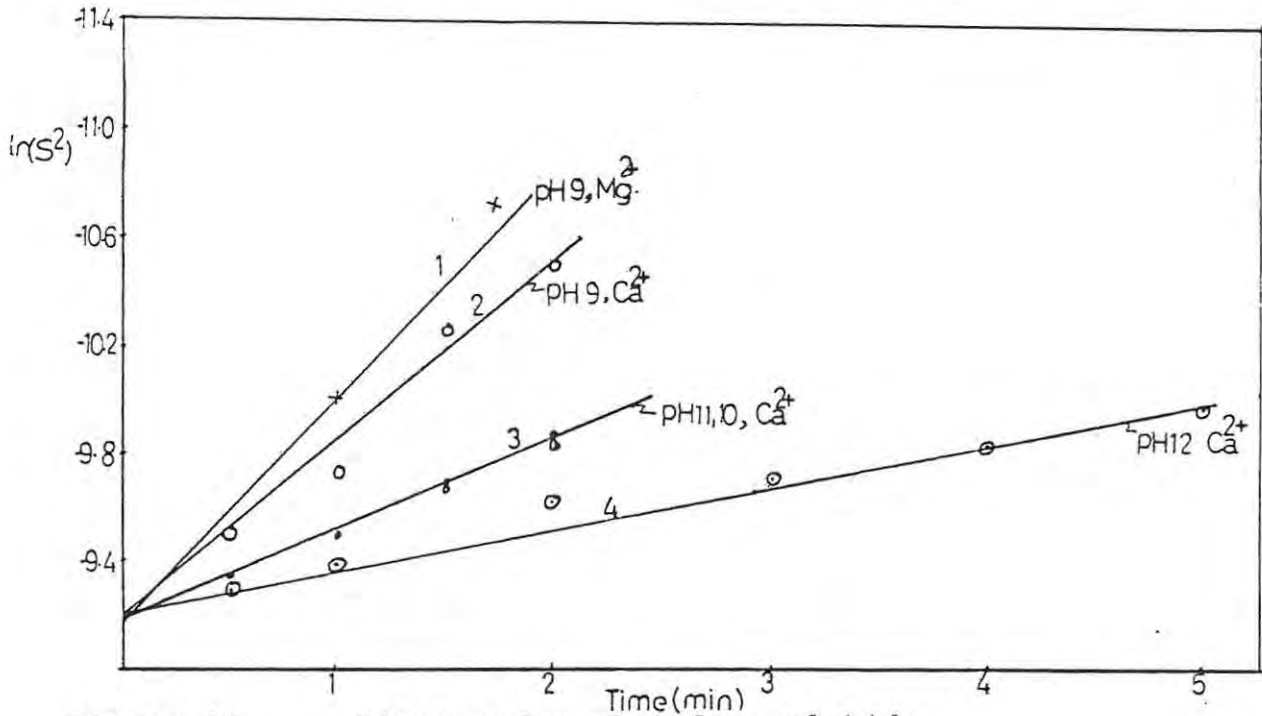


Figure.46. First order plot for sulphide interaction with cerussite in the presence of 1.25×10^{-3} mol/l Ca^{2+} and 2.06×10^{-3} mol/l Mg^{2+} at pH 9.

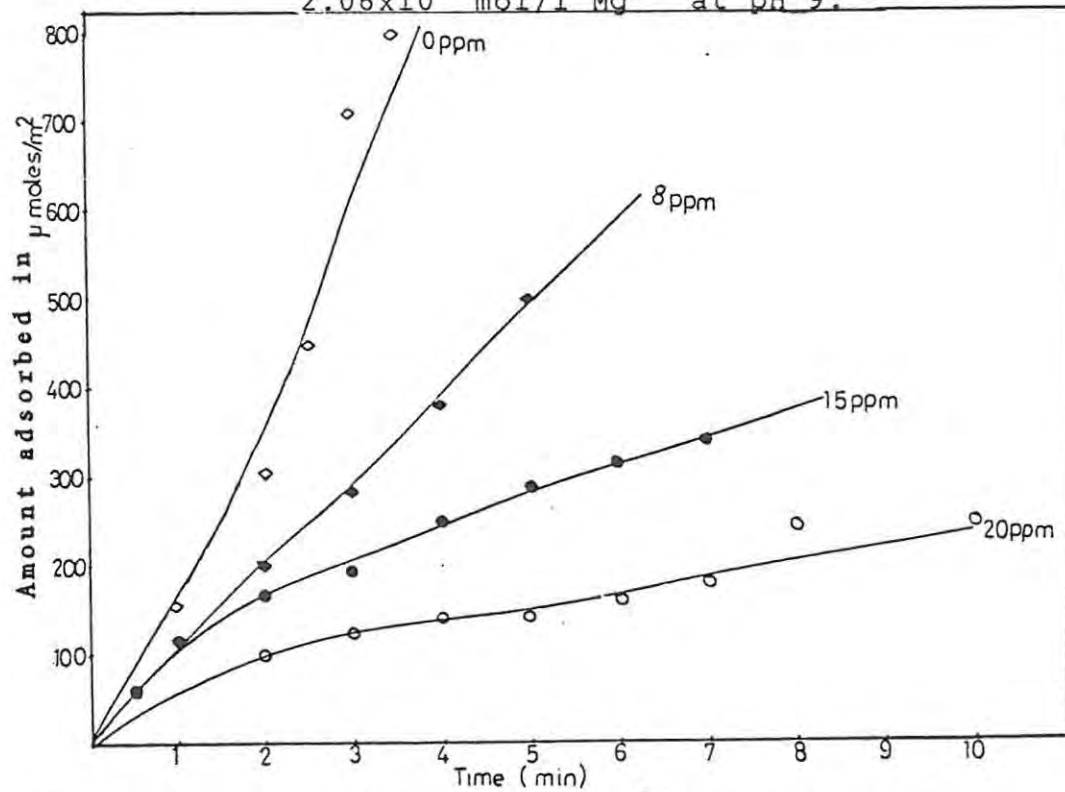


Figure.47. Variation with Ca^{2+} concentration of the rate of sulphide uptake on cerussite at pH 11, 0.5g of cerussite was used, concentration = 1×10^{-4} mol/l sulphide was used.

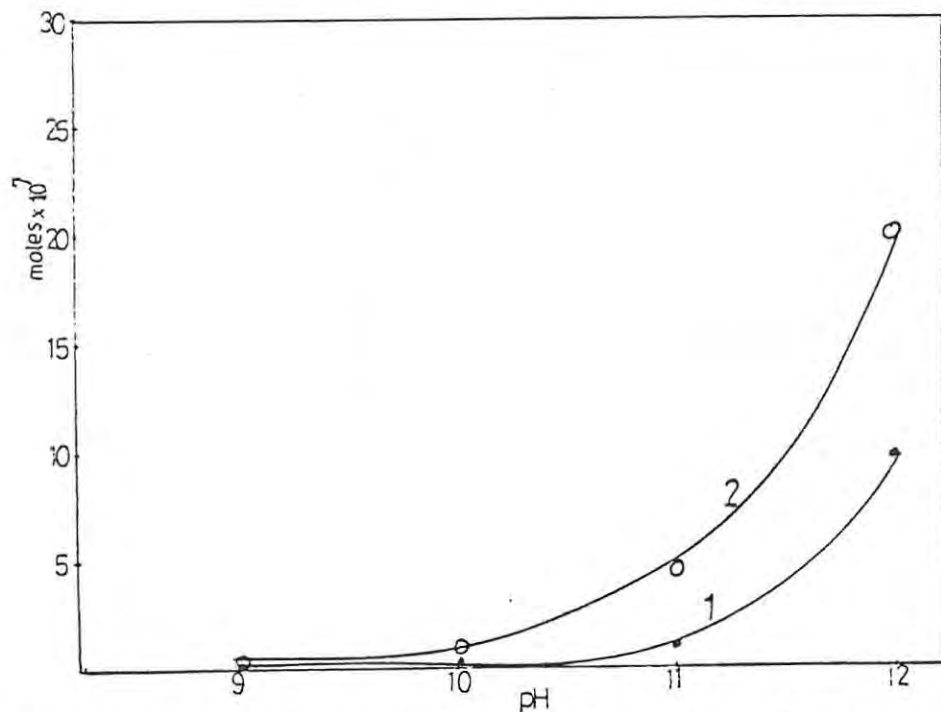


Figure.48. Variation with pH of the bulk precipitate (1) in the presence and (2) absence of calcium.

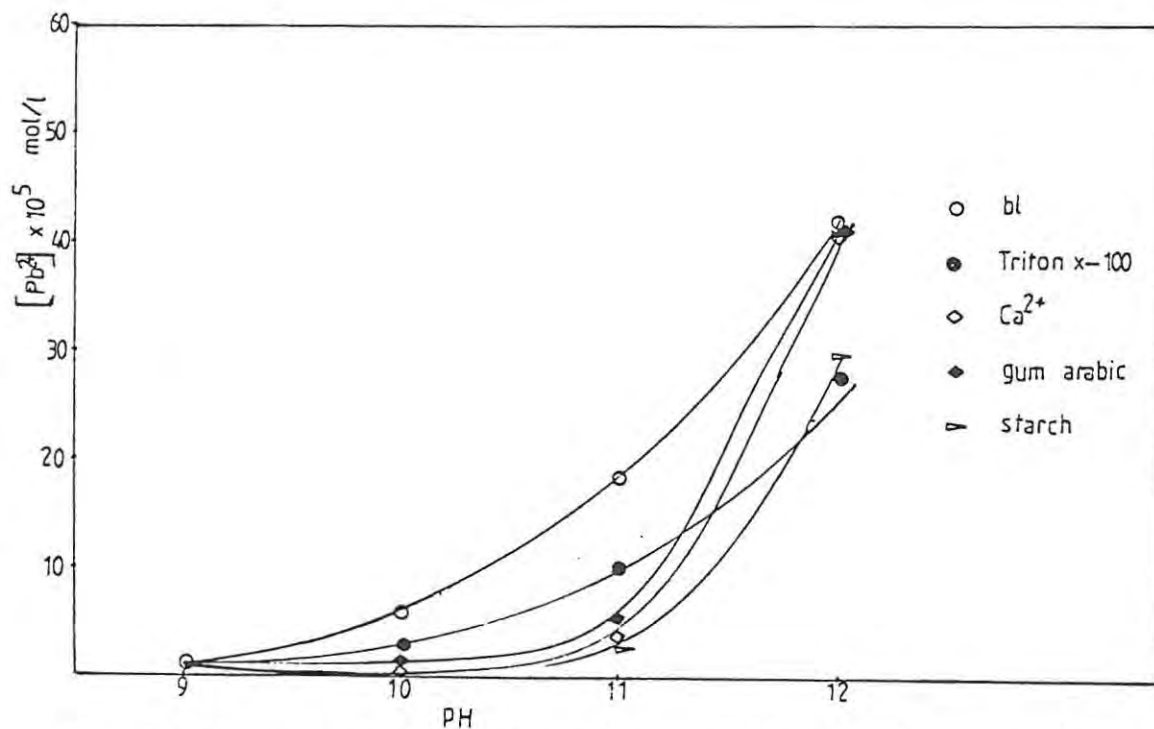


Figure.49. Solubility of cerussite in the presence of 50ppm Triton X-100, Ca^{2+} , gum arabic and starch bl = solubility in the absence of other species.

also found to increase with an increase in pH (Table III).

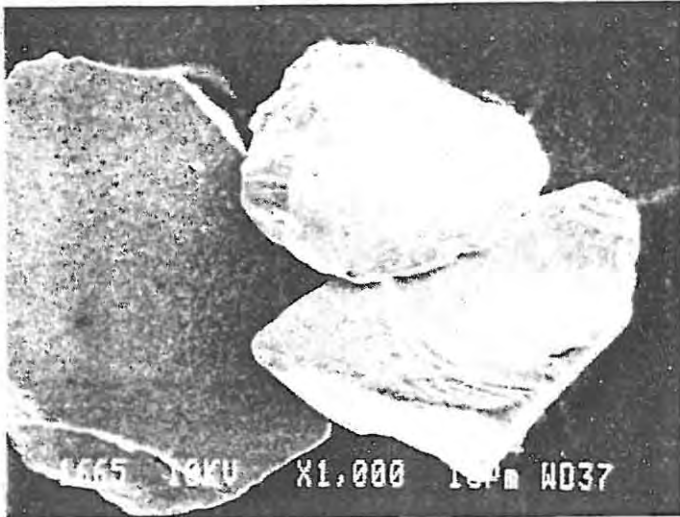
Table III Concentration of Mg^{2+} and Ca^{2+} adsorbed as a function of pH during the dissolution of cerussite initial $Ca^{2+} = 1.25 \times 10^{-3} \text{ mol/l} = 50 \text{ ppm}$, $Mg^{2+} = 2.06 \times 10^{-3} \text{ mol/l} = 50 \text{ ppm}$

pH	$[Ca^{2+}] \text{ eq mol/l}$	$[Ca^{2+}] \text{ ads mol/l}$	$\text{mmoles} \times 10^{-3} \text{ adsorbed}$
9	1.15×10^{-3}	9.48×10^{-5}	9.48
10	1.05×10^{-3}	2.00×10^{-4}	19.96
11	8.91×10^{-4}	3.56×10^{-4}	35.55
12	9.17×10^{-4}	3.30×10^{-4}	33.05
pH	$[Mg^{2+}] \text{ eq mol/l}$	$[Mg^{2+}] \text{ ads mol/l}$	$\text{mmoles} \times 10^{-3} \text{ adsorbed}$
9	1.05×10^{-3}	1.01×10^{-3}	50.60
10	5.14×10^{-4}	1.54×10^{-3}	77.16
11	3.86×10^{-4}	1.67×10^{-3}	83.60
12	1.29×10^{-4}	1.93×10^{-3}	96.46
ads. = adsorbed eq = equilibrium			

This, together with the results illustrated in Figs. 45 and 47 show that the amount of Ca^{2+} adsorbed can play an important role in reducing the rate of sulphide uptake whereas the amount of Mg^{2+} adsorbed seems to facilitate the rate of sulphide uptake.

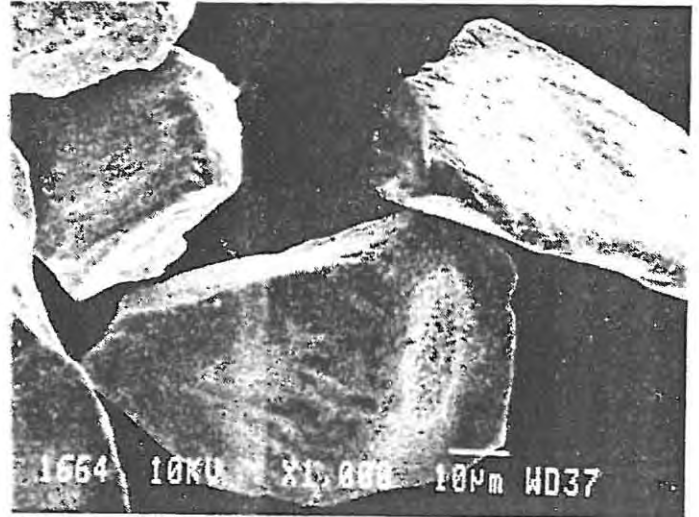
The amount of carbonate released during sulphidization at pH 11 in the presence of Ca^{2+} was lower than that obtained when sulphidization was conducted in the absence of Ca^{2+} . The results displayed in Fig. 50 show the reduction in CO_3^{2-} released as Ca^{2+} concentration is increased.

Cerussite particles produced after sulphidization in the presence of Mg^{2+} and Ca^{2+} at pH 9 and 10 showed a colour change from white and black, i.e. a change from A to C in Fig.43. Particles obtained after sulphidization in the presence of Mg^{2+} showed a decrease in colour intensity when the pH was increased. The formation of light coloured particles can be represented by the colour change from A to B in Fig. 43. The results obtained from SEM are similar to those represented by micrographs 21, 25 and 26. However, particles obtained after sulphidization in the presence of Ca^{2+} did not show a change in colour intensity when the pH was increased. The colour change observed was from white to black (A to C in Fig.43). SEM results showed what can be interpreted as a uniform coverage of these particles by PbS (micrographs 29 to 31).



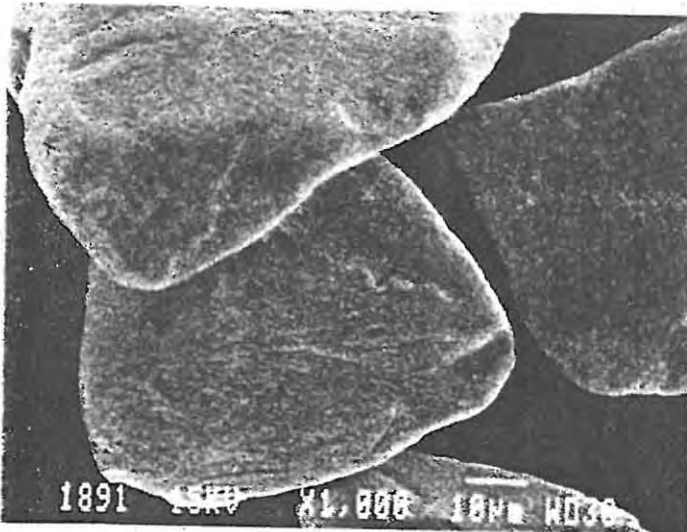
Micrograph.29.

Cerussite conditioned with 1×10^{-4} mol/l sulphide at pH 9 in the presence of 1.25×10^{-3} mol/l Ca^{2+} .



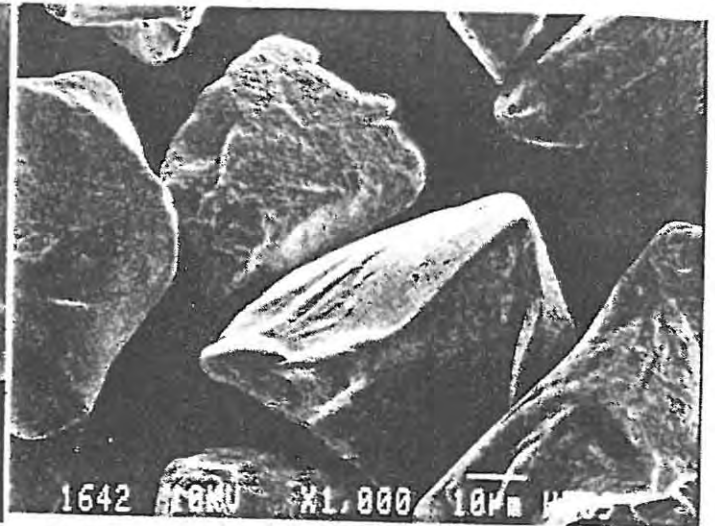
Micrograph.30.

Cerussite conditioned with 1×10^{-4} mol/l sulphide at pH 11 in the presence of 1.25×10^{-3} mol/l Ca^{2+} .



Micrograph.31.

Cerussite conditioned with 1×10^{-4} mol/l sulphide at pH 12 in the presence of 1.25×10^{-3} mol/l Ca^{2+} .



Micrograph.32.

Cerussite particles conditioned with 1×10^{-4} mol/l sulphide of 50ppm starch at pH 11.

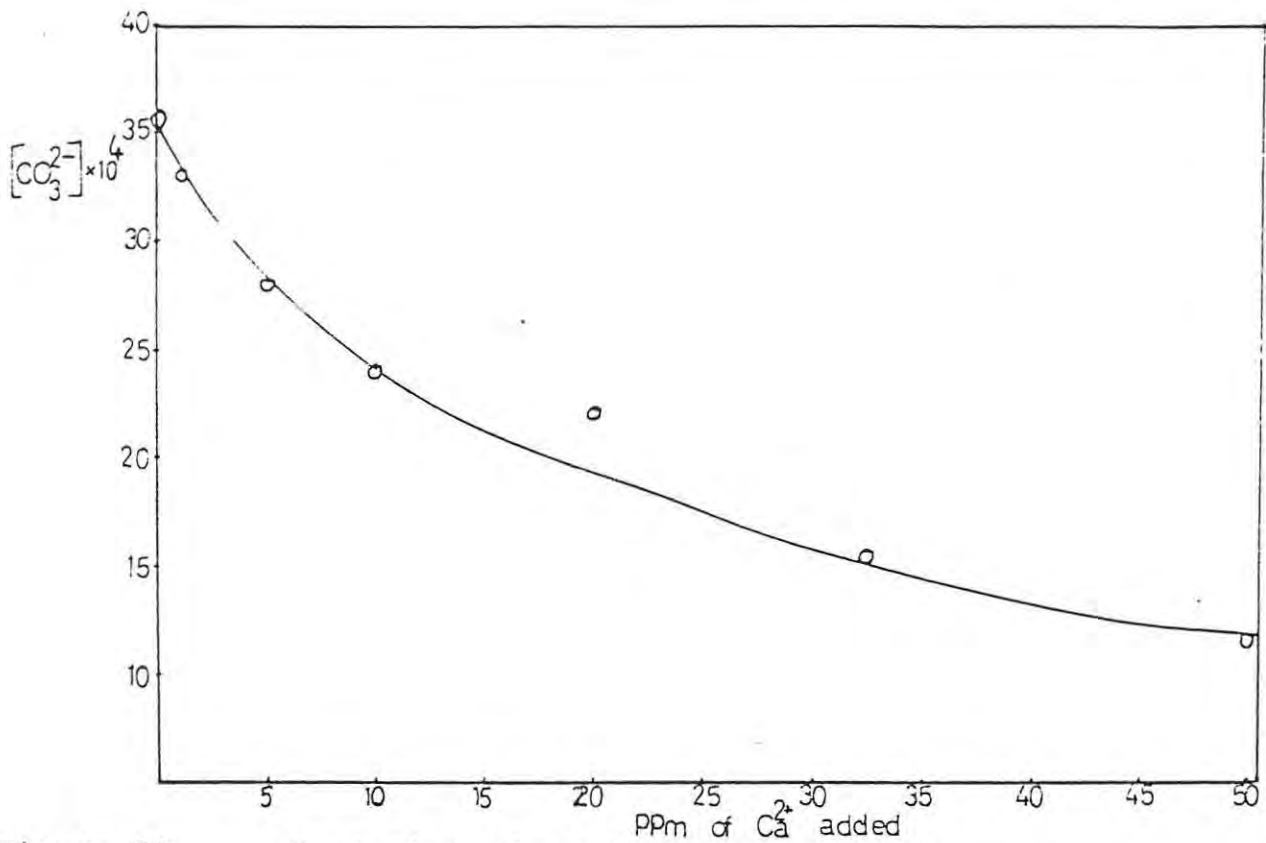


Figure.50. Variation of equilibrium carbonate concentration with Ca^{2+} concentration during sulphidization at pH 11.

Concentration = 1×10^{-4} mol/l sulphide was used.

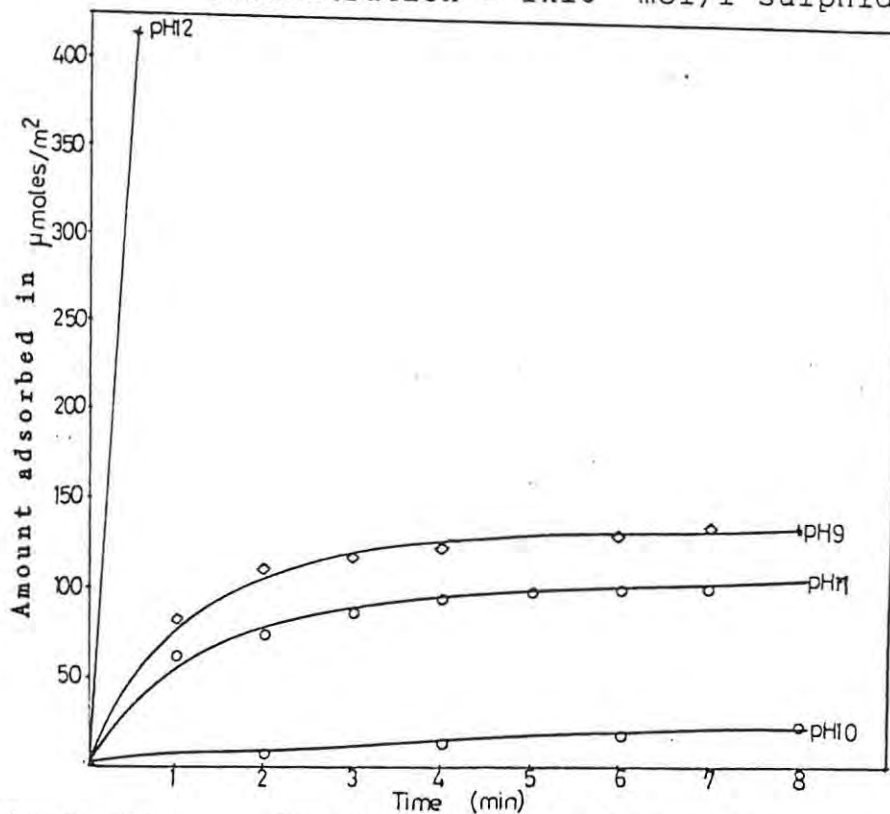


Figure.51. Kinetics of sulphide uptake on cerussite in the presence of 50ppm starch at various pH values 1×10^{-4} mol/l was used.

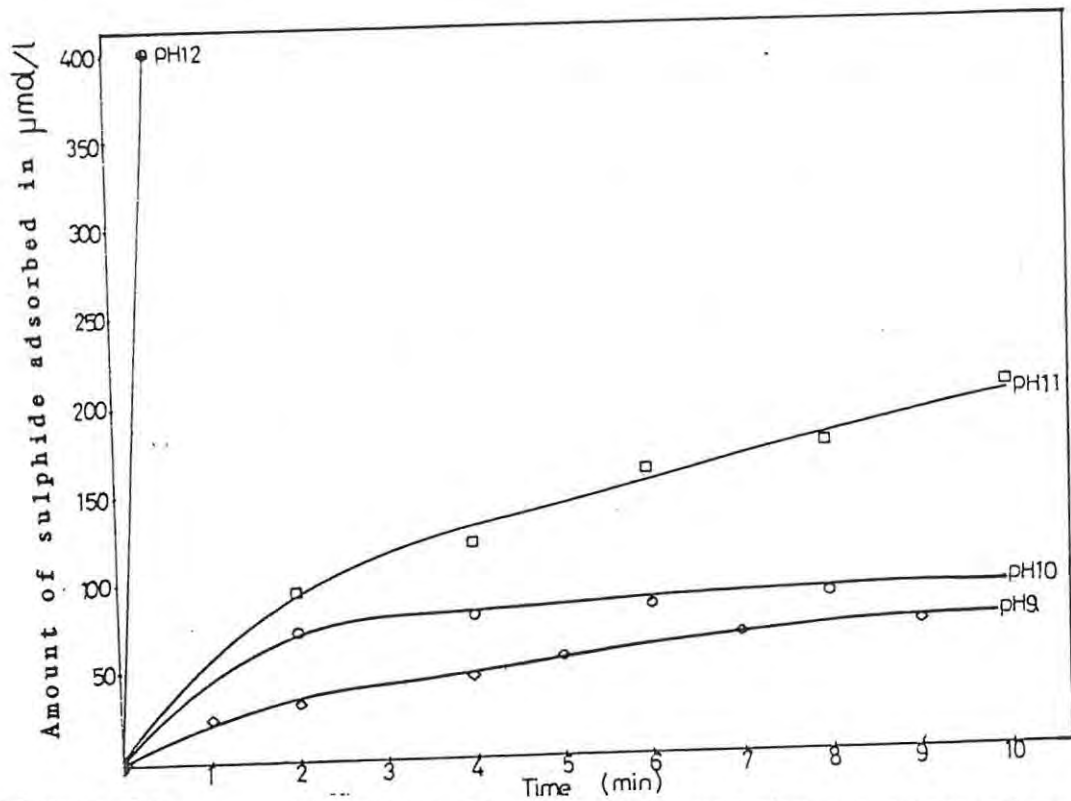


Figure.52. Kinetics of sulphide uptake on cerussite in the presence of 50ppm gum arabic at various pH values 1×10^{-4} mol/l sulphide was used.

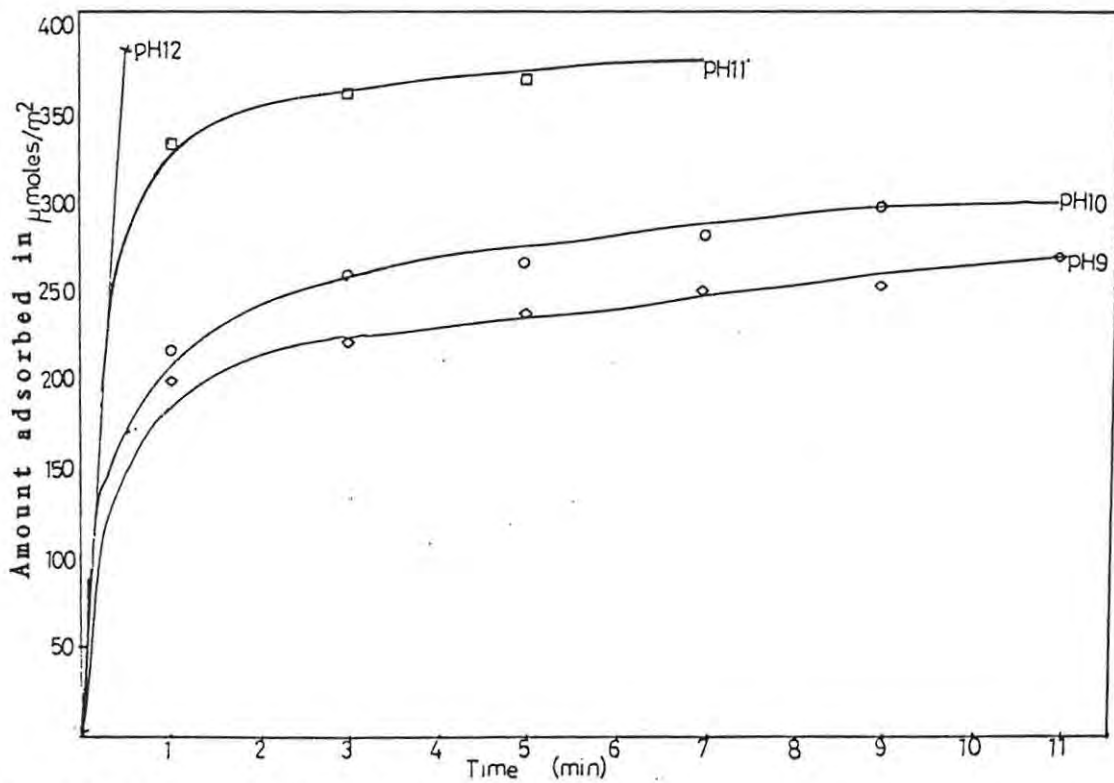


Figure.53. Kinetics of sulphide uptake on cerussite in the presence of 50ppm Triton X-100, 1×10^{-4} mol/l sulphide was used.

Electron microprobe results also confirmed the presence of sulphide and Ca^{2+} on the surface. Although a large amount of Mg^{2+} seemed to be adsorbed on the mineral surface (Table III), electron microprobe showed that there was a minimum amount of Mg^{2+} adsorbed at pH 12.

3.3.4. The kinetics of sulphide uptake on cerussite in the presence of starch, gum arabic and Triton X-100.

The rate of sulphide uptake in the presence of starch, gum arabic and Triton X-100 was also studied. In section 3.2.4. it was shown that these compounds interfered with sulphide adsorption on CuO .

Consequently it was considered necessary to determine whether these reagents could similarly interfere with sulphide adsorption on cerussite. The results of these kinetic studies are shown in Figs. 51, 52 and 53 for starch, gum arabic and Triton X-100 respectively. From these figures it is clear that between pH 9 and 11, the rate of sulphide uptake is reduced by these polymers. The rate of sulphide uptake in the presence of starch was found to increase with an increase in pH i.e. from pH 10 to 12.

However, at pH 9 the rate of sulphide uptake was found to increase (Fig.51). In the presence of gum arabic the rate of uptake was found to increase with an increase in pH of sulphidization. It was also observed that between pH 9 and 11 sulphidization in the presence of starch did not reach completion even when the samples were conditioned for 2 hours. This was also found to be the case for gum arabic and Triton X-100 at pH 9 and 10.

Results illustrated in Figs. 54 and 55 indicate that the rate of sulphide uptake is also influenced by the concentration of starch and gum arabic. Starch, as shown in Fig. 54, has a greater effect than gum arabic (Fig.55). Furthermore, these polymers were found to have an influence on the solubility of cerussite and in all cases, the solubility of cerussite was reduced, Fig.49. The depression in solubility of cerussite at pH 11 and 12 in the presence of gum arabic was however, much less than that observed with Triton X-100 and starch. As it is illustrated in Fig.56, the bulk precipitate was found to be decreased from about 7×10^{-7} moles at pH 9 to about 2×10^{-7} moles at pH 10 in the presence of starch and gum arabic. Thereafter it increased at higher pH values of 11 and 12.

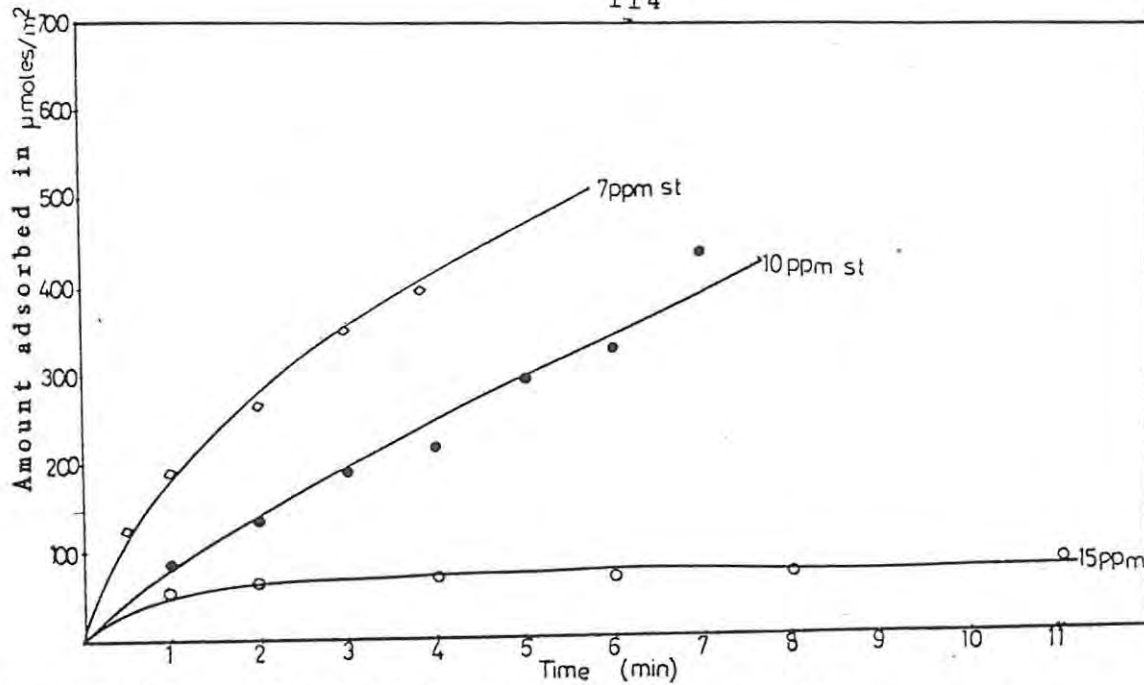


Figure.54. Variation with starch concentration of the rate of sulphide uptake on cerussite at pH 11, 0.5g of cerussite was used. 1×10^{-4} mol/l sulphide was used.

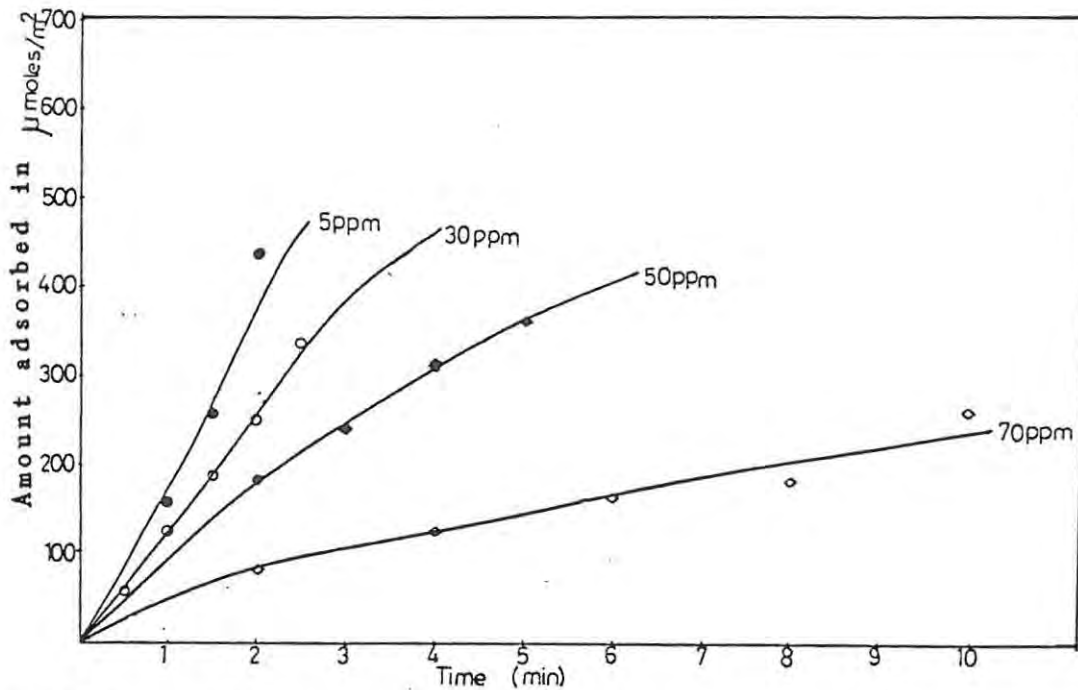


Figure.55. Variation with gum arabic concentration of the rate of sulphide uptake on cerussite at pH 11, 0.5g of cerussite was used. 1×10^{-4} mol/l sulphide was used

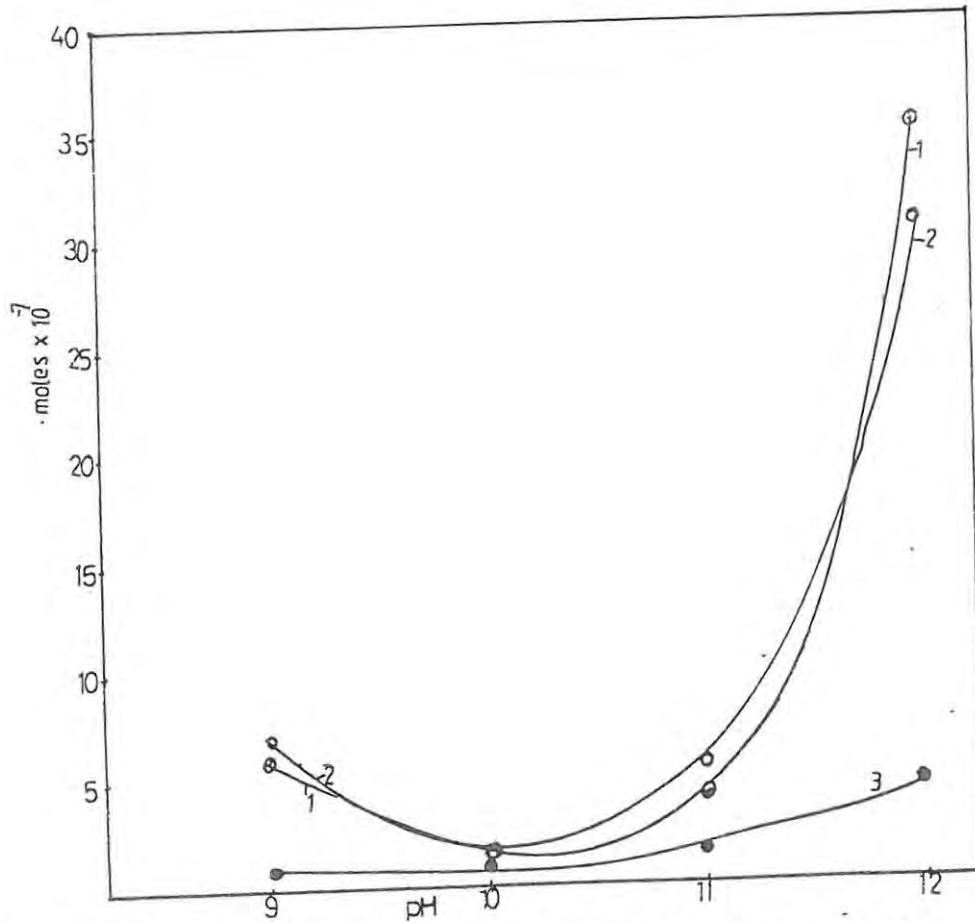


Figure.56. The variation with pH of the bulk precipitate after sulphidization in the presence of (1) starch and (2) gum arabic and (3) Triton X-100.

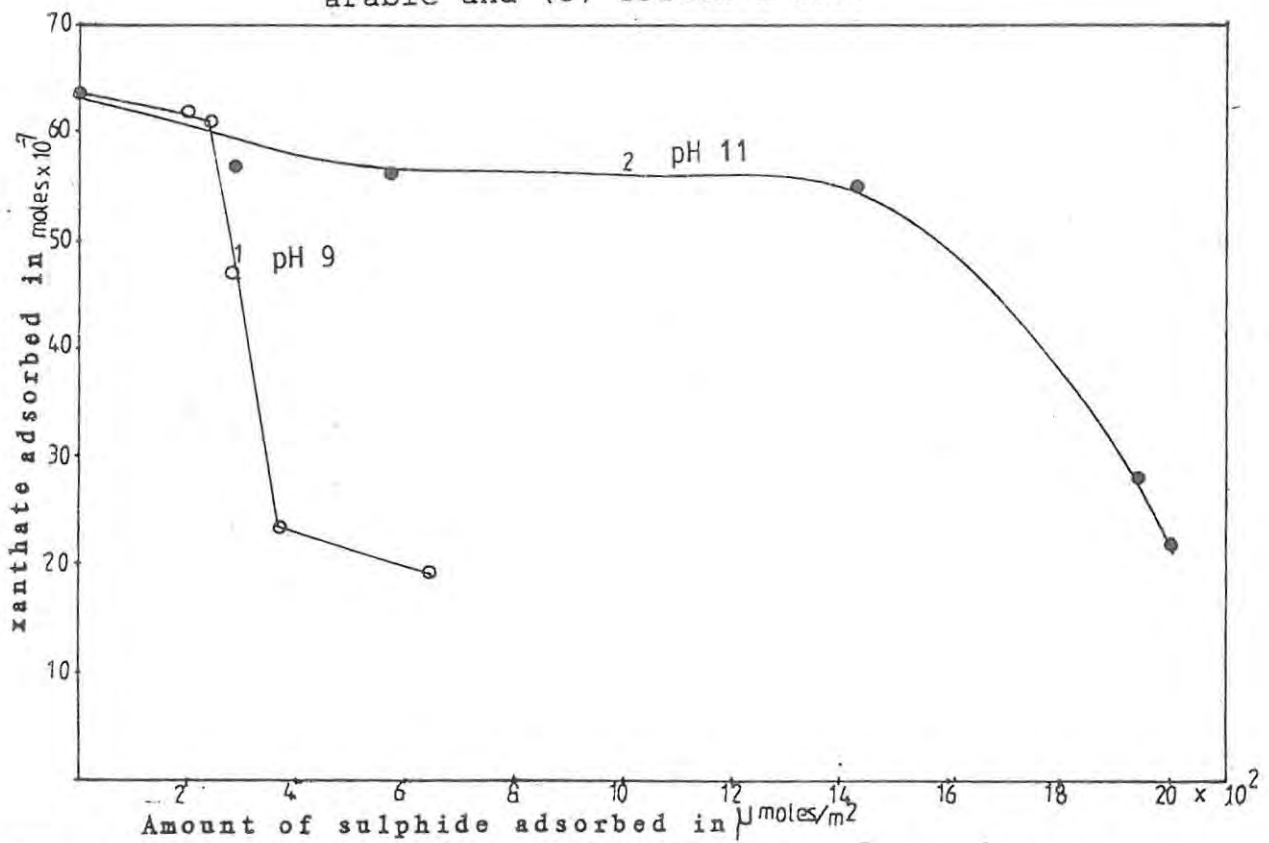
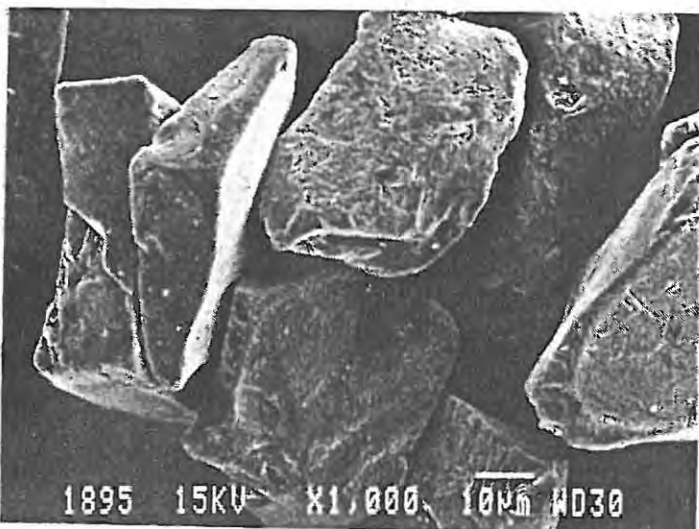


Figure.57. Variation in xanthate uptake on cerussite with sulphidization level.



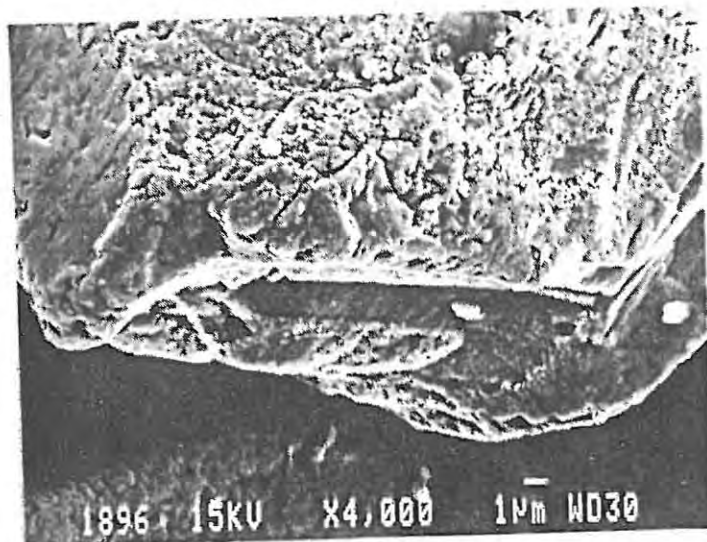
Micrograph.33.

Cerussite conditioned with 1×10^{-4} mol/l in the process of 50ppm gum arabic at pH 11.



Micrograph.34.

Cerussite conditioned with 1×10^{-4} mol/l sulphide in the presence of 50ppm Triton X-100 at pH 11.



Micrograph.35.

Cerussite conditioned with 1×10^{-4} mol/l sulphide in the presence of 50ppm Triton X-100 at pH 11.

In the presence of Triton X-100 however, the bulk precipitate was low. Cerussite particles obtained after sulphidization in the presence of these polymers showed a colour change from white to light brown, i.e. change from A to B (Fig. 43). Again, SEM micrographs showed what can be interpreted as uniform coverage of cerussite particles by PbS (micrographs 32 and 33). At pH 11 in the presence of Triton X-100 small crystals of PbS could be seen at high magnification (micrographs 34 and 35).

3.3.5 Reaction of xanthate with sulphidized cerussite at pH 9 and 11.

A series of sulphidization experiments were conducted at different sulphide ion concentrations at pH 9 and 11. Sulphide solution was decanted and the samples were washed several times with deaerated water prior to xanthate addition. N₂ gas was also passed through the solution during xanthate reaction. Table IV shows the different conditions used.

Table IV Conditions under which xanthate experiments were conducted at (a) pH 9* and (b) pH 11*
 $[X^-]$ = Xanthate concentration

	Initial $[S^{2-}]$ mol/l	$[S^{2-}]$ after 15 mins.	Amount of $[S^{2-}]$ adsorbed in $\mu\text{mol}/\text{m}^2$	Initial $[X^-]$ in mol/l $\times 10^{-5}$	Amount of X^- adsorbed in $\text{mol} \times 10^{-7}$
(a)	-	-		7.35	62.80
	7.0×10^{-5}	0	199.93	7.35	62.00
	8.5×10^{-5}	0	242.67	7.35	61.30
	1.0×10^{-4}	0	285.71	7.35	47.12
	1.5×10^{-4}	2.0×10^{-5}	371.18	7.35	23.60
	3.0×10^{-4}	7.5×10^{-5}	642.85	7.35	19.50
(b)	1.0×10^{-4}	0	285.71	6.63	56.50
	2.0×10^{-4}	0	571.43	6.63	56.30
	5.0×10^{-4}	0	1428.57	6.63	55.70
	7.0×10^{-4}	1.8×10^{-5}	1948.53	6.90	28.30
	1.0×10^{-3}	3.0×10^{-4}	2000.00	6.90	22.80

* lg of Cerussite with $0.035 \text{m}^2/\text{g}$ area was used.

Results illustrated in Fig.57 indicate that xanthate uptake was reduced when surface coverage by the metal sulphide was increased, and also that this reduction depended on the pH of sulphidization. At pH 11 higher sulphide concentration was necessary for complete coverage than pH 9 (micrographs 21 and 25).

3.3.6. Discussion.

The work described above shows that a relationship exists between the rate of sulphide uptake on the mineral and the mineral solubility e.g. compare Figs.39 and 41. These figures show that where the mineral solubility is low, as at pH 9 the rate of sulphide uptake is also low. At pH 12 where the rate of sulphide uptake is high, mineral solubility is also high. These effects reflect the type of surface coverage formed by sulphide. It has been noticed in this investigation that high rate of sulphide uptake gave a non-uniform surface coverage and a low rate of sulphide uptake gave a uniform one.

In discussing these generalizations, a system where sulphidization was conducted in the absence of metal ions (i.e. Mg^{2+} and Ca^{2+}) and polymers will be considered first.

Adsorption of sulphide on cerussite at low mineral solubility i.e. pH 9 and 10 which gave rise to uniform coverage, can be regarded as taking place via a surface precipitation or a chemisorption type process. This may be due to the predominance of $\text{Pb}(\text{OH})^+$ species which is surface active at these pH values (69). Fuerstenau et al (69) showed that at pH 9 and 10, 99% and 88% respectively of lead ions in solution exist as $\text{Pb}(\text{OH})^+$ (Table II). It is most likely that under these conditions reported by Fuerstenau et al, adsorption can occur via a chemisorption process with initial formation of monolayer coverage. A multilayer build up that follows which is equivalent to more than 20 monolayers (this was calculated on the assumption that the area covered by one molecule of HS^- is 10\AA^2 (29)) is formed by a slow diffusion of sulphide ions to the surface. Thus, making it possible to represent this adsorption phenomena as a first order process.

However, at a point where the mineral solubility is high sulphide uptake can be suggested to occur via the formation of a metal-sulphide complex in solution which is then followed by the nucleation of this metal-sulphide on the surface (7). Reactions in solution unlike chemisorption can be caused by the fact that at pH 11 and 12 where solubility is high, most of the lead ion species

are in the form of $\text{Pb}(\text{OH})_2$ and $\text{Pb}(\text{OH})_3^-$ and they are not as surface active as $\text{Pb}(\text{OH})^+$. Consequently, precipitation in solution will be preferred over chemisorption or surface precipitation. Another evidence which tends to support this, is the fact that the amount of bulk precipitate measured after sulphidization at pH 11 and 12 was high as compared to that at pH 9 and 10 where the mineral solubility is low. This then indicates that metal-sulphide complex formation followed by nucleation on the surface predominates at high pH values. SEM results also showed a non-uniform surface coverage of cerussite particles by sulphide when sulphidization was conducted under these conditions.

Other experimental evidence showed that compounds that lower the solubility of cerussite will as a result lower the rate of sulphide uptake on the mineral surface (compare Fig. 49 with 51, 52 and 53). Experimental evidence provided showed that the presence of Ca^{2+} reduces the mineral solubility thus reducing the rate of sulphide uptake on cerussite (Figs. 49 and 45). On the other hand results given in Fig. 50 and Table III suggest that this reduction in rate of sulphide uptake is probably due to the formation of $\text{CaCO}_3(\text{s})$ which can compete with sulphide ions for surface sites.

The fact that the rate of sulphide uptake in the presence of Ca^{2+} decreases as the pH is increased can be due to the decrease in solubility of CaCO_3 (61) and as a result more adsorption of CaCO_3 on cerussite (Table III) as the pH is increased is favoured. Evidence provided in Fig. 49 however, show that cerussite is highly soluble at pH 12 in the presence of Ca^{2+} . This seems to contradict the results shown in Fig. 45 which indicate a low rate of sulphide uptake at this pH. Experimental evidence given in Fig. 58 showed that the solubility of cerussite at pH 12 in the presence of Ca^{2+} is influenced by the conditioning time with the equilibrium being attained after 30 minutes, whereas in the absence of Ca^{2+} , equilibrium is attained after only 10 minutes. SEM micrographs obtained after sulphidization in the presence of Ca^{2+} show that mineral particles are uniformly covered by sulphide throughout the pH range studied.

Polymers such as gum arabic, starch and Triton X-100 that tend to reduce the solubility of cerussite were as a result found to reduce the rate of sulphide uptake. This may be influenced by their dispersing and flocculating ability.

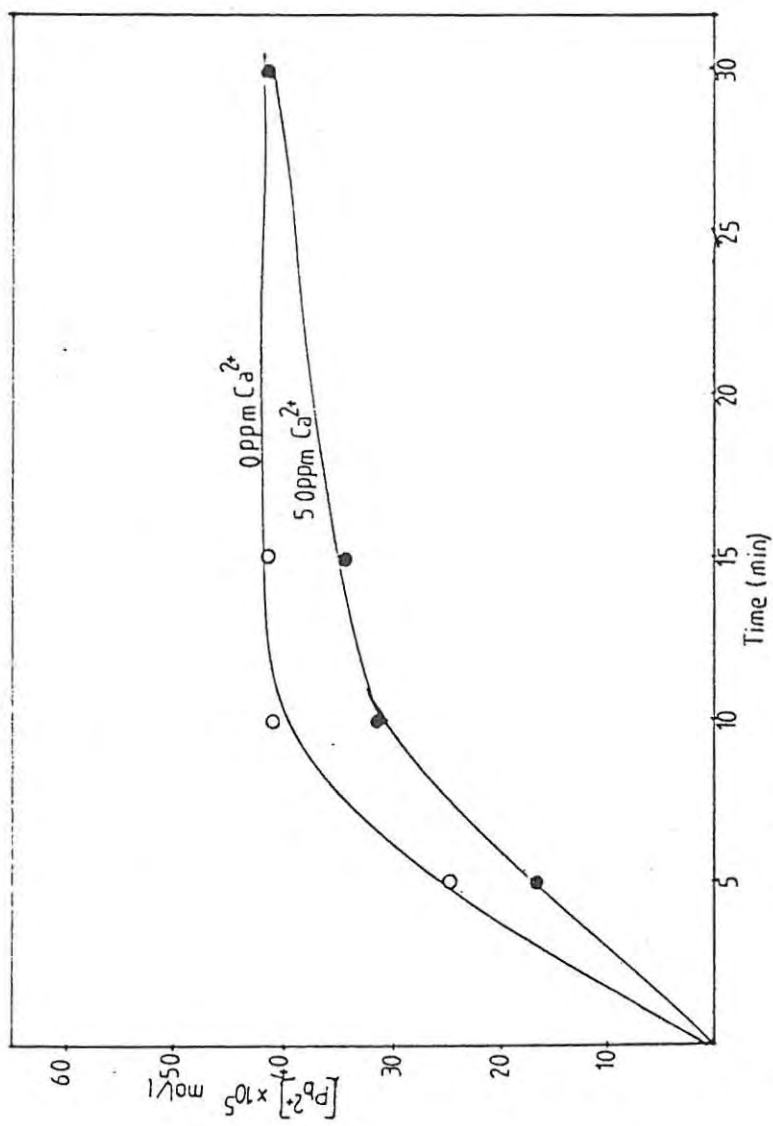


Figure.58. Kinetics of cerussite dissolution at
pH 12.

These polymers are known to adsorb on the surface of most minerals (2,63,65,66) and they can reduce the rate of the reaction of sulphide ions with the surface. In the case of gum arabic this tendency was found to decrease with increasing pH of sulphidization (Fig.52) and the resultant monolayers of sulphide adsorbed ranged between 3 and 8. Starch on the other hand seems to have a greater influence than gum arabic with the exception of pH 9. The highest dispersing action was observed at pH 10 and the amount of sulphide adsorbed at this pH value is equivalent to 2 monolayers. The rate of sulphide uptake was reduced by the presence of Triton X-100. From the bulk precipitate results given in Fig. 56 it can be seen that starch and gum arabic offer a great dispersing action, whereas Triton X-100 tends to cause flocculation (67,68) of the precipitate, and hence the bulk precipitate in the presence of Triton X-100 was much lower than in the presence of the other polymers.

Results for the interaction of xanthate with sulphide surface (Fig.57), indicate that reduction of xanthate adsorption is caused by the manner in which the surface is covered. If the surface is uniformly covered by sulphide, as in the case where sulphidization was conducted at pH 9,

the release of Pb^{2+} that can react with xanthate from an impervious surface is slow. Therefore the amount of xanthate adsorbed is reduced. On the other hand at pH 11 where the surface is not uniformly covered, lead ions can be released from the exposed cerussite surface. This will cause an increase in xanthate adsorption which can only be reduced if high sulphide concentrations are used which will react with most of the soluble lead species and hence effectively block the surface again. From Fig. 57, it can be seen that for sulphidization at pH 9, a low amount of sulphide is required to form an impervious layer than when sulphidization is conducted at pH 11.

CHAPTER 4

4.1 Conclusion.

Interesting features that emerge from this work are that sulphide uptake on cerussite is influenced mainly by the mineral solubility whereas sulphide uptake on copper (II) oxide also is affected by the sulphide concentration. The rate of sulphide uptake on cerussite was found to increase with an increase in pH of the solution. In the case of copper (II) oxide, the rate of sulphide uptake did not increase with an increase in pH of conditioning

instead, a minimum rate of uptake was obtained at pH 10 and 11 when 1×10^{-3} mol/l and 1×10^{-4} mol/l sulphide was used respectively.

The presence of other species Ca^{2+} , starch, gum arabic and Triton X-100 reduced the rate of sulphide uptake on these minerals. Again this depended on the pH of the solution. The presence of Mg^{2+} did not reduce the rate of sulphide uptake on cerussite whereas a reduction in rate in the presence of Mg^{2+} was observed on CuO . The ability of these polymers and metal ions in reducing the rate of sulphide uptake was postulated to be caused by the blocking of the oxide surface by the species, which in turn can reduce the mineral solubility or cover some of the reactive surface sites. Cerussite showed a colour change when treated with soluble sulphide. The colour intensity decreased with an increase in pH. The colour intensity remained high during conditioning in the presence of Ca^{2+} at all pH values studied. It was also observed that high colour intensity (black) corresponded with the uniform surface coverage by sulphide, and a low colour intensity with non-uniform coverage.

A low colour intensity was also observed for experiments conducted in the presence of starch, gum arabic and Triton X-100. In this case a low colour intensity corresponded with uniform

coverage because the amount of sulphide adsorbed on the surface was low (equivalent to 2 monolayers).

SEM micrographs obtained for copper (II) oxide particles that were sulphidized in the presence of Ca^{2+} , Mg^{2+} , starch and gum arabic showed a non-uniform coverage under all pH values studied. Smaller crystallites of CuS were observed on the surface after sulphidization in the presence of Triton X-100. This may be due to flocculation caused by the presence of Triton X-100 which caused rapid precipitation of CuS on the surface.

In the absence of oxygen surface coverage by sulphide prevented xanthate from reacting with the surface. A uniformly covered cerussite reacted with less xanthate than a non-uniform one.

Surface coverage of CuO by sulphide also prevented xanthate from reacting with the surface. However, when the sulphidization level was increased beyond 1800 mol/m^2 sulphide, the xanthate adsorption increased with an increasing sulphidization level.

REFERENCES

- (1) FUERSTENAU, D.W. Chemistry of flotation in: Principles of mineral flotation. The Wark Symposium ed. M.H. JONES AND WOODCOCK J.T., (1984), 7-29.
- (2) LEJA, J. Surface chemistry of froth flotation. (1982) Plenum press.
- (3) IVES, J.K. The Scientific basis of flotation NATO ASI Series. Series E. Applied sciences No. 75 (1984) Martinus Nishoff Publishers, Boston, 3-52, 229-288.
- (4) HARRIS, P.J. P.Proc. Conf. on : Recent advances in Mineral Science and Technology. Sandton, South Africa. March (1984) 221-226.
- (5) KLASSEN, V.I. and MOKROUSKOV, V.A. An Introduction to the Theory of Flotation, Butterworths, London, (1963)
- (6) GUTZEIT, G. Flotation process. Chem. Abstr. 40 p2777, (1946).
- (6) BRYSON, M.A.W. The adsorption of chelating reagents on oxide minerals, PhD Thesis, Rhodes University, 1984.
- (8) MARABINI, A.M. Trans Instn. Min. Metall (Sec C: Mineral Process. Extr. Metall) (1978), 87 C75-C78 .

- (9) BUSTAMANTE, H. Trans, Instn, Min, Metall
SHERGOLD, H.L. (Sec : Mineral Process Extr.
Metall) (1983), 92-C201-C215.
- (10) SOMASUNDARAN, P. Chemistry and application of
and chelating agents in flotation
NAGARAJ, D.R. and flocculation in : Reagents
in the mineral industry.
Edited by M.J. JONES AND R.
OBLAH, (1984) IMM.
- (11) CECILE, J.L. J. Coll. Interface Sci. (1981)
CRUZ, M.I. 80, 2,589
BARBERY, G. AND
FRIPIAT, J.J
- (12) REY, M. and The flotation of oxidized zinc
RAFFINOT, P. ores in : Recent Developments
in Mineral Dressing (London :
IMM, 1953), 571-579.
- (13) FLEMING, M.G. Effects of soluble sulphide in
the flotation of secondary
lead minerals. In Recent
Developments in Mineral Dressing
(London : IMM, 1953) 521-554.
- (14) CAPRONI, G., The processing of oxidized lead
CICCU, R. and zinc ores in the CAMPO PISANO
GHIANI, M., and and SAN GIOVANNI plants (SARDINIA)
TRUDU, I. in : Processing of oxidized and
mixed oxide-sulphide lead-zinc
ores XII international mineral
processing congress, Warsaw
1979, LASKOWSKI, J.ed) Warsaw :
Polish Scientific publishers,
1979, 71-89

- (15) CASES, J.M. Concentration par flotation D'un
TRABELSI ,K., minerai D'oxyde de zinc et de
PREDALI,J.J., plomb in : ref 14, 95-119.
BRION, D.
- (16) KOZO, S., Flotation of Copper ore in :
HIDETO,H., Chem Abstr. 90,155129 f.
YOSHIO,M. and
TADASHI, K.
- (17) KOZO,S., Flotation of Copper ore in :
HIDETO,H., Chem Abstr 90,155128 e.
YOSHIO,M. and
TADASHI,K.
- (18) QUEIROLO,C. and Trans. Instn. Min. Metall.
CASTRO,S. (Sec. C: Mineral Process. Extr.
Metall.) (1976), 85,C166-C168.
- (19) CASTRO,S., Int. J. Miner. Process (1974),
GOLDFARB,J. and 1, 151-161.
LASKOWSKI, J.
- (20) FUERSTENAU,M.C. Sulphide mineral flotation :
in: principles of flotation
edited by R.P.KING. S.A. Instn.
Min. Metall (1982), 159-182.
- (21) SOTO,H. and Trans. Instn. Min. Metall (Sec C :
LASKOWSKI,J. Mineral Process.Extr.Metall)
(1973), 82,C153-157.
- (22) LASKOWSKI , J. Redox conditions in flotation of
oxides in : Interfacial phenomena
in mineral processing ed. B. YARAR
and D.J. SPOTTISWOOD. Proc.
Engineering foundation conf.
Franklin Pierce College, Rindge,
New Hampstown (1981).

- (23) BOWDISH, F.W. and TSE PU CHEN. Trans. Soc. Mining Eng. AIME (1963), 226, 21-24.
- (24) FUERSTENAU, D.W., SOTILLO, F. and VALDIVIESO, A. 15th Int. Min. Proc. Congr. Cannes (1985) 74-86.
- (25) REY, M. Trans. Instn, Min, Metall, (Sec C: Mineral Process. Extr. Metall) (1979), 88, C245-C250.
- (26) MARABINI, A.M. ALLESSE, V., and GARBASS, F. Role of sodium sulphide, xanthate and amine in flotation of lead-zinc oxidized ores. In : Reagent in the Mineral Industry edited by M.J. JONES and R. OBLAH. (1984), IMM, 125-136.
- (27) MASSACI, P., BELADI, G and BONIFAZI, G. Heat of reaction at solid-liquid interface in flotation of lead and zinc oxidized minerals in: Ref (26) 137-143.
- (28) GARBASS, F. and MARABINI, A.M. J. Chem. Soc. Faraday Trans I. (1986), 82, 2043-2055.
- (29) GASTRO, S., GOLDFARB, J., and LASKOWSKI, J. Int. J. Miner. Process (1974), 1, 141-149.
- (30) BOWDISH, F.W., and STAHMANN, W.S. Trans. Soc. Mining. Eng. AIME (1967), 238, 118-122.

- (31) RAGHAVAN, S., Int. J. Miner Process (1984),
ADAMEC, E., and 12, 173-191.
LEE, L.
- (32) CHANDER, S., Trans. Soc. Mining Eng. AIME
FUERSTENAU, D.W. (1972), 252, 62-69.
- (33) FINKELSTEIN, N.P. Natural and induced hydrophobicity
ALLISON, A.S., in sulphide minerals systems.
LOVELL, V.M., and In : P.SOMASUNDARAN and R.B.GIEVES
STEWART, B.V. (ed). Advances in interfacial
phenomena of particulate/solution/
gas systems Am. Inst. Chem. Eng. symp.
Ser. (1975) 150, 71 : pp165-175.
- (34) FUERSTENAU, M.C. Int. J. Miner. Process (1981),
and 8, 79-84.
SABACKY, B.J.
- (35) EADINGTON, P. and Trans. Instn. Min. Metall.
PROSSER, A.P. (Sec C: Mineral Process. Extr.
Metall), (1969), 78, C74-82
- (36) GRANVILLE, A., Trans. Instn. Min. Metall
FINKELSTEIN, N.P, (Sec C : Mineral Process,
and ALLISON, S.A. Extr. Metall), (1972), 81, C1-C30.
- (37) REHBINDER et al : Introduction to the Theory of
cited in Flotation edited by KLASSEN, I.
and MOROUSKOV V.A., Butterworths
(1963), 311-313.
- (38) BUSTAMANTE, H. and Trans. Instn. Min. Metall
CASTRO, S. (Sec C : Mineral Process.
Extr. Metall) (1975). 86 C167-C171

- (39) ALLISON, S.A., Met. Trans. (1972), 3, 2613-2618
 GOOLD, L.A.,
 NICOL, M.J. and
 GRANVILLE, A.
- (40) CASTRO, S., Int.J. Miner Process (1976),
 GAYTAN, H., and 3, 71-82.
 GOLDFARB, J.
- (41) TRAHAR, W.J. Int.J. Miner. Process. (1983),
 11, 57-74.
- (42) LUTTRELL, G.H. and Colloids and Surfaces (1984),
 YOON, R.H. 12, 239-254.
- (43) HARRIS, P.J. and National Institute of Metallurgy
 FINKELSTEIN, N.P. Report no: 1894 (1977).
- (44) HARRIS, P.J. and National Institute of Metallurgy
 FINKELSTEIN, N.P. Report no: 1896 (1977)
- (45) JONES, M.H., Trans. Instn. Min. Metall
 WOODCOCK, J.T. (Sec C: Mineral Process. Extr.
 Metall) (1978), 87, C99-105.
- (46) JONES, M.H., Proc. Australas. Instn. Min.
 WOODCOCK, J.T. Metall (1978), 266, 11-9.
- (47) JONES, M.H. Application of pulp chemistry of
 WOODCOCK, J.T. regulation of chemical environment
 in sulphide mineral flotation in :
 Principles of mineral flotation.
 The Wark Symposium ed. M.H. JONES
 and WOODCOCK, J.T. (1984), 147-183.
- (48) ORION, 1979 Instruction manual for sulphide
 ion selective electrode, silver
 ion electrode model 94-18,
 9930 (Orion Research Incorporated:
 Cambridge. Mass.

- (49) FRIES, J. and GETROST, J. Organic Reagents for Trace Analysis (1977), pp344. E. MERCK DRAMSTADT.
- (50) DU BOIS, M., GILLES, K.A., HAMILTON, J.K. REBERS, P.A., and SMITH, G. Anal. Chem. (1956), 28, 350-356.
- (51) BASSETT, J., DENNEY, R.C. JEFFERY, G.H. and MENDHAM, J. Vogel's Textbook of Quantitative Inorganic Analysis 4th ed (1978), Longman 309-310
- (52) HULLINGER, F. Structure and Bonding (1968), 4, 83-229.
- (53) EMELEUS, H.J. Inorganic Chemistry series one Vol.5. Transition Metals part 1 ed: SHARP, D.W. Butterworths, London, (1973), 372-375.
- (54) BAILAR, J.C. EMELEUS, H.J. NYHOLM, R., and TROTMAN-DICKENSON, A.F. Comprehensive Inorganic Chemistry Vol 2 : Pergamon Press, Oxford, (1973), 927-929.
- (55) JELLINEK, F. Sulphides in : Inorganic Sulphur Chemistry edited by G. NICKLESS, Elsevier publishing company, London (1968), 670-747.
- (56) PAUL, R.L. Council for Mineral Technology, Randburg, South Africa. Private Communication.

- (57) MOELLER, T. Inorganic Chemistry, John Wiley and Sons, New York, (1982), 607-610.
- (58) SOTO, R., and Trans. Instn. Min. Metall,
GOLDFARB, J. (Sec C: Miner Process. Extr. Metall)
(1975), 86, C267-268.
- (59) BAES, C.F. and The Hydrolysis of Cations, John
MESMER, R.E. Wiley and Sons, New York, (1976), 273.
- (60) ATTIA, Y.A. Trans. Instn. Min. Metall (Sec C:
Miner Process. Extr. Metall) (1975),
84, C221-230.
- (61) SOMASUNDARAN, Colloids and Surfaces (1985), 15,
OFORI AMANKONAH, J. 309-333.
and
ANANTHAPADMABHAN, K.P.
- (62) In : HUNTER, R.J. Zeta Potential in Colloid Science,
Principles and Applications.
Academic Press, London, (1981),
326-334.
- (63) STEENBERG, E., S.Afr. J. Chemistry (1984), 37 (3),
and 85-90.
HARRIS, P.J.
- (64) YUEYING, G., Chem. Abstr. (1986), 104, 75780d.
WAILANG, L., LI, X.
and TIREN, G.
- (65) LEVITS, P., J. Phy. Chem. (1984), 88,
VAN DAMME, H., and 2228-2235.
KERAVIS, D.

- (66) LEVITS, P., and VAN DAMME, H. J. Phy.Chem. (1986), 90, 1302-1310.
- (67) RUBIO, J. and KITCHENER, J.A. Trans. Instn. Min. Metall. (Sec C : Mineral Process. Extr. Metall) (1977), 86, C87-C100
- (68) RUBIO, J. Colloids and Surfaces (1981), 3, 79-95.
- (69) FUERSTENAU, M.C. SOMASUNDARAN, P. FUERSTENAU, D.W. Trans. Instn. Min. Metall (1965), 381-391.
- (70) STUMM, W. and MORGAN, J.J. Aquatic Chemistry, New York, John Wiley and Sons, (1970), 749-757.